Ore Geology Reviews 76 (2015) 360–394

Contents lists available at ScienceDirect

Ore Geology Reviews

journal homepage: www.elsevier.com/locate/oregeorev

Basin-related uranium mineral systems in Australia: A review of critical features

Subhash Jaireth, Ian C. Roach *, Evgeniy Bastrakov, Songfa Liu

Geoscience Australia, GPO Box 378, Canberra, ACT 2601, Australia

ARTICLE INFO

Article history:
Received 29 October 2014
Received in revised form 6 August 2015
Accepted 6 August 2015
Available online 12 August 2015

Keywords:
Australia's uranium deposits
Unconformity-related uranium
Sandstone-hosted uranium
Calcrete-uranium

ABSTRACT

This paper reviews critical features of basin-related uranium mineral systems in Australia. These mineral systems include Proterozoic unconformity-related uranium systems formed predominantly from diagenetic fluids expelled from sandstones overlying the unconformity, sandstone-hosted uranium systems formed from the influx of oxidised groundwaters through sandstone aquifers, and calcrete uranium systems formed from oxidised groundwaters flowing through palaeochannel aquifers (sand and calcrete). The review uses the so-called 'source-pathway-trap' paradigm to summarise critical features of fertile mineral systems. However, the scheme is expanded to include information on the geological setting, age and relative timing of mineralisation, and preservation of mineral systems. The critical features are also summarised in three separate tables. These features can provide the basis to conduct mineral potential and prospectivity analysis in an area. Such analysis requires identification of mappable signatures of above-mentioned critical features in geological, geophysical and geochemical datasets. The review of fertile basin-related systems shows that these systems require the presence of at least four ingredients: a source of leachable uranium (and vanadium and potassium for calcrete-uranium deposits); suitable hydrological architecture enabling connection between the source and the sink (site of accumulation); physical and chemical sinks or traps; and a post-mineralisation setting favourable for preservation. The review also discusses factors that may control the efficiency of mineral systems, assuming that world-class deposits result from more efficient mineral systems. The review presents a brief discussion of factors which may have controlled the formation of large deposits in the Lake Frome region in South Australia, the Chu-Sarysu and Syrdarya Basins in Kazakhstan and calcrete uranium deposits in the Yilgarn region, Western Australia.

1. Introduction

Basin-related uranium mineral systems, which include uranium deposits formed during various stages of basin evolution (sedimentation, diagenesis and post-sedimentation fluid-flow), account for a significant portion of worldwide uranium resources. Uranium resource data in the International Atomic Energy Agency's (IAEA) UDEPO database (1140 deposits worldwide) show that they account for around 74% of resources, almost three times more than resources in the magmatic-related uranium systems (Fig. 1). Of the basin-related uranium mineral systems, close to 59% of resources are associated with various types of phosphorites (Fig. 2). In general, phosphorite-related deposits are of low grade (between 200 ppm U and 600 ppm U) and large tonnage (Dahlkamp, 2009). Sandstone-hosted uranium deposits contain close to 23% of known uranium resources (Fig. 2) and, at present, represent the largest economically extractable resources of uranium of any type. Although unconformity-related uranium deposits account for around only 8% of uranium resources, some of the world's highest grade deposits are of this type. Calcrete uranium deposits (termed surficial in the UDEPO database) contain around 2% of the world's uranium resources. Amongst sandstone-hosted deposits, the roll-front type contains up to 54% of known uranium resources (Fig. 3) followed by tabular (37%) and basal-channel types (7%).

In Australia, basin-related uranium mineral systems account for around 21% of uranium resources (Fig. 4). A large contribution of magmatic-related mineral systems (78%) is due to one single deposit, the low-grade but large-tonnage 'supergiant' Olympic Dam deposit. More than 60% of the resources in basin-related systems are associated with unconformity-related uranium deposits (Fig. 5). Sandstone-hosted uranium and calcrete uranium deposits account for 24% and 16% of uranium resources, respectively (Fig. 5).

The predominance of basin-related uranium systems in the global metallogeny of uranium can be explained by oxidation–reduction reactions, which control transport (in oxidised conditions) and deposition (in reduced conditions) of uranium. Changes in the oxygenation level of Earth's atmosphere triggered intensive removal of uranium from rocks and its transport in oxidised fluids. The oxygenation of the atmosphere occurred in a number of stages (Holland, 2006). During Stage 1 (3.85 Ga to 2.45 Ga), the atmosphere and the oceans were largely or

* Corresponding author.
E-mail address: Ian.Roach@ga.gov.au (I.C. Roach).

http://dx.doi.org/10.1016/j.oregeorev.2015.08.006
0169-1368/

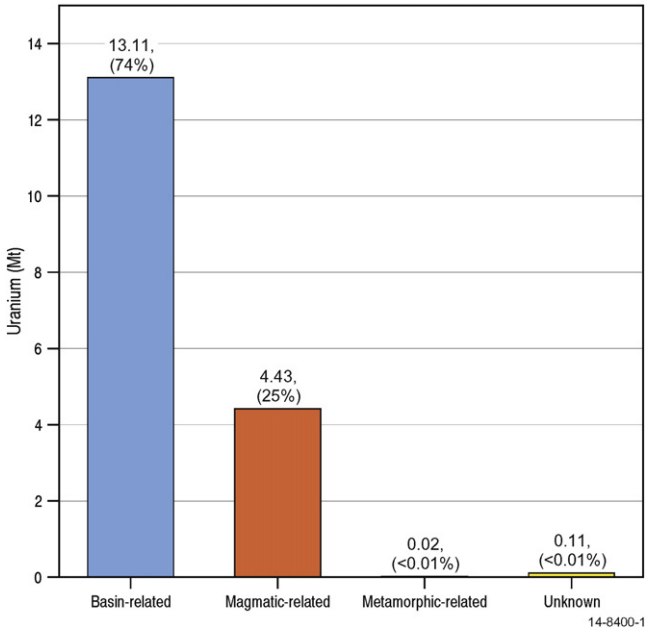

Fig. 1. Uranium resources of four major classes of uranium deposits. Data are sourced from the IAEA's UDEPO database (IAEA, 2009). Data accessed in January 2014 (https://infcis.iaea.org/UDEPO/About.cshtml).

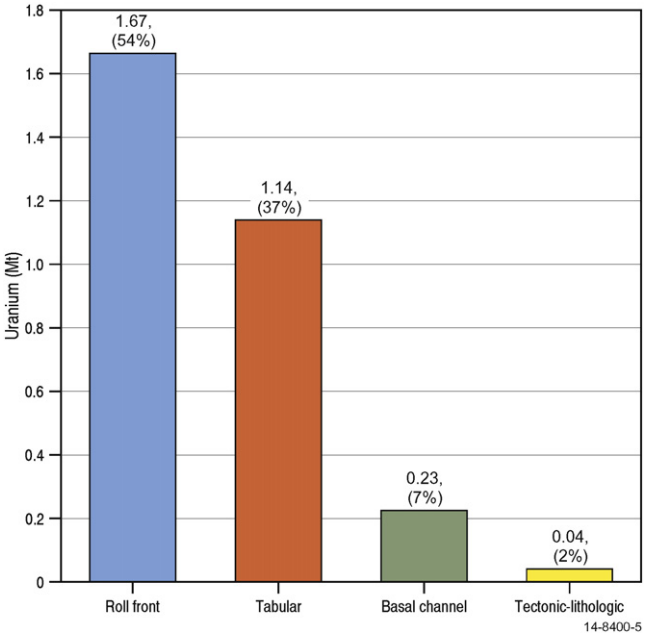

Fig. 3. Uranium resources of sandstone-hosted uranium deposits. Data are sourced from the IAEA's UDEPO database (IAEA, 2009). Data accessed in January 2014 (https://infcis.iaea.org/UDEPO/About.cshtml).

entirely anoxic. These conditions favoured the accumulation of detrital uraninite and formation of uraniferous quartz-pebble conglomerates (e.g. the Witwatersrand Basin in South Africa and the Blind-River and Elliot Lake area in Canada; Dahlkamp, 2009). During Stage 2 (2.45 Ga to 1.85 Ga), the oxygen level in the atmosphere increased to between 0.02 atm. and 0.04 atm. and shallow regions of oceans were mildly oxygenated. Proterozoic unconformity-related uranium deposits formed predominantly between ~1750 Ma and 1600 Ma in Australia (Lally and Bajwah, 2006) and between 1600 Ma and 1300 Ma (the Athabasca and Thelon basins in Canada; Jefferson et al., 2007). This time period overlaps with Stage 3 of oxygenation (1.85 Ga to 0.85 Ga) when atmospheric oxygen levels did not change significantly from the Stage 2 (2.45 Ga to 1.85 Ga) levels. The atmospheric oxygen levels during Stage 4 (0.85 Ga to 0.54 Ga) increased ten times to reach values of ~0.2 atm. The atmospheric oxygen levels probably rose to a maximum value of ~0.3 atm. during Stage 5 (540 Ma to present). This is the time period when most large sandstone-hosted uranium deposits in the world were formed.

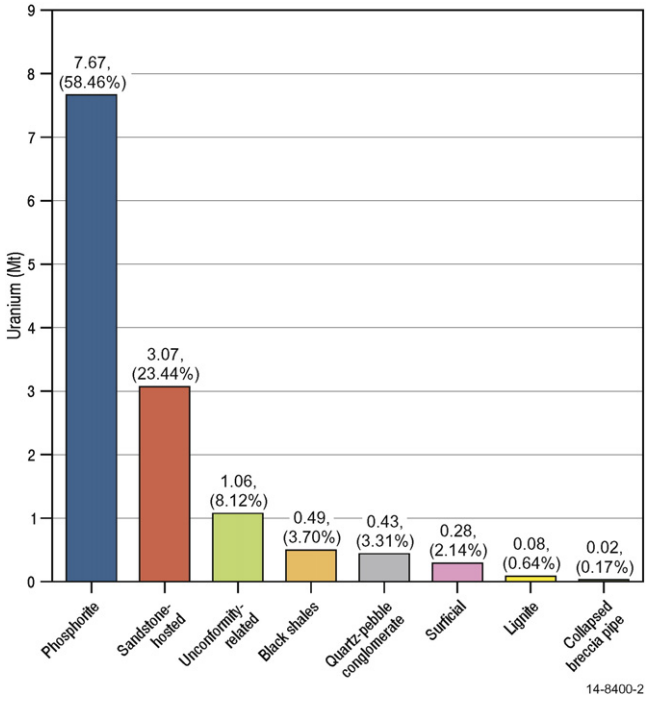

Fig. 2. Uranium resources of basin-related uranium deposits. Data are sourced from the IAEA's UDEPO database (IAEA, 2009). Data accessed in January 2014 (https://infcis.iaea.org/UDEPO/About.cshtml).

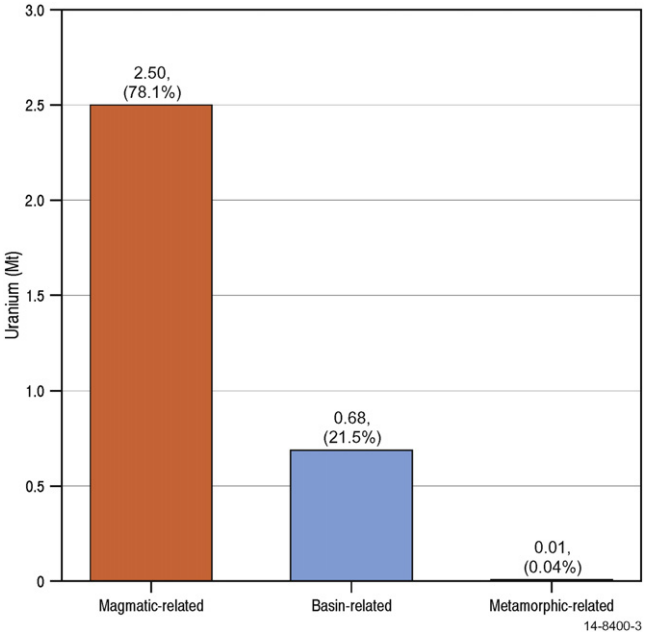

Fig. 4. Uranium resources of four major classes of uranium deposits in Australia. Data are sourced from Geoscience Australia's OZMIN dataset. Data accessed in January 2014. Selective data can be downloaded from http://www.australianminesatlas.gov.au/.

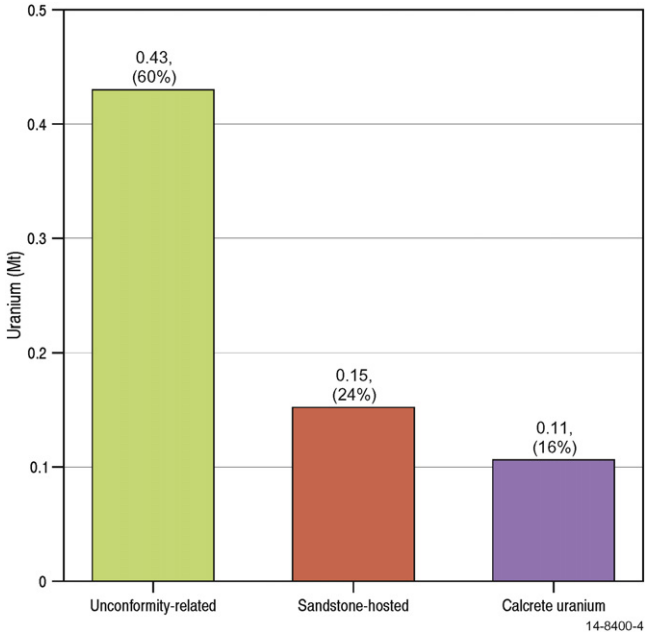

Fig. 5. Uranium resources of basin-related uranium deposits in Australia. Data are sourced from Geoscience Australia's OZMIN dataset. Data accessed in January 2014. Selective data can be downloaded from http://www.australianminesatlas.gov.au/.

However, oxygenation of the atmosphere was only one of the two critical factors, which could have controlled the formation of basin-related uranium deposits. The other important factor was the appearance of vascular plants in sedimentary basins. It has been suggested that after the emergence of vascular plants on the Earth (in the Late Silurian or even as early as the Late Ordovician; Cuney, 2010), deposition of continental siliciclastic sediments did not lead to the formation of thick strata of uniformly oxidised 'red sandstones', a characteristic feature of basins hosting Proterozoic unconformity-related deposits, but was more conducive to the formation of strata comprising alternating successions of oxidised and reduced (rich in carbonaceous material) sediments (Cuney, 2010). The creation of intraformational redox gradients provided ideal conditions for the formation of sandstone-hosted uranium deposits. Calcrete-uranium deposits appeared in the Cenozoic when valley calcretes were formed in areas of relatively arid climate conditions. In these mineral systems uranium and vanadium are transported in oxidised groundwaters and carnotite is deposited, not due to changes in redox conditions, but from changes in pH, and in the concentration of CO_2 in groundwaters caused by seasonal fluctuation of groundwater levels (see Section 4).

This paper presents a review of three major types of basin-related uranium mineral systems in Australia: unconformity-related; sandstone-hosted; and, calcrete uranium. The three systems are responsible for the formation of many of the major uranium deposits in Australia (Fig. 6).

Since the initial definition (Fyodorov, 2005), the concept of a mineral system has evolved and a number of different formulations of this concept have been developed (see Huston, 2010, this volume). This review uses the so-called 'source-pathway-trap' paradigm to summarise critical features of mineral systems. However, the scheme is expanded to include information on the geological setting, age and relative timing of mineralisation, and preservation of mineral systems.

2. Unconformity-related uranium mineral systems

In Australia, unconformity-related uranium deposits and prospects are located in the Northern Territory (NT, Pine Creek Orogen — PCO-region), Western Australia (WA, Capricorn and Paterson regions) and South Australia (SA, Gawler region). Minor uranium occurrences are also recorded in the Granites–Tanami region (NT and WA), the Halls Creek region (WA), and the Tennant Creek region (McKay and Miezitis, 2001).

Unconformity-related uranium deposits in Australia range from very small deposits (<~1 tonne uranium) to world-class deposits, such as Jabiluka (123 000 tonnes uranium) and Ranger (211 000 tonnes uranium). In general the deposits have uranium grades of >~0.1 wt.% (Fig. 7). However the highest grades in the PCO are significantly lower than the grades recorded for similar deposits in the Athabasca Basin. For example, the highest grade in the PCO is reported at the Palette uranium mine (2.45% U). However, this deposit is small with total uranium resource of 124 tonnes. The Nabarlek deposit is much larger (9200 tonnes U) with an average grade of 1.54 wt.% U. In the Athabasca Basin ore grades for some of the largest deposits are significantly higher (17.5 wt.% U at Cigar Lake and 19.5 wt.% U at McArthur River).

Polymetallic uranium mineralisation in the Paleoproterozoic sandstone-hosted deposits in the Westmoreland region (NT) is spatially distant from the Proterozoic unconformity, but it shows many features similar to the unconformity-related deposits in Australia and Canada. As the genesis of these deposits is controversial, they are not discussed in this review. More detailed descriptions of these deposits can be found in Bastrakov et al. (2010), Lally and Bajwah (2006), Polito et al. (2005a, 2005b), and McKay and Miezitis (2001).

This review is largely based on the geology of unconformity-related uranium deposits in the PCO. The uranium deposits in the PCO are generally grouped in three separate fields (Fig. 8, Table 1): the Alligator Rivers Uranium Field; the South Alligator Valley Mineral Field; and, the Rum Jungle Mineral Field. In recent years a number of new uranium prospects (e.g., Thunderball, Bella Rose and Corkscrew) have been discovered in a zone between Adelaide River and Emerald Springs. This new Hayes Creek Mineral Field also contains the Fleur De Lys deposit that was discovered in the early 1960s. Uranium deposits in the PCO have been described in detail in many publications (e.g., Ahmad and Hollis, 2013; Ahmad et al., 2006; Lally and Bajwah, 2006; McKay and Miezitis, 2001). Outside the PCO, a brief description of Kintyre uranium deposit in the Paterson region of WA can be found in Cross et al. (2011), Huston et al. (2010), McKay and Miezitis (2001) and Jackson and Andrew (1990).

2.1. Geological setting of the Pine Creek Orogen

Geological architecture of unconformity-related uranium systems in the PCO can be defined by three important components, which include: 1. major unconformity; 2. reduced Paleoproterozoic metasedimentary rocks below the unconformity; and 3. a relatively thick (>4 km to 5 km) package of Paleoproterozoic coarse-grained, dominantly fluvial sedimentary rocks overlying the unconformity.

2.1.1. Major unconformity

In the Nimbuwah Domain, the major unconformity is between reduced metasedimentary rocks of the Paleoproterozoic Cahill Formation and Nourlangie Schist (both broadly equivalent of the South Alligator River Group) and relatively oxidised sediments of the overlying Katherine River Group (Fig. 9). In the Central Domain, the unconformity is between reduced metasedimentary rocks of the South Alligator River Group and the Katherine River Group in the eastern part of the Domain. In the South Alligator Valley Mineral Field, the unconformity between the overlying El Sherana Group that contains a package of oxidised sediments (Coronation Sandstone) and the underlying reduced metasedimentary rocks of the South Alligator River Group could have played an important role in generating fertile mineral systems. In the Rum Jungle Mineral Field, the important unconformity is between reduced metasedimentary rocks of the Mount Partridge Group (Whites Formation) and the oxidised sediments of the Depot Creek Sandstone

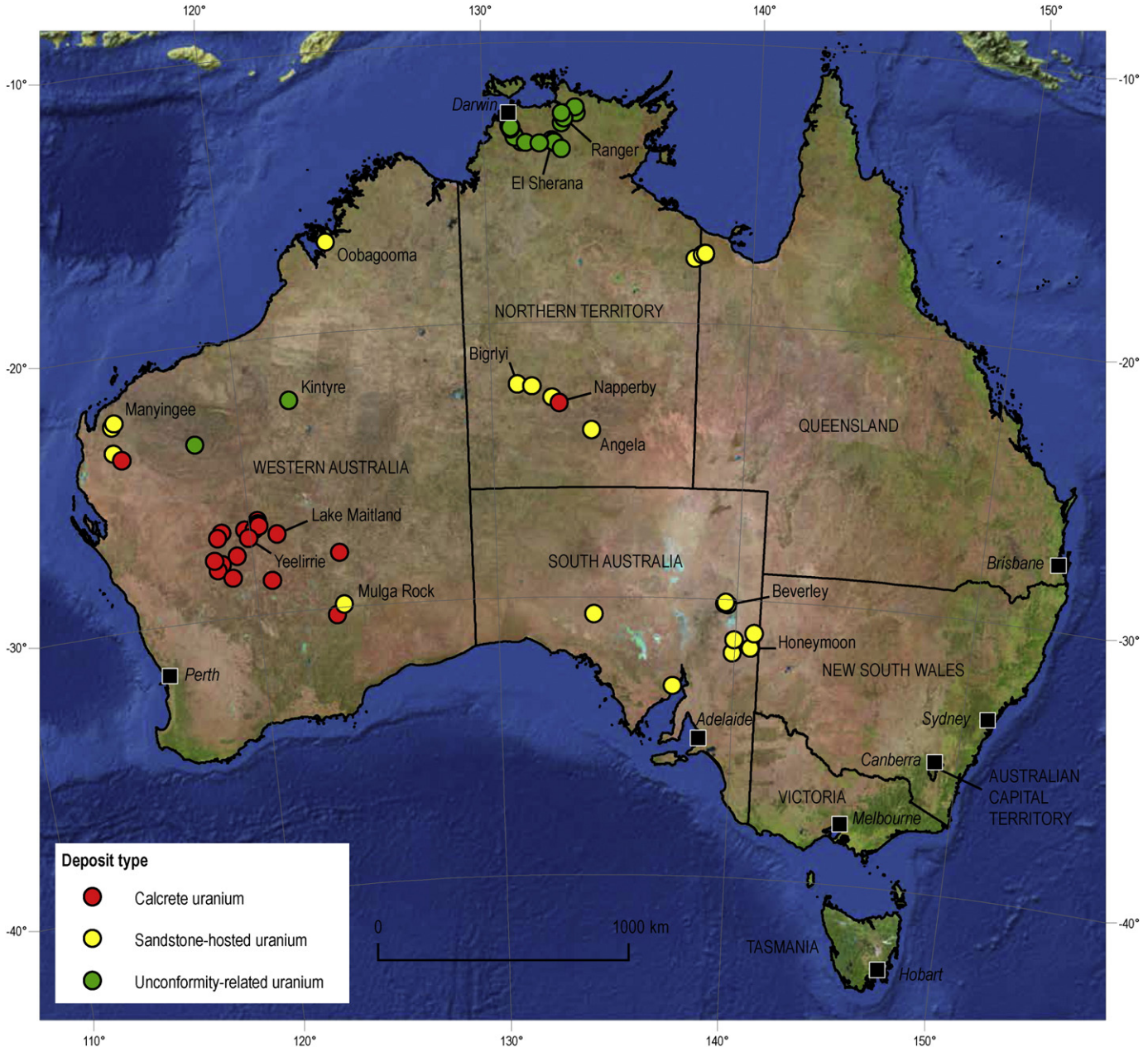

Fig. 6. Map showing location of major basin-related uranium deposits in Australia. Data are sourced from Geoscience Australia's OZMIN dataset. Data accessed in January 2014. For more detailed maps see Figs. 8, 11, 15, 16, and 19.

within the Tolmer Group (Fig. 9), most of which have been eroded. Similarly, in the Hayes Creek Uranium Field a large portion of the original package of oxidised sediments (the Depot Creek Sandstone) has most probably been eroded. Where present, rocks of the Depot Creek Sandstone overlie reduced metasedimentary rocks of the South Alligator River Group (Koolpin Formation). Remnants of the Depot Creek Sandstone outline margins of the Paleozoic Daly Basin and continue under the Basin. Airborne electromagnetic (AEM) data reveals the presence of the unconformity between the Depot Creek Sandstone and reduced metasedimentary rocks of the South Alligator River Group, a relationship supported by drilling records (Craig, 2011). In the northern Litchfield Domain, it is possible that the Depot Creek Sandstone unconformably overlies the graphite-bearing metasedimentary rocks of the Welltree Metamorphics.

In the Arnhem Land Plateau (Nimbuwah Domain, Fig. 8), the unconformity commonly has a local relief of up to 20 m (Needham, 1988). Pebble-filled palaeovalleys up to 20 m across have been observed along the unconformity. Locally, steep palaeovalleys are filled with massive breccia-conglomerate which grades into coarse conglomerate, and coarse quartz sandstone (Needham, 1988). A truncated regionally extensive palaeo-saprolitic profile (commonly over 50 m thick), developed in rocks of the Nanambu Complex, has been described by Needham (1988). The profile shows mineralogical and geochemical zoning from the chlorite zone just above the protolith to a hematite zone at the top. The profile was most probably modified following burial under the Kombolgie Subgroup sediments. A hematite–apatite-rich breccia (Scinto Breccia) in the South Alligator Valley is interpreted by Stuart-Smith et al. (1980) as an in situ regolith developed over carbonate-bearing rocks (mainly Koolpin Formation) at the unconformity surface. However, it has also been interpreted to be of hydrothermal origin (Ferenczi and Sweet, 2004). Hematite–quartz breccia within the Geolsec Formation in the

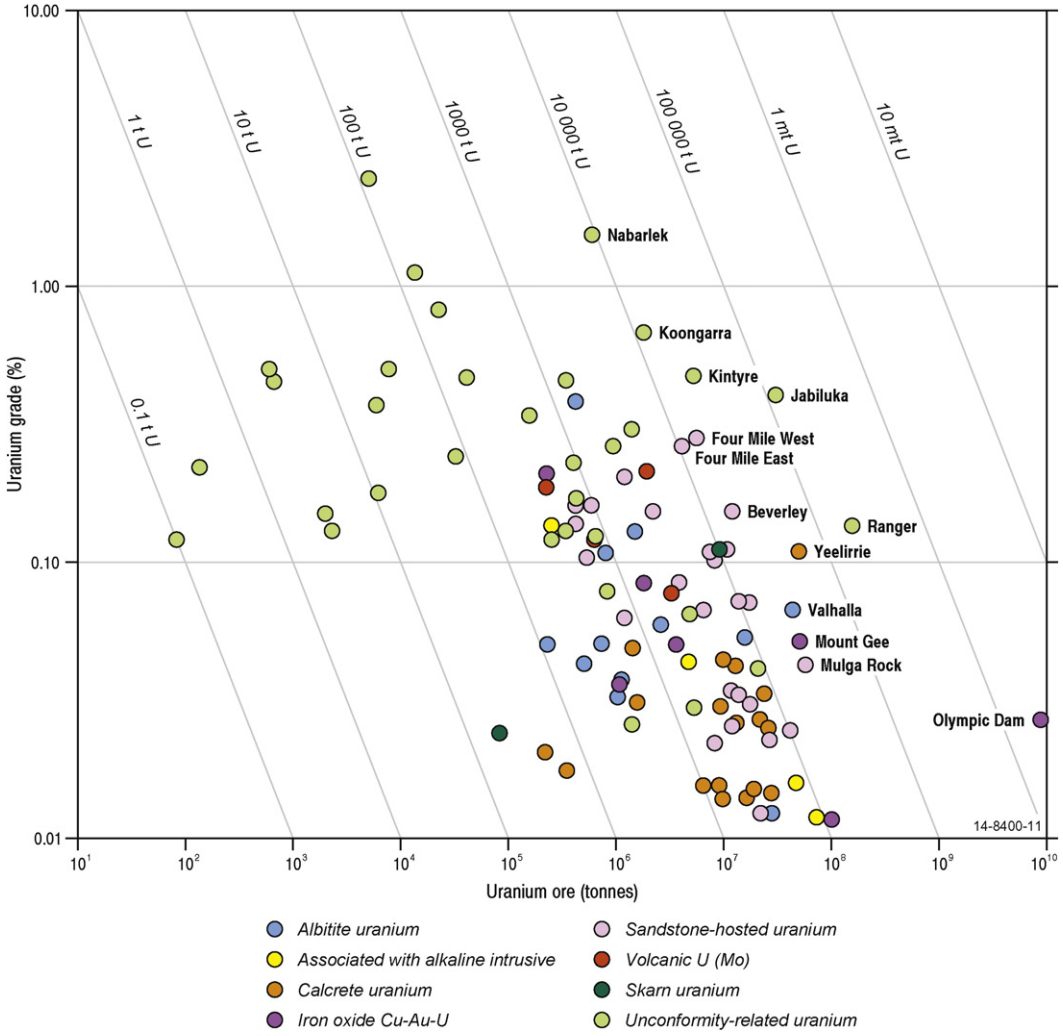

Fig. 7. Grade and tonnage data of Australian uranium deposits. Data are sourced from Geoscience Australia's OZMIN dataset. Data accessed in January 2014.

Rum Jungle Mineral Field has some similarities with the Scinto Breccia. It is considered to be either the product of in situ weathering and collapse of the Coomalie Dolostone, or a reworked talus slope breccia (Ahmad et al., 2006).

2.1.2. Reduced Paleoproterozoic metasedimentary rocks below the unconformity

Paleoproterozoic metasedimentary rocks that are enriched in carbonaceous material (graphite) and/or Fe^{+2}-bearing silicates (such as chlorite) include the Whites Formation (Rum Jungle Mineral Field), the Koolpin Formation (Hayes Creek Mineral and South Alligator Valley Mineral Fields), the Cahill Formation (Alligator Rivers Uranium Field) and the Welltree Metamorphics (Litchfield Domain). The metasediments were metamorphosed in the greenschist and amphibolite-to-granulite facies, which produced Fe^{+2}-bearing silicates (amphibole, biotite, garnet and chlorite). A characteristic feature of the metasedimentary package is the presence of calcareous sediments (dolomudstone in the Koolpin Formation; dolostones of the Coomalie Dolomite interbedded with the Whites Formation and with dolomitic rocks in the Cahill Formation). The significance of calcareous sediments in the favourable host rocks is not clear, although it may indicate that the favourable package was deposited in low-energy supratidal to subtidal conditions rather than in deeper-marine turbiditic environments.

2.1.3. A relatively thick (>4 to 5 km) package of Paleoproterozoic coarse-grained, dominantly fluvial sediments overlying the unconformity

In both the Nimbuwah and Central Domains, the bulk of the Katherine River Group sediments (>3 km in thickness; Needham, 1988) represent alluvial fan to braided fluvial facies. Although sediments of the Tolmer Group (>4 to 5 km in thickness; Malone, 1962) have not been studied in as much detail as the Katherine River Group, the available information suggests that the bulk of them were also deposited in similar conditions (Malone, 1962). The Depot Creek Sandstone (the basal unit of the Tolmer Group) occupies a similar stratigraphic position to that of the Mamadawerre Sandstone (basal unit of the Katherine River Group) and is interpreted to have formed in fluvial conditions (Carson et al., 2011). Matrix minerals in the sandstones contain hematite and some units in the Katherine River Group are distinctly ferruginous (e.g., the Marlgowa Sandstone and McKay Sandstone; Needham, 1988; Carson et al., 1999). Similarly the sandstone in the Tolmer Group contains lenses of hematite-rich calcarenite (Malone, 1962). The presence of ferruginous minerals in the sandstone can be an important indicator of the oxidation state of fluids formed from the diagenesis of these sediments.

2.2. Setting with respect to unconformity

The unconformity-related deposits in the PCO are described as Proterozoic sub-unconformity deposits because mineralisation is located

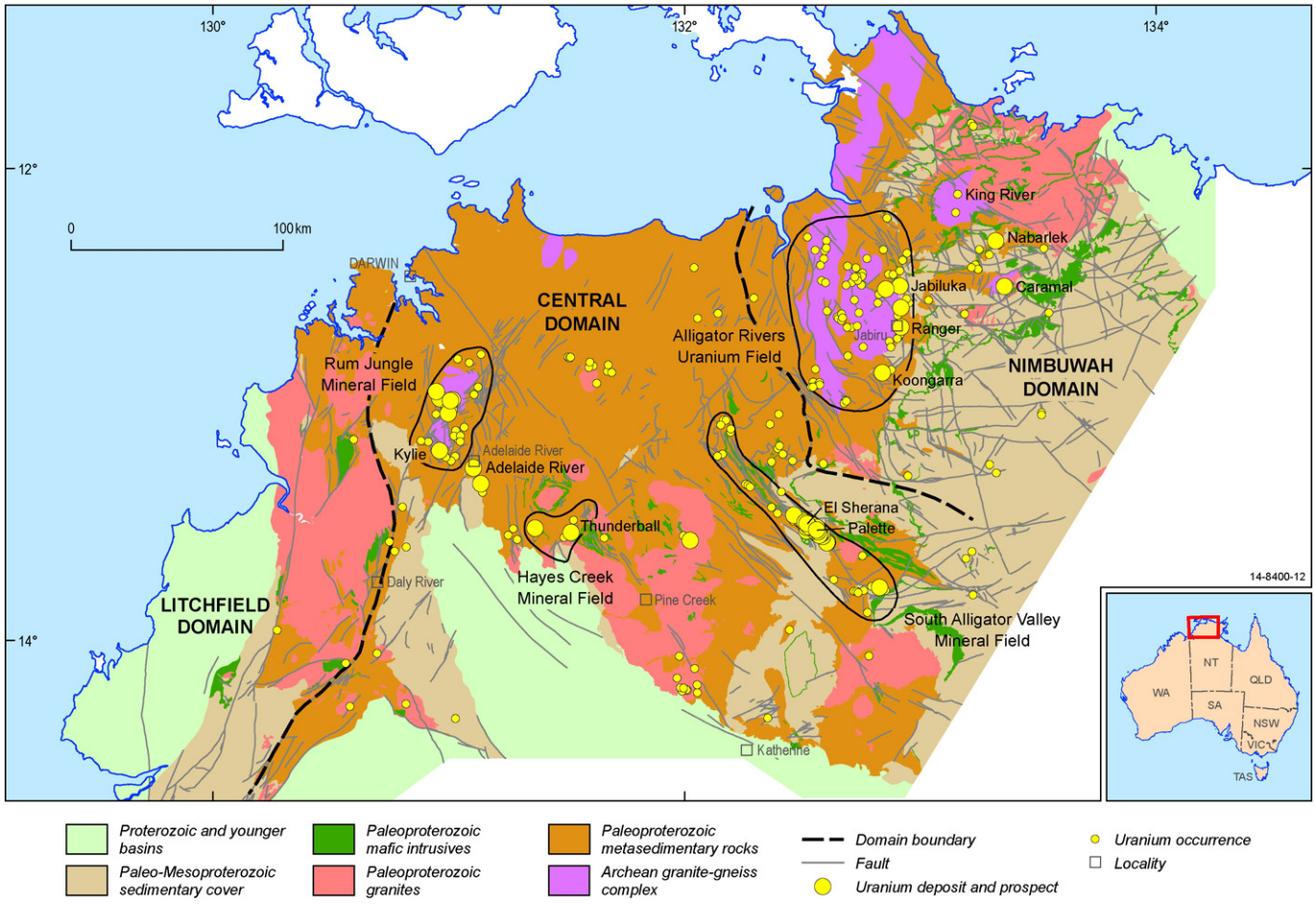

Fig. 8. Map of the Pine Creek Orogen showing uranium deposits and occurrences. The map is based on an NTGS (2005) dataset Pine Creek Orogen interpreted geology. Deposits, prospects and occurrences are from GA's OZMIN and MINLOC dataset (http://www.australianminesatlas.gov.au/).

within reduced metasedimentary rocks below the unconformity (Dahlkamp, 2009). In Canada similar deposits are classified as 'Ingress-style' in contrast to the 'Egress-style' deposits in which the mineralisation is hosted in the sandstone package overlying the unconformity (Jefferson et al., 2007). The Katherine River Group and Tolmer Group sediments overlying the unconformity have been preserved only in and near a few deposits. The known deposits and prospects in the PCO can be grouped into four types (Fig. 10):

1. Deposits in which the Proterozoic sandstone package is preserved (such as Jabiluka);
2. Deposits in which the Proterozoic sandstone package is partially preserved (such as Koongarra where the Mamadawerre Sandstone is present in the footwall of a shear zone);
3. Deposits in which the Proterozoic sandstone package is located within a few kilometres of the mineralised zone (such as Nabarlek and Caramal); and,
4. Deposits in which the mineralised zone is covered by Phanerozoic rocks (such as Ranger 68 and Austatom). At these deposits, the mineralised zones are unconformably overlain by Cretaceous rocks. The uranium mineralisation, however, is interpreted to be related to a Proterozoic rather than a Cretaceous unconformity.

2.3. Source of uranium

Although Archean and Paleoproterozoic metasediments and felsic intrusive rocks in the PCO contain abundant uranium (Ahmad et al., 2006; Lally and Bajwah, 2006) and could have been the first-stage source of uranium for the deposits, the immediate source of uranium remains uncertain. Two types of immediate sources of uranium have been postulated for unconformity-related uranium deposits: primary detrital heavy minerals in the sandstones overlying the unconformity; or, uranium-bearing minerals in the metasedimentary rocks below the unconformity (Kyser and Cuney, 2009). It has been suggested that diagenesis of the Athabasca Group in Canada caused extensive mobility of rare-earth elements and that rare-earth elements and uranium were most likely derived from detrital fluorapatite and zircon in the sandstone (Fayek and Kyser, 1997). In the Athabasca Group, primary detrital heavy minerals are essentially absent except for rare zircon and tourmaline, but fluorapatite and zircon are abundant as inclusions in detrital quartz. Detrital zircon in the matrices of sandstones is commonly corroded and shows evidence of increase in uranium relative to zirconium, hence detrital zircon could not have been the source of uranium (Kyser and Cuney, 2009). However, in situ alteration of monazite results in the formation of uranium-poor phosphate minerals, releasing excess uranium into diagenetic fluids (Hecht and Cuney, 2000). The former presence of detrital monazite in sandstones is indicated by high thorium contents of 18 ppm in the lower Manitou Formation of the eastern Athabasca Basin (Quirt et al., 1991). Although no detailed studies have been carried out in the Katherine River and Tolmer groups, a scenario similar to the one in the Athabasca Basin has also been suggested in the PCO (Kyser and Cuney, 2009).

As the uranium content of metasedimentary rocks, granites, and pegmatites below the unconformity is an order of magnitude higher than in the sandstones overlying the unconformity, they can be another possible source of uranium (Mercadier et al., 2013a, 2013b; Kyser and

Table 1
Major unconformity-related uranium mineral fields in Australia. Information sourced from Lally and Bajwah (2006) and Huston et al. (2010).

Attribute\uranium field	Alligator rivers	South Alligator Valley	Rum Jungle	Hayes Creek	Kintyre
Orogen	Pine Creek	Pine Creek	Pine Creek	Pine Creek	Paterson
Domain	Nimbuwah	Central	Central	Central	
Resource (tonnes U_3O_8)	408 055	2649	6354	0.1	36 023
Number of deposits	7	11	5	2	1
Metal association	U, Au	U, Au, PGEs	U, Cu, Pb, Zn, Co, Ni	U, PGE	U, Cu, Bi, Mo
Host rocks	Cahill Formation	Koolpin Formation, Coronation Sandstone	Whites Formation	Mount Bonnie Formation, Gerowie Tuff	Yandagooge Formation (Rudall Complex)
Age of host rock (Ma)	ca. 1870	ca. 1860, ca. 1829	ca. 2019	ca. 1860	ca. 2015–1765 Ma
Sandstone above unconformity	Mamadawerre Sandstone	Mamadawerre Sandstone	Depot Creek Sandstone, Geolsec Formation	Depot Creek Sandstone	Throssell Range Group (includes Broadhurst Formation and Coolbro Sandstone)
Metamorphic grade of the host (facies)	Amphibolite	Greenschist	Greenschist	Greenschist	Granulite to Amphibolite
Nearby Archean complex	Nanambu, Arrarra Gneiss, Kukalak Gneiss	Unknown	Rum Jungle	Unknown	Unknown
Age of Archean complex (Ma)	2670, 2640, 2520		2545, 2520	Unknown	Unknown
Associated mafic rocks (<1800 Ma)	Oenpelli Dolerite (?), mafic volcanics in the Katherine River Group	Oenpelli Dolerite (?)	None	None	Mafic intrusives (ca. 830 Ma)
Mafic rocks (>1800 Ma)	Zamu Dolerite present near Caramal	Zamu Dolerite, Goodparla Dolerite	Zamu Dolerite	Zamu Dolerite	Mafic–ultramafic rocks in the Rudall Complex
Alteration in the metasedimentary rocks	Chloritic, sericitic, hematitic, desilicification	Chloritic, sericitic, hematitic, desilicification	High-Mg chloritic, Fe–Mg Chloritic, sericitic, hematitic. In some deposits magnesite, dolomite and tourmaline present	Sericitic	Chloritic, magnetite, hematite, carbonate
Alteration in the sandstone	Chloritic, sericitic hematitic, desilicification	Hematitic	Hematitic	Unknown	Unknown

Cuney, 2009). The Archean granites in the Rum Jungle Complex have anomalously high uranium (2.9 to 39.9 ppm; average 12.5 ppm; McCready et al., 2003). The Archean and Paleoproterozoic rocks generally contain abundant zircon and monazite, alteration of which can provide a good source of uranium. Altered zircons from these basement rocks in the Athabasca Basin, however, are depleted in zirconium and silicon and are enriched in phosphorus, yttrium, iron, calcium and uranium. Hence zircon may not be a good source of uranium unless it is completely altered (Hecht and Cuney, 2000). Monazite, on the other hand, is the dominant uranium-bearing mineral in the basement rocks below the unconformity and has undergone intensive alteration in proximity to uranium deposits, suggesting that around 75% of its uranium has been leached. Thus monazite in the basement rocks interacting with fluids can be a good potential source of uranium in unconformity-related uranium deposits (Kyser and Cuney, 2009).

In the PCO the sandstones in the Katherine River Group are not anomalously enriched in uranium. In the drill hole DAD006 (~90 km east of El Sherana deposit, Fig. 7), the concentration of uranium in the sandstone units of the Kombolgie Subgroup varies between 0.29 ppm and 5 ppm. The uranium concentration increases to ~20 ppm at the upper and lower contact with mafic units (Nungbalgarri and Gilruth Volcanics) within the Kombolgie Subgroup (Jaireth et al., 2007). A

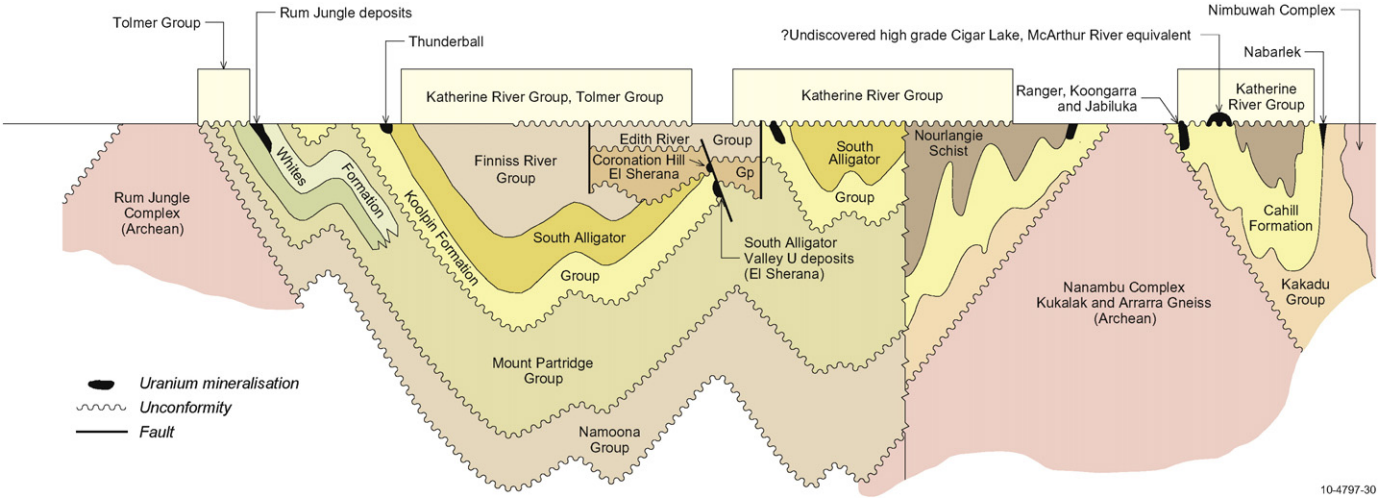

Fig. 9. Schematic cross section of the Pine Creek Orogen showing the position of major uranium deposits in relation to the unconformity. Modified after McKay and Miezitis (2001).

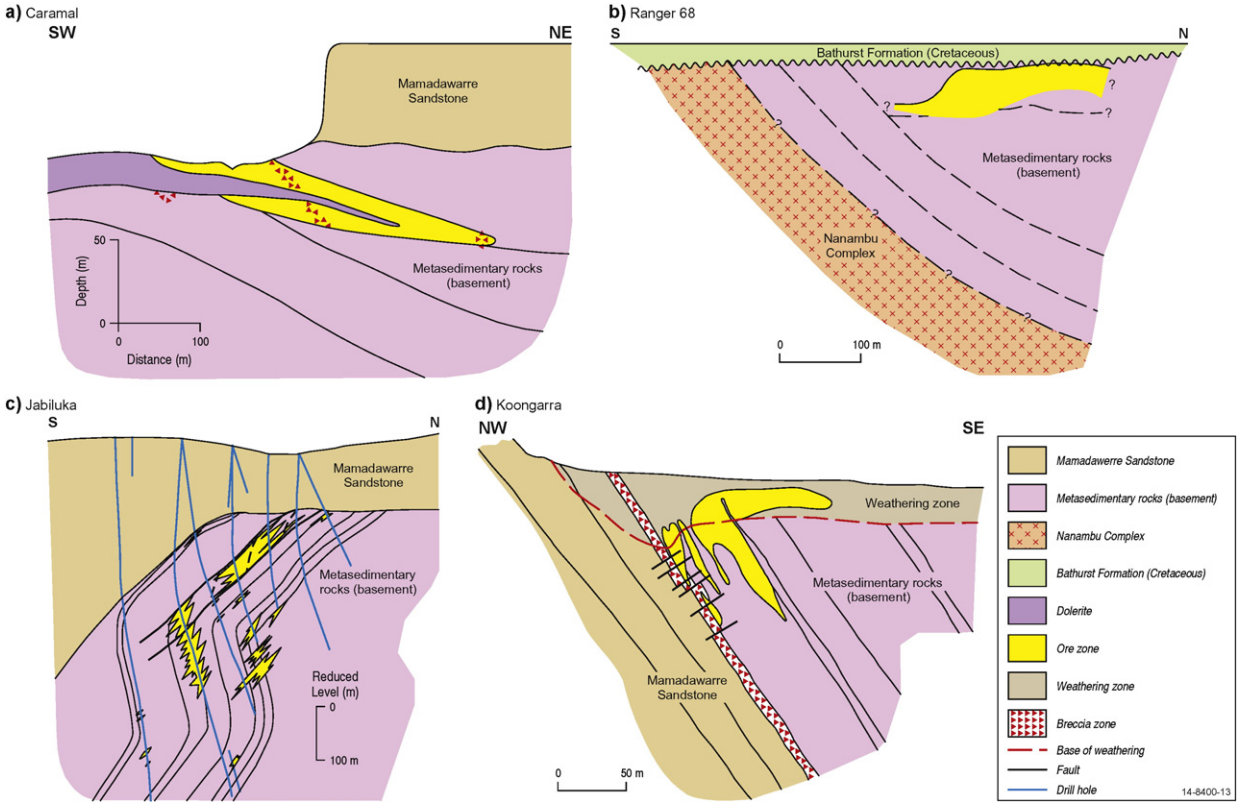

Fig. 10. Schematic cross-sections showing four types of settings of unconformity-related uranium deposits in the Pine Creek Orogen. Modified after Lally and Bajwah (2006).

similar variation is observed in the drill holes DAD002 (~120 Km northeast of El Sherana deposit, Fig. 7) and DAD007 (~90 km east of El Sherana deposit, Fig. 8).

Saprolitic palaeoweathering zones, such as those described at Granite Hill (Needham, 1988), can also be good sources of uranium. At Granite Hill, the palaeoweathering zone has lost up to 5 ppm of uranium compared to the unweathered Nanambu Complex protolith. Although the origin of the Geolsec Formation in the Rum Jungle Mineral Field and the Scinto Breccia in the South Alligator Valley Mineral Field is not clear, such palaeoweathering zones overprinted and altered by later fluid influx can also be effective sources of uranium. Similar zones of palaeoweathering have been described in the basement beneath the Athabasca Basin (Kyser and Cuney, 2009; Wilson, 1986).

2.4. Source and nature of fluids

Numerous fluid inclusion studies in the PCO and in the Athabasca Basin suggest that uranium deposits formed during peak diagenesis of the sandstone units overlying the unconformity at temperatures between 180 °C and 250 °C (Polito et al., 2011; Kyser and Cuney, 2009 and references therein). Derome et al. (2003) studied fluid inclusions in quartz-breccia veins in the basal sandstone units of the Kombolgie Subgroup and showed the presence of three distinct fluids: (1) a sodium-rich brine corresponding to a diagenetic fluid at a temperature close to 150 ± 5 °C; (2) a calcium-rich brine, probably corresponding to a residual basinal evaporitic brine that had reacted with the rocks below the unconformity; and (3) a low-salinity fluid heated in the basement. Wilde et al. (1989) documented similar hypersaline fluids (ca. 23 eq. wt.% $CaCl_2$) in secondary halite-saturated inclusions in altered host rock quartz and in early hydrothermal quartz veins. A detailed reconstruction of fluid evolution based on fluid inclusion studies in the unconformity deposit at McArthur River (Athabasca Basin) revealed two similar types of fluids: (1) a NaCl-rich brine (25 wt.% NaCl, up to 14 wt.% $CaCl_2$, and up to 1 wt.% $MgCl_2$) interpreted to be basinal fluid expelled from evaporites; and (2) a $CaCl_2$-rich brine (5 to 8 wt.% NaCl, 20 wt.% $CaCl_2$, and up to 11 wt.% $MgCl_2$) interpreted to have formed during the interaction of the basinal fluid with Ca-rich minerals in the rocks below the unconformity (Derome et al., 2005). At the Coronation Hill deposit in the South Alligator Valley Mineral Field the syn-ore fluid is likewise highly saline (20 to 25 wt.% $CaCl_2$) with median homogenisation temperatures of 140 °C (Mernagh et al., 1994). The interpreted temperatures of formation of 180 °C to 250 °C suggest that the sandstone package overlying the unconformity was at least 5 km thick (assuming a geothermal gradient of 35 °C/km).

Thus, at least two fluids are interpreted to be involved in the formation of these deposits: a basinal fluid derived from the diagenesis of sandstone overlying the unconformity, and, a fluid resulting from the interaction of the basinal fluid with rocks below the unconformity. The presence of halite crystal casts, indicative of evaporites, have been reported in the McKay Sandstone (upper part of the Kombolgie Subgroup) and in the Cottee Formation, overlying rocks of the Kombolgie Subgroup (Kyser and Cuney, 2009; Ferenczi and Sweet, 2004). The analysis of halogen and noble gases and composition of the uranium-bearing fluid inclusions in uranium deposits in the Athabasca Basins show that fluid composition was strongly controlled by subaerial evaporation and subsequent interaction with sedimentary rocks (Richard et al., 2011, 2014). It is more than likely that high-salinity fluids documented in the Kombolgie Subgroup sandstones were also at least partially generated by similar processes.

2.5. Sources of energy (energy drivers of fluid-flow)

The exact nature of the energy drivers of fluid-flow in these systems remains uncertain. Different fluid flow drivers and models have been

proposed, which include (Chi et al., 2013): large-scale convection caused by geothermal gradient; deposit-scale convection associated with the high heat conductivity of graphite; compaction-driven flow; and deformation-induced fluid flow.

In the Athabasca Basin, where sedimentary rocks overlying the unconformity are largely preserved, numerical modelling of regional-scale fluid flow by Raffensperger and Garven (1995a, 1995b) shows that compaction and heat (with average basement heat flow values) can create basin-scale free convection of fluid. Basin geometry and hydrostratigraphy constitute two important factors, which can influence flow patterns. The modelling demonstrates that reducing total basin thickness below 3 km can effectively shut off the free convection system. This highlights the importance of basin depth and the thickness of sandstone in generating fertile mineral systems.

As all known mineral deposits in the Athabasca Basin and PCO are structurally controlled (located both in sandstones overlying the unconformity and in the reduced basement rocks below the unconformity), the numerical model proposed by Raffensperger and Garven (1995a, 1995b) required modification in order to understand the possible contribution of tectonically-driven fluid flow. Numerical modelling by Cui et al. (2012) shows that in unconformity-related systems, free convection of fluid in the basin is significantly affected by thermal structure and by tectonic activation of faults. The modelling demonstrates that thermally driven free convection can develop throughout the sandstone sequence under a normal geothermal gradient (25 to 35 °C/km). During extensional deformation, because of their relative low permeability, the basement rocks experience reduction of pressure faster than the basinal rocks, and the basinal brines begin to penetrate the basement along fault zones. In contrast, during compressional deformation, a more rapid accumulation of pore pressure in the basement rocks causes expulsion of fluids (mainly along fault zones) from the basement into the sedimentary rocks above the unconformity.

2.6. Fluid-flow pathways

Unconformity-uranium systems involve two major types of fluid-flow pathways. Within the sandstone sequence overlying the unconformity, the fluid-flow is predominantly controlled by a system of aquifers and aquitards in the sequence. In a detailed study of the Manitou Formation in the Athabasca Basin, Hiatt and Kyser (2007) showed that depositional environment of sediments not only determine aquifer properties but also their basin-scale geometries, which in turn determine the degree of compartmentalisation of aquifers. Their analysis demonstrates that in the Athabasca Basin, the juxtaposition of a major aquifer over the palaeoweathering surface on the basal unconformity may have channelized flow along the unconformity. The geometry of the aquifer (its thinning and onlapping onto the unconformity) may have also focused fluid-flow toward the underlying basement in the eastern portion of the Basin, which hosts major uranium deposits.

In the Kombolgie Subgroup, diagenesis of the sediments produced a system of aquifers and aquitards, which could have also controlled fluid-flow in the basin (Kyser and Cuney, 2009; Kyser et al., 2000). The first stage of diagenesis in the lower Kombolgie Subgroup resulted in quartz overgrowth, which caused pronounced reduction in the porosity, particularly in the well-sorted lithologies (Hiatt et al., 2007). This event created basin-wide diagenetic aquitards capable of directing fluid-flow toward zones of higher permeability such as diagenetic aquifers (sediments without quartz cement) and fault zones (Kyser and Cuney, 2009). This early diagenesis (prior to the intrusion of Oenpelli Dolerite at ~1720 Ma, Worden et al., 2008) and resulting aquitards along with other volcanic units in the Kombolgie Subgroup were capable of subdividing the Kombolgie Subgroup into different compartments (Kyser et al., 2000).

Unlike in the Athabasca Basin, palaeo-saprolitic profiles in the PCO, at this stage, have been only locally mapped (see Section 2.1.1). It is possible that some sections of palaeo-saprolitic zones could have also served as fluid pathways.

The second major type of fluid-flow pathways is represented by major faults. As all major deposits are structurally controlled, faults, to a large extent, controlled deposit-scale fluid-flow. Numerical modelling discussed in the previous section demonstrates that extensional and compressional activation of these faults could have channelled fluids along these faults.

Some of the basin-scale fluid-flow pathways can be recognised through two regional-scale alteration assemblages: basin-wide pre-ore diagenetic alteration of sandstone identified in the Athabasca Basin, as well as in the Kombolgie Subgroup (Jefferson et al., 2007; Kyser and Cuney, 2009); and, sub-basin scale alteration haloes outlining clusters of uranium deposits in the Athabasca Basin (Jefferson et al., 2007). Extensive inner and outer halos of alteration in the basement rocks, as well as in the sandstone, also represent footprints of fault-controlled fluid-flow in uranium deposits. At the Ranger deposit, wall-rock alteration halos and rare-earth-element fractionation patterns around the ore body have been used to interpret fluid-flow, in upward direction along structures in the basement host rock (Fisher et al., 2013). This interpretation contrasts with models of downward flowing ore fluids proposed by Wilde et al. (1989), Polito et al. (2005a, 2005b), and for basement-hosted deposits beneath the Athabasca Basin (Kyser and Cuney, 2009 and references within).

2.7. Physical and chemical sinks/traps

2.7.1. Faults and shear zones

All known deposits in the PCO are structurally controlled. At the Nabarlek deposit mineralisation is located along a northwest-trending reverse fault/shear zone (Wilde and Wall, 1987). At the Jabiluka deposit, mineralisation is structurally controlled within semi-brittle shears that are sub-conformable to the basement stratigraphy, and within breccias developed along the hinge zone of fault-related folds adjacent to shears (Polito et al., 2005a, 2005b). The Ranger 1 deposits occur along the sheared contact (north–south trending low-angle reverse fault) between the Cahill Formation and the underlying Nanambu Complex (Lally and Bajwah, 2006). At the Koongarra deposit, mineralisation is located at the faulted and brecciated contact (northwest trending, steeply dipping reverse fault) between the Cahill Formation and the Mamadawerre Sandstone (Lally and Bajwah, 2006).

In the South Alligator Valley Mineral Field all major deposits are within the northwest-trending Rockhole–El Sherana–Palette Fault system and were formed in dilational zones at fault bends or intersections (Valenta, 1991).

A similar structural control is described for uranium deposits in the Rum Jungle Mineral Field. Four uranium deposits and the Browns basemetal deposit lie along a northeast-trending shear zone located on the northern limb of a northeast-trending asymmetric syncline (Ahmad et al., 2006). At the Rum Jungle Creek South deposit, the uranium ore body is located within the hinge zone of a northwest-trending doubly-plunging syncline in proximity to a northwest-trending steep fault (Ahmad et al., 2006). There is limited information on uranium prospects in the Hayes Creek Uranium Field, but the main uranium prospects appear to be located within a structural zone defined by the northeast-trending Hayes Creek and Bella Rose faults (Thundelarra Exploration, 2010).

2.7.2. Mobile and/or in situ reductant

All major host rocks of uranium deposits in the PCO are enriched in carbonaceous material (graphite), which is interpreted as being the main reducing agent for uranium-bearing hydrothermal fluids (Kyser and Cuney, 2009). However, a genetic link between basement graphite and uranium deposits is not clear and has been questioned by many researchers (Cuney, 2005). Graphite has not been reported in the host sequence at the Nabarlek deposit (Polito et al., 2004). In the Athabasca

Basin significant uranium deposits are hosted by geological units which do not contain graphite (Jefferson et al., 2007). An additional problem with graphite functioning as a reductant is the relatively low reactivity of graphite at temperatures below 300 °C (French, 1966; Frost, 1979).

In the absence of graphite in the host rock (as at the Nabarlek deposit), Fe^{+2}-bearing silicates, especially Fe-chlorite, can be good reductants. A reaction between relatively oxidised uranium-bearing fluids with Fe-chlorites can liberate Fe^{+2} to reduce the fluid. The evidence of such a reaction may be found in the presence of Mg-chlorite and of illite in the inner alteration halo proximal to ore zones.

At the Nabarlek deposit, the outer alteration halo extends as far as 1 km from the Nabarlek Fault and is dominated by chlorite and sericite. In this zone, biotite, muscovite and hornblende in the schists are partially-to-completely replaced by Fe-chlorite and minor fine-grained sericite, which also replaces plagioclase. The inner alteration halo comprises illite, hematite, and Fe-chlorite, but completely lacks quartz. Finely disseminated hematite, making up to 20% of the assemblage, is the distinguishing feature of this zone. The abundance of illite increases toward the ore zone. Within the ore zone, illite locally forms a massive monomineralic rock. The deposit also contains post-ore chloritic alteration, which crosscuts the uraninite–illite–hematite assemblage (Polito et al., 2004).

At the Jabiluka deposit, the outer and inner alteration halos are mineralogically similar, but the content of chlorite and illite/sericite increases in the inner halo. Within the mineralised areas, multiple generations of chlorite and sericite occur with and/or without quartz, uraninite and hematite (Polito et al., 2005a, 2005b).

Radioelement-rich bitumen, occurring in both Archean granites and the Paleoproterozoic metasedimentary rocks, has been reported in the Rum Jungle Mineral Field (McCready et al., 2003). Landais (1996) reported similar carbon isotope compositions between barren bitumen (U < 500 ppm) and graphite in metasediments below the unconformity with the Athabasca Basin and suggested that this bitumen could have formed due to hydrogenation of carbon. A similar model is proposed for the bitumen in the Rum Jungle Mineral Field, where hydrogenation is thought to be related to the fluids which caused sericitic alteration of organic-rich metasediments of the Whites Formation (McCready et al., 2003). It is not clear if bitumen generated by hydrogenation of organic material has played a role in reducing uranium-bearing diagenetic fluids, but such a possibility cannot be ruled out. However, according to Jefferson et al. (2007), it is unlikely that hydrocarbons were involved in the reduction of uranium-bearing fluids because of the sluggishness of the reaction at temperatures below 400 °C, and also because bitumen observed in many deposits is paragenetically post-uraninite. For 'Egress-style' mineral deposits (mineralisation located in the sandstone above the unconformity), it is possible that reaction of fluids with graphite and sulphides in the basement rocks could have produced mobile reductants, such as H_2S, N_2, H_2 and CH_4, capable of causing reduction of uranium-bearing fluids (Jefferson et al., 2007; Pascal, 2014; Potter, 2014).

2.8. Age and relative timing of mineralisation

Results of geochronological studies of major uranium deposits have been summarised by Lally and Bajwah (2006). Some of the more cited ages for uranium deposits in the PCO are shown in Table 2. The oldest age of ca. 2000 Ma for the Whites East deposit in the Rum Jungle Mineral Field is probably not correct as discussed by von Pechmann (1992). The other ages lying between ca. 1740 (Ranger) Ma and ca. 1600 Ma (Coronation Hill; Table 2.) are interpreted by Kyser and Cuney (2009 and reference therein) to suggest that mineralisation was closely related to the diagenesis of sediments of the Katherine River Group.

A four-step plateau $^{40}Ar/^{39}Ar$ age of illite from an aquitard in the lower Kombolgie Subgroup (sampled near the Jabiluka deposit) of 1798 ± 13 Ma is interpreted as the age of the earliest diagenetic event in the sandstones (Polito et al., 2005a, 2005b). This earliest phase of diagenesis is represented in the sandstone by the formation of hematite and of syn-compaction quartz overgrowth on detrital quartz grains. The diagenetic silicification greatly reduced the porosity of the sandstones and converted them into basin-scale aquitards (Polito et al., 2005a, 2005b; Kyser and Cuney, 2009). An ion probe U–Pb dating of low-Th monazite in an assemblage of hydrothermal mica and Fe-rich chlorite from an alteration zone at the Ranger 1 No 3 ore body yielded an age of 1800 ± 9 Ma. Mercadier et al. (2013a, 2013b) interpret this age to represent an important hydrothermal event at the Ranger 1 deposit possibly related to the tectonothermal activity of the Shoobridge Event at ~1.8 Ga in the PCO, and suggest that this pre-ore alteration and tectonism could have been a key factor in localising later unconformity-related uranium mineralisation. However, it is possible that this age (1.8 Ga) may also represent an event representing incursion of the diagenetic fluid (earliest phase) into the basement rocks. The Kombolgie Subgroup unconformably overlies the Nabarlek Granite (dated to have been emplaced at 1818 ± 8 Ma; Worden et al., 2008), providing the maximum age of deposition of the sediments. This and the 1798 ± 13 Ma age of the earliest phase of diagenesis suggest that the sedimentation of the Kombolgie Subgroup could have started between ca. 1820 Ma and 1800 Ma.

Peak diagenesis in the Kombolgie Subgroup began with the dissolution of detrital feldspar, smectitic clays, quartz overgrowths and detrital quartz grains in fluvial sediments (Polito et al., 2005a, 2005b). Illite was the principal diagenetic mineral formed in this phase. It was replaced by variable amounts of chlorite. A plateau $^{40}Ar/^{39}Ar$ age of illite of 1747 ± 9 Ma, formed in a diagenetic aquifer, is interpreted as the age of peak diagenesis (Polito et al., 2005a, 2005b). This event is indistinguishable from the ~1745 Ma Wonga Event in the Mount Isa Basin (Murphy

Table 2
Ages of unconformity-related uranium deposits in the Pine Creek Orogen.

Deposit	Domain	Age	Error	Comment	Reference
Kylie	Central	1627	45	Whole rock U–Pb age of uraninite from upper intercept of concordia	1
Adelaide River	Central	701	190	LA-HR-ICPMS age of uraninite. Upper intercept of the concordia	1
El Sherana	Central	1600		Whole rock U–Pb age of uraninite. Upper intercept of concordia; La-HR-ICPMS of uraninite gives 1573 ± 160 Ma	1, 3
Coronation Hill	Central	1607	26	LA-ICPMS dating of uraninite	4
Koongarra	Central	870		Whole rock U–Pb age of uraninite from upper intercept of concordia	5
Palette	Central	841	94	LA-HR-ICPMS age of uraninite. Upper intercept of the concordia	2
Ranger	Nimbuwah	1737	20	Whole rock U–Pb date of ore. Upper intercept of concordia	6
Jabiluka	Nimbuwah	1680	17	LA-HR-ICPMS age of uraninite. Ar/Ar age of illite in the sandstone gives 1683 ± 11 Ma. Resetting at 1302 ± 37 Ma, 1191 ± 27 Ma and 802 ± 57 Ma	7
Nabarlek	Nimbuwah	1642	33	LA-HR-ICPMS age of uraninite. Ar/Ar age of illite in the sandstone gives 1683 ± 11 Ma. Resetting at ca. 1360 Ma, ca. 1100 Ma, and ca. 900 Ma	8

1: Pechmann (1992); 2: Chipley et al. (2007); 3: Greenhalgh and Jeffery (1959); 4: Orth et al. (2014); 5: Hills and Richards (1976); 6: Ludwig et al. (1987); 7: Polito et al. (2005a, 2005b) 8: Polito et al. (2004).

et al., 2011) and the mid-Tawallah inversion event in the Southern McArthur Basin (Ferenczi and Sweet, 2004; Bull and Rogers, 1996). What is more important is that the whole-rock U–Pb dating of uraninite from the Ranger deposits gives an age of 1737 ± 22 Ma (Ludwig et al., 1987). Thus it is possible that the formation of uranium mineralisation at the Ranger deposit was closely related to the fluids released during peak diagenesis of the Kombolgie Subgroup, triggered by the mid-Tawallah inversion event. These events overlap with the age of intrusion of Oenpelli Dolerite (1723 ± 6 Ma; cited in Worden et al., 2008) in the Kombolgie Subgroup, which could have provided an additional thermal trigger for the movement of ore forming fluids.

The $^{207}Pb/^{206}Pb$ ages of 1679 ± 17 Ma and 1685 ± 17 Ma, obtained by LA-ICPMS dating of uraninite from the Jabiluka deposit have been interpreted to suggest that uranium mineralisation began to form at this deposit at ca. 1680 ± 17 Ma (Polito et al., 2005a, 2005b). The oldest of these ages are close to an $^{40}Ar/^{39}Ar$ age of 1683 ± 11 Ma from a illite sampled above the deposit and to many $^{40}Ar/^{39}Ar$ ages from illite obtained from diagenetic aquifers in the Kombolgie Subgroup (Kyser et al., 2000), suggesting that the formation of Jabiluka deposit may be related to diagenetic fluids released from the aquifers around that time (Polito et al., 2005a, 2005b).

The $^{207}Pb/^{206}Pb$ age of 1642 ± 33 Ma age (LA-ICPMS dating) of a highly reflective homogenous grain of uraninite from the Nabarlek deposit provides a good estimate of the age when uranium mineralisation began to form at this deposit (Polito et al., 2004). This age is comparable to the 1616 ± 50 Ma Sm–Nd age reported by Maas (1989). The age of initial uraninite precipitation at the Nabarlek deposit appears to coincide with two bends on the Australian apparent polar wander path at 1650 Ma and 1640 Ma, which according to Polito et al. (2004) represent the timing of tectonic events in the region that could have also caused reactivation of the Nabarlek Fault.

A U–Pb analysis of uraninite at the Kylie deposit in the Rum Jungle Mineral Field yielded an age of 1627 ± 45 Ma (Table 2; Pechmann, 1992). This age is close to the 1642 ± 33 Ma chemical age of uraninite at the Nabarlek deposit (Polito et al., 2004). The diagenetic history of the Depot Creek Sandstone in the Rum Jungle Mineral Field is unknown and hence, at this stage, it cannot be directly linked to the uranium deposition age at Nabarlek. McCready et al. (2004) note that uranium minerals at the Browns deposit (Rum Jungle Mineral Field), are observed either in association with secondary digenite-chalcocite minerals or within postmetamorphic organic material. According to them no genetic link exists between uranium and basemetal mineralisation at this deposit. A Pb–Pb model age of galena at the Browns deposit constrains the age of basemetal mineralisation at ca. 1690 Ma (Jaireth, 2011a, 2011b). If the basemetal mineralisation at the Browns deposit and unconformity-related uranium mineralisation at the Kylie deposit were formed from similar diagenetic fluids expelled during the diagenesis of Depot Creek Sandstone, the age of uranium mineralisation in the Rum Jungle Mineral Field could be close to ca. 1690 Ma, an age similar to the age of uranium mineralisation at the Jabiluka deposit.

Geochronological studies at uranium deposits in the South Alligator Valley Mineral Field yield a much wider spectrum of ages. In a recent study, LA-ICPMS U–Pb dating of uraninite from high-grade uranium core samples gave an age of 1607 ± 27 Ma (Orth et al., 2014). At the El Sherana deposit in the same uranium field, the upper intercept of the U–Pb concordia of uraninite gave ages of 1600 Ma (Greenhalgh and Jeffery, 1959). Chipley et al. (2007) reported an LA-ICPMS age of 1573 ± 160 Ma for uraninite from the same deposit. However, Chipley et al. (2007) reported a much younger LA-ICPMS age (841 ± 94 Ma) for uraninite from the nearby Palette deposit. At this stage, it is not clear if uranium deposits in the South Alligator Valley Mineral Field represent two different episodes of mineralisation (Paleoproterozoic and Neoproterozoic) or if the Neoproterozoic ages (between ca. 850 Ma and 700 Ma), so often reported from uranium deposits in PCO, represent remobilisation of older uranium and/or isotopic resetting of ages.

Both $^{40}Ar/^{39}Ar$ analysis of alteration and diagenetic minerals and U–Pb analysis of uraninite at various deposits in the PCO consistently show resetting of ages at ca. 1300 Ma, ca. 1190 Ma, and ca. 800 Ma, which can be related to several proximal and distal thermal events, such as the intrusion of Maningkorrir/Mudginberri phonolitic dykes and the Derim Derim Dolerite between 1370 Ma and 1316 Ma, the Grenville Orogeny at ca. 1140 Ma and the breakup of Rodinia between 1000 Ma and 750 Ma (Polito et al., 2005a, 2005b).

2.9. Preservation

In the PCO, the Katherine River and Tolmer group sediments overlying the unconformity have been preserved only in and near a few basement-hosted deposits (see Section 2.2). The thickness of the McArthur Basin rocks (Katherine River Group) increases in the eastern and south-eastern parts of the PCO, but no deposits (either sandstone- or basement-hosted) have yet been found in the area. More targeted exploration is required to assess the fertility of this region. However, the absence of sandstone-hosted ('Egress-style') uranium deposits in the PCO may be, in part, related to partial or full erosion of the Katherine River Group (which includes the Kombolgie Subgroup) in some areas.

The Tolmer Group, which was deposited in the Central and Litchfield domains (western part of the PCO), is thought to be correlative of the Katherine River Group (Needham, 1988). Sedimentation of the Tolmer Group occurred in the Birrindudu Basin resulting from N–S directed extension (Calvert Extension; de Vries et al., 2008). However, recent SHRIMP U–Pb data on detrital zircon from the Depot Creek Sandstone (Tolmer Group) provide a maximum age of deposition of 1837 ± 15 Ma, which is quite similar to the maximum deposition ages obtained from the Kombolgie Subgroup (Carson et al., 2011), suggesting that the Tolmer Group may also be related to the Leichhardt Extension. Limited SHRIMP U–Pb studies of detrital zircon show that the sediments of both the Kombolgie Subgroup in the Nimbuwah Domain and of the Depot Creek Sandstone (Tolmer Group) in the Litchfield Domain may have been derived from local Archean and Paleoproterozoic rocks (Carson et al., 2011). The pre-erosional extent of the Katherine River and Tolmer Group rocks in the PCO has not been estimated. However, limited palaeocurrent measurements in the sandstones suggest that these rocks could have covered a much larger area (Jaireth, 2011a, 2011b).

2.10. Kintyre deposit

Although mineralisation at the Kintyre deposit in the Paterson Orogen is located at the unconformity between Paleoproterozoic rocks of the Rudall Complex and Neoproterozoic rocks of the Throssell Range Group, there is still some uncertainty regarding its genesis (McKay and Miezitis, 2001). This is because, unlike other unconformity-related deposits in the PCO and the Athabasca Basin in Canada, the Yeneena Basin sediments overlying the unconformity were deformed during the Paterson Orogeny (ca. 650 Ma). This deformation also affected the unconformity, as well as uranium mineralisation.

The Neoproterozoic Kintyre deposit is hosted by Paleo- to Mesoproterozoic carbonaceous metasedimentary rocks of the Yandagooge Formation (Rudall Complex) adjacent to the unconformity with the Neoproterozoic Coolbro Sandstone (Throssell Range Group) of the Yeneena Basin (Fig. 12).

The deposit is located ~2 km northeast of a northwest striking thrust fault mapped by Hickman and Clarke (1993). The mineralised veins are hosted by chlorite–quartz schist, chlorite–carbonate–quartz schist and chloritic and garnetiferous quartzite (Jackson and Andrew, 1990), which form a stratigraphic unit that is structurally overlain by dolomite and underlain by biotite–graphite schist.

The host succession is folded by a recumbent (Bagas, 2004) fold with a shallowly dipping axial plane, which appears to be refolded by an asymmetric regional fold. The uraniferous veins tend to be concentrated in the hinges of regional folds and have an orientation sub-parallel to

the axial planes (Fig. 12). Northwest striking faults, parallel to the axial planes of the asymmetric regional fold, separate the ore lenses (Bagas, 2004).

Although the host unit contains a wide variety of rock types, the more competent siliceous chloritic and garnetiferous quartzite preferentially hosts the uraniferous veins (Root and Robertson, 1994). The host rocks are extensively chloritised, with primary garnet totally altered to chlorite near mineralised zones. Other alteration minerals include carbonate and martite (hematite), which replaced magnetite. The pre-ore magnetite ± carbonate ± Fe-chlorite alteration is overprinted by syn-mineralisation alteration of Mg-chlorite ± carbonate with weak to moderate silicification (Large et al., 2014).

The veins are dominated by a chlorite–carbonate assemblage, with carbonate minerals including dolomite, ankerite and calcite. Colloform pitchblende is the dominant ore mineral, with minor bismuthinite, chalcopyrite, bornite and galena, and trace native bismuth and gold. Platinum-group elements have also been noted with gold, which has a geochemical association with copper and bismuth (Jackson and Andrew, 1990).

The coarse-grained arkosic sediments of the Coolbro Sandstone were formed in a fluvial–deltaic environment (Large et al., 2014). Geochronological data constrain deposition of sediments in the Yeneena Basin to between ca. 910 Ma, the age of the youngest detrital zircon in the basal Coolbro Formation (Bagas and Nelson, 2007), and ca. 830 Ma, the age of intermediate to mafic rocks that intrude the lower part of the basin (D. Maidment, unpublished data). These constraints are compatible with a Pb–Pb isochron age for carbonate rocks of the Isdell Formation (stratigraphic equivalent of the Throssell Range

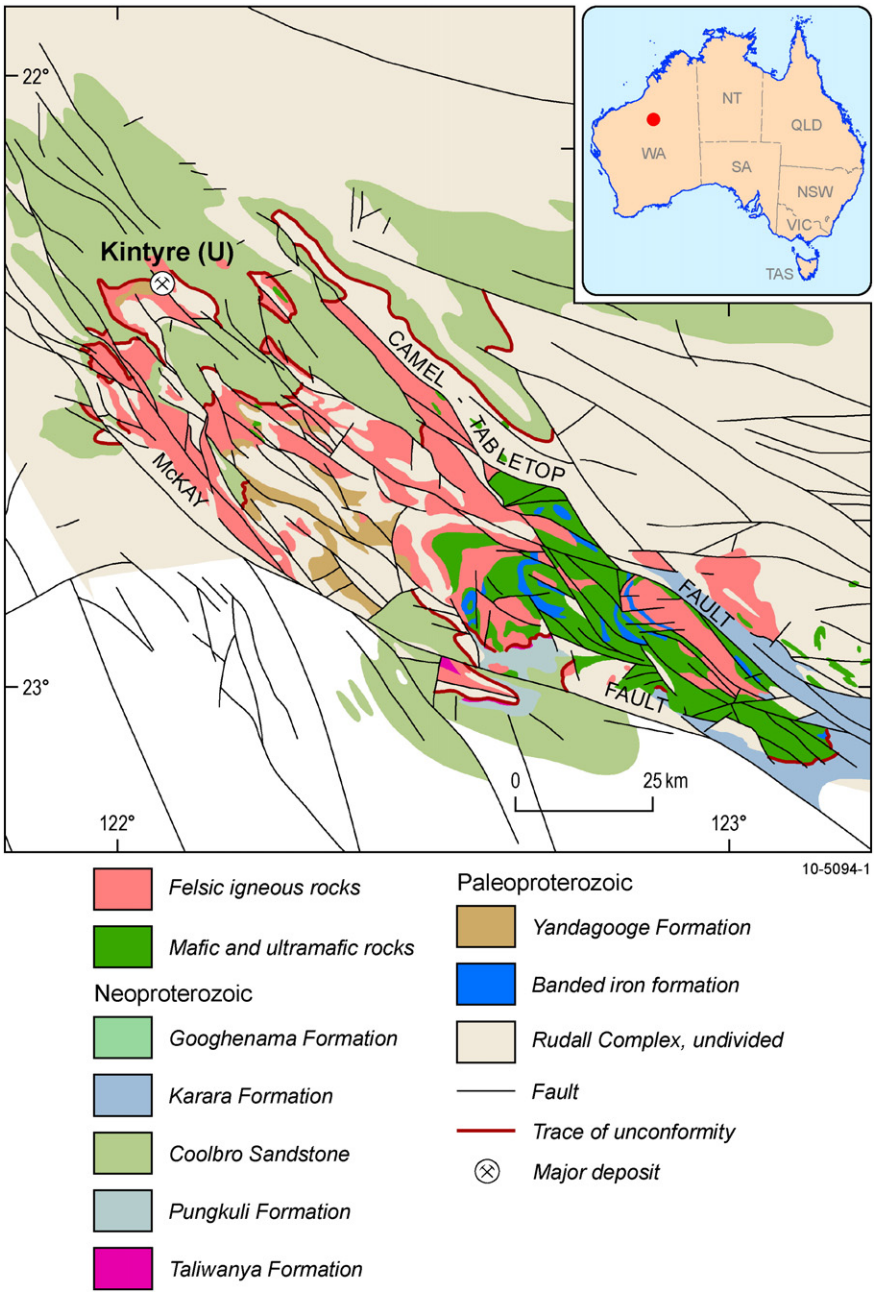

Fig. 11. Geological map of the Paterson region showing the Kintyre uranium deposit and the extensions of the potentially mineralised Paleoproterozoic–Neoproterozoic unconformity. Modified after Liu and Jaireth (2010).

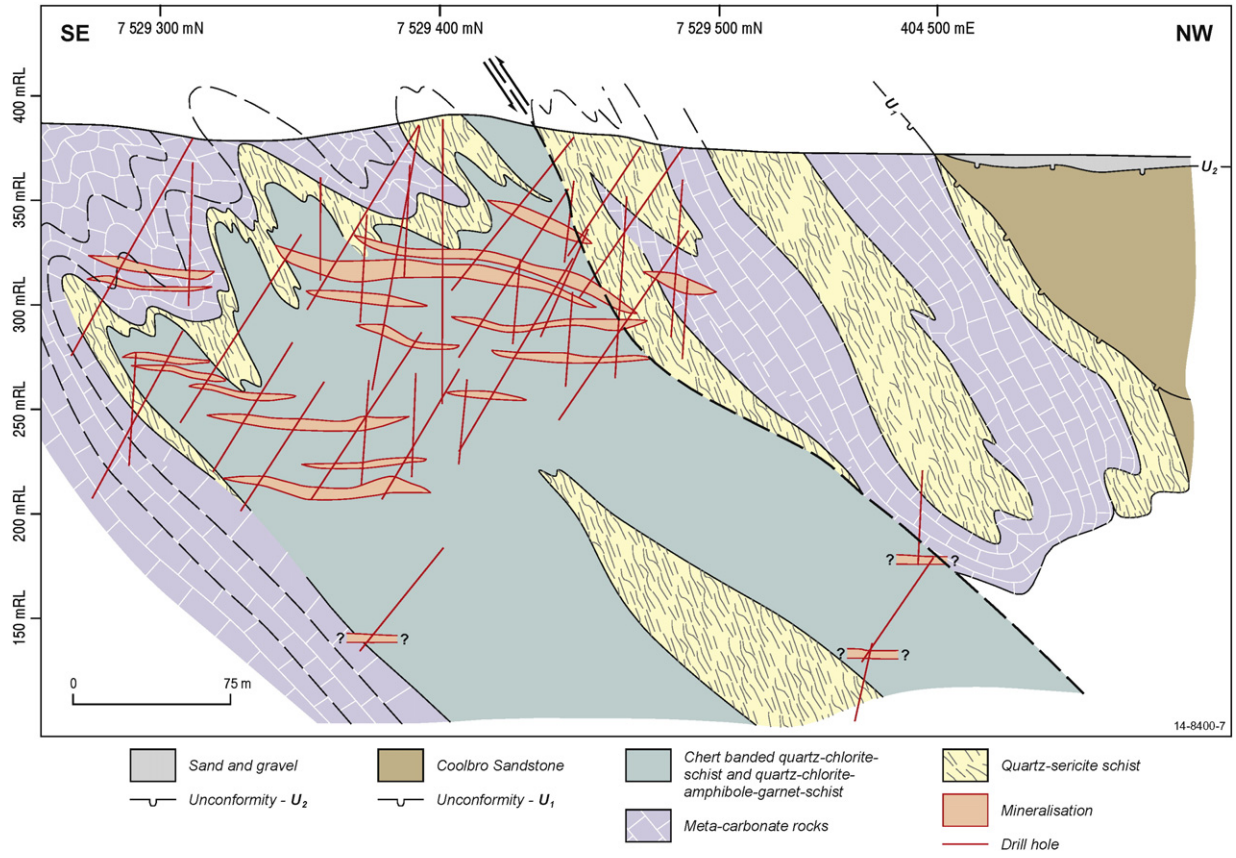

Fig. 12. Geological cross section, Kintyre deposit.
Modified after Dorling et al. (2011).

Group) of ca. 860 Ma, which is interpreted as a diagenetic age (Maas, R. and Huston, D.L., unpublished data). Electron Probe Micro-analyser (EPMA) U–Th–Pb chemical dating of uraninite yielded an age of 837 + 35/− 31 Ma, suggesting that the initial uranium mineralisation occurred during or after the latest period of sedimentation in the Yeneena Basin, and could have been formed from diagenetic fluids released during diagenesis at ca. 860 Ma (Cross et al., 2011). The chemical age for the Kintyre uraninite is in good agreement with an inferred age for the deposit of ca. 845 Ma (R Maas, unpublished data, Sm–Nd isotope data cited in Huston et al., 2010).

Critical features of unconformity-related uranium mineral system discussed in the above section are summarised in Table 3.

3. Sandstone-hosted uranium mineral systems

The known sandstone-hosted uranium deposits in Australia are located in Paleozoic and Cenozoic basins. Within Cenozoic basins, mineralisation is hosted by Paleogene and Neogene sandstones (Table 4). Around 46% of uranium resources are in the Cenozoic Callabonna Sub-basin (Lake Eyre Basin) in South Australia (SA). The geology of some major deposits and prospects is described in McKay and Miezitis (2001), Lally and Bajwah (2006) and Curtis et al. (1990). Descriptions of individual uranium deposits are available in Fidler et al. (1990; Bigrlyi deposit), Borshoff and Faris (1990; Angela and Pamela deposits), Brunt (1990; Oobagooma deposit), and Mulga Rock (Fulwood and Barwick, 1990; Mulga Rock deposit). The geology of multi-element mineralisation at the Anderson prospect (Mulga Rock) was described in a recent paper by Douglas et al. (2011).

Sandstone-hosted uranium deposits in Australia are generally of small to medium tonnage (<~40 million tonnes) with low to medium grades (<~0.28 wt.% U; Fig. 6).

This review is largely based on the geology of sandstone-hosted deposits in the Lake Frome region in South Australia.

3.1. Geological setting

An important feature of the Lake Frome region is its embayment shape, in which the mineralized sedimentary basins are surrounded on three sides by Proterozoic rocks enriched in uranium (Fig. 13). Similar shapes are observed in many mineralized areas such as the Chu-Sarysu and Syrdariya basins in Kazakhstan (Dahlkamp, 2009; Jaireth et al., 2008). This particular shape of the embayment has resulted from the prolonged geological history of the region.

In the south, the basins in the Lake Frome area are bounded by Paleoproterozoic metasedimentary rocks of the Willyama Supergroup (southern Curnamona Province). The north–south trending Benagerie Ridge runs through the central part of the Lake Frome area and is entirely concealed by Phanerozoic rocks (Fabris et al., 2010). In the west, the Lake Frome area is flanked by the Proterozoic Mount Painter and Mount Babbage inliers (northern Curnamona Province), part of the northern Flinders Ranges.

The Lake Frome area is filled with sediments of three major basins: the Arrowie Basin (Cambrian); the Eromanga Basin (Early Jurassic to Late Cretaceous); and, the Callabonna Sub-basin (part of the Lake Eyre Basin, Cenozoic). The gross architecture of the Lake Frome area is largely determined by the structures generated during a series of Neoproterozoic to Cenozoic basin-forming and orogenic events, which created new structures and reactivated older structures (Teasdale et al., 2001).

The Cenozoic Callabonna Sub-basin, which hosts more than 90% of known mineralisation in the Lake Frome region, resulted from a west–northwest to east–southeast compression during which major faults

Table 3
Critical features of unconformity-related uranium mineral systems.

Deposit types (including synonyms)
- Ingress-type, Egress-type; Unconformity-contact (fracture-bound, clay-bound) Proterozoic subunconformity-epimetamorphic.

Geological setting
- Unconformity between Paleoproterozoic metasedimentary rocks and Paleo- to Mesoproterozoic sandstones.
- Basement of Archean domes/inliers flanked by Paleoproterozoic metasedimentary rocks.
- Metasediments formed in shallow marine conditions rather than turbiditic, containing units enriched in carbonaceous material.
- Thick (>~5 km) package of Paleoproterozoic to Mesoproterozoic sediments containing sandstones formed in braided, fluvial conditions. Flat-lying at the time of mineralisation (often foreland basin). Often partially or fully eroded.

Source (fluid, metal, energy)

Fluids
- Fluid 1: Diagenesis of sedimentary package overlying the unconformity. High salinity fluids formed from dissolution of evaporite.
- Fluid 2: Evolved from Fluid 1 after reacting with metasedimentary rocks below the unconformity. High salinity but higher Ca/Na ratio than Fluid 1.
- Fluid 3: Hydrocarbon-rich fluid formed from hydrogenation of carbonaceous material in metasediments below the unconformity.

Uranium
- Uranium-bearing detrital minerals in the sandstone such as monazite and/or zircon. Felsic volcanics or their fragments in the sandstone package overlying the unconformity.
- Uraninite and or uranium-bearing minerals (monazite and/or zircon) in the granites and/or metasediments below the unconformity.
- 'Palaeoregolith', often altered by reaction with fluids.

Energy drivers of fluid-flow
- Compaction of sediments in the basin.
- Heat (radiothermal, produced by granitoids and Archean rocks in the basement, and by intrusives emplaced in the sandstone overlying the unconformity). Compaction and heat can initiate basin-scale convection of fluid.
- Tectonic activity along faults and shear zone.

Fluid pathway
- Unconformity surface with or without palaeoregolith.
- Aquifers in the sandstone package overlying the unconformity.
- Faults and breccia zones leading up to and/or cutting the unconformity.

Trap

Physical
- Unconformity surface.
- Breccia zones and faults (in the basement rocks and in the sandstones overlying the unconformity).

Chemical
- Carbonaceous (graphite) rocks below the unconformity.
- Rocks with Fe^{+2}-bearing silicates such as chlorite either below the unconformity or in the sandstone package above the unconformity.
- Reduced fluid resulting from the hydrogenation of carbonaceous material.
- Presence of calcareous rocks (affecting pH, not fully clear).

Age and relative timing of mineralisation
- Proterozoic age important for world-class deposits.
- Mineralisation closely linked with the timing of diagenesis in the sandstone package overlying the unconformity.
- Mineralisation linked to compression during basin inversion in the basin overlying unconformity.
- During extension diagenetic fluids accumulate, during inversion the fluids move outward from the basin.

Preservation
- Presence of sandstone above the unconformity indicates high probability of preservation of unconformity type uranium deposits.
- Most known deposits show remnants of the sandstone package overlying unconformity in close proximity.

Main references
Dahlkamp (2009), Kyser and Cuney (2009), Jefferson et al. (2007), Lally and Bajwah (2006), McKay and Miezitis (2001)

surrounding the Lake Frome region were reactivated (Teasdale et al., 2001). The uplift generated minor foreland flexure in the area, and up to 800 m of clastic sediments were deposited in the subsequent basin.

A number of major faults have been mapped in the Beverley area (Fig. 14). Most of them are long-lived structures with a prolonged history of reactivation. These faults are considered to have played important roles in determining the present-day and palaeo-architecture of the Lake Frome region. Some of the important faults include the:

- Paralana Fault: a shallow west-dipping thrust fault, which has been active since the Neoproterozoic (as a normal fault) and controlled deposition of Adelaidean sediments. The Paralana Hot Springs are controlled by this fault;
- Wooltana Range Front Fault (also known as the Vidnee Yarta Fault Zone near Beverley): a west-dipping thrust fault with splays mapped along the eastern scarp of the Flinders Ranges near Wooltana Station;
- Wooltana Fault: a steep west-dipping fault outlined on gravity data (Heathgate Resources, 2007);
- Four Mile Fault: northeast–southwest trending fault running west of the Four Mile East and Four Mile West deposits; and,
- Poontana Fault Zone: a west-dipping thrust fault with splays identified in drilling through variations in the thickness of the Cenozoic units on either side.

Movements along the Paralana Fault could have controlled palaeorelief in the Lake Frome region, especially near the Beverley and Four Mile deposits. Drill hole and geophysical data suggest that a block defined by the Wooltana Fault in the west and the Poontana Fault Zone in the east forms an upthrusted inlier (the Poontana Inlier) separating the Beverley deposit to its east and the Four Mile deposits to its west (Fig. 13).

The Paralana Embayment to the west of the Poontana Inlier hosts the Paralana Trough, which contains several important uranium deposits and prospects (Heathgate Resources, 2008; McConachy, 2009). Movements along the Poontana Fault Zone could have also controlled the shape of the Miocene palaeovalley which hosts the Beverley deposit (Heathgate Resources, 2007).

The role of deformation and exhumation is also significant for the sandstone-hosted uranium deposits in the Amadeus (Angela and Pamela deposits) and Ngalia basins (Bigryli and Walbiri deposits). In these basins deformation during the 450 Ma–300 Ma Alice Springs Orogeny caused exhumation of the basement, which became a major source of detritus for the host rocks, the Late Devonian to Carboniferous Mount Eclipse Sandstone (Ngalia Basin) and the Brewer Conglomerate (Amadeus Basin). The source rocks of both these units included uranium-rich granites of the Arunta Region. The subsequent peak of deformation terminated deposition in the basins and initiated major thrusting and associated thrust-related folding in and near the basins (Edgoose, 2013a, 2003b).

3.2. Source of uranium

The Callabonna Sub-basin is surrounded on three sides by felsic rocks enriched in uranium (Fig. 13 and Table 5). The average uranium concentration in the rocks varies between 4 and 100 ppm, but some felsic rocks in the Mount Painter and Mount Babbage inliers contain up to ~400 ppm uranium. However, the total uranium in rocks only provides a rough guide to their potential as a source of uranium. A more important guide is the concentration of readily leachable uranium in the rocks. The most leachable uranium minerals in rocks are uranium oxides (such as uraninite). In their absence uranium-bearing rock-forming and accessory minerals (e.g. allanite, monazite, xenotime, zircon, epidote and apatite) become important. Limited experimental leaching studies indicate that in minerals such as allanite, 80% of uranium can be leachable (Larsen and Gottfried, 1961).

The Yerilla Granite (4 to 270 ppm uranium) in the Mount Babbage Inlier, the Mount Neill Granite (3 to 380 ppm uranium) and the Hot Springs Gneiss (7 to 427 ppm uranium) in the Mount Painter Inlier are possibly the best sources of leachable uranium (Table 5 and Fig. 15). The medium- to coarse-grained Yerilla Granite contains uraninite and other uranium-bearing accessory minerals including monazite,

Table 4
Sandstone-hosted uranium deposits and prospects. Geological information sourced from Mckay and Miezitis (2001) and Roach et al. (2014). Resource data from Geoscience Australia's OZMIN database.

Name	State	Basin	Host unit	Host age	Deposit type	Ore (Mt)	Grade (%)	U (t)
Angela	NT	Amadeus	Undandita Member	Late Devonian to Late Carboniferous	Roll front	10.7	0.111	11886
Bennett Well	WA	Carnarvon	Birdrong Sandstone and Yarraloola Conglomerate	Cretaceous	Basal channel	26.7	0.023	6047
Beverley	SA	Callabonna Sub-basin	Namba Formation	Neogene	Basal channel	12	0.153	18317
Bigrlyi	NT	Ngalia	Mount Eclipse Sandstone	Late Devonian to Late Carboniferous	Roll front	7.5	0.109	8160
Billeroo	SA	Callabonna Sub-basin	Eyre Formation	Paleogene	Basal channel	12	0.025	3053
Blackbush	SA	Pirie Basin	Kanaka Beds	Paleogene	Roll front	41.5	0.025	10170
Carley Bore	WA	Carnarvon Basin	Birdrong Sandstone and Yarraloola Conglomerate	Cretaceous	Basal channel	13.8	0.033	4564
East Kalkaroo	SA	Callabonna Sub-basin	Eyre Formation	Paleogene	Basal channel	1.2	0.063	753
Four Mile East	SA	Callabonna Sub-basin	Eyre Formation	Paleogene	Roll front	4.1	0.263	10778
Four Mile West	SA	Callabonna Sub-basin	Bulldog Shale	Cretaceous	Roll front	5.6	0.282	15766
Goulds Dam	SA	Callabonna Sub-basin	Eyre Formation	Paleogene	Basal channel	17.6	0.031	5373
Honeymoon	SA	Callabonna Sub-basin	Eyre Formation	Paleogene	Basal channel	1.2	0.204	2442
Kalkaroo	SA	Callabonna Sub-basin	Eyre Formation	Paleogene	Basal channel			
Manyingee	WA	Carnarvon Basin	Birdrong Sandstone and Yarraloola Conglomerate	Cretaceous	Basal channel	13.8	0.072	9933
MacDonnell Creek	SA	Callabonna Sub-basin	Eyre Formation	Paleogene	Basal channel			
Mulga Rock	WA	Narnoo Basin	Narnoo Sequence	Paleogene	Basal channel	57.3	0.042	24295
Oban	SA	Callabonna Sub-basin	Eyre Formation	Paleogene	Basal channel	8.2	0.022	1808
Oobagooma	WA	Canning Basin (Yampi Embayment)	Yampi Sandstone	Early Carboniferous	Roll front	8.2	0.102	8333
Pannikin	SA	Callabonna Sub-basin	Eyre Formation	Paleogene	Roll front			
Pepegoona	SA	Callabonna Sub-basin	Eyre Formation	Paleogene	Roll front	2.2	0.153	3358
Walbiri	NT	Ngalia Basin	Mount Eclipse Sandstone	Paleozoic	Roll front	0.42	0.137	582
Warrior	SA	Eucla basin	Pidinga Formation	Paleogene	Basal channel	11.8	0.034	4003
Yagdlin	SA	Callabonna Sub-basin	Namba Formation	Neogene	Basal channel			
Yarramba	SA	Callabonna Sub-basin	Eyre Formation	Paleogene	Basal channel			

NT = Northern Territory; SA = South Australia; WA = Western Australia.
http://lws-60603:3000/deposits/mineral_system.csv?commodity=U.
http://lws-60603:3000/deposits/mineral_system.csv?commodity=U3O8.

allanite, zircon, apatite and xenotime. It also shows extreme enrichment in rare earth elements (REE), niobium, fluorine, thorium, yttrium and tungsten (Teale, 1993). Wülser (2009) document intensive metasomatic overprints (Proterozoic and Ordovician in age) and the gneissic varieties contain allanite-rich lenses. Uraninite and uranothorite inclusions are present in zircons. The uranium-enriched Hot Springs Gneiss also shows a similar metasomatic overprint and a red metasomatic gneiss contains brannerite veins, allanite-rich zones and thorite mineralisation (Wülser, 2009). Elburg et al. (2001) explained the presence of trondhjemite, gneiss and schist within the Mount Neill Granite as the result of metasomatic alteration. It is possible that some samples containing up to 300 ppm uranium represent metasomatically altered A-type Mount Neill Granite.

In addition to uranium-enriched felsic rocks, the Mount Painter Inlier also contains a variety of magmatic-hydrothermal and epithermal prospects and deposits of uranium such as Mount Gee, Mount Painter and Radium Ridge. Uraninite is the major ore mineral in these prospects. Other uranium-bearing minerals are brannerite, gummite, xenotime, allanite, apatite, titanite, ilmenite, monazite, samarskite, torbernite, uranophane and zircon (Coats and Blissett, 1971; Drexel and Major, 1990).

More than 80% of uranium resources in the Lake Frome region are located in close proximity to the Mount Painter and Mount Babbage inliers. A number of deposits (Four Mile East, Four Mile West, Pepegoona and Pannikin) are also within the Paralana Embayment (Paralana Trough), to the south-western end of which are located not only uranium-enriched felsic rocks (Hot Springs Gneiss, Mount Neill Granite), but also many uraninite-bearing deposits and prospects. The relatively high uranium endowment of this area could thus be associated with the presence of source rocks containing leachable uranium.

Uranium-enriched felsic rocks (average concentration of uranium varying between 2 ppm and 28 ppm) are also present in the southern Lake Frome region (Table 5 and Fig. 16). However, the maximum uranium concentration is less than 110 ppm (Table 5). The most enriched of these is the Mindamereeka Trondhjemite (Crocker Well Suite) with up to 110 ppm uranium and the Honeymoon Granite with up to 40 ppm uranium. The trondhjemites have undergone intensive sodic metasomatism and grade into alaskites, which occur as dykes, veins and pegmatitic bodies (Wade, 2011). The Honeymoon Granite, which is spatially associated with the Honeymoon and East Kalkaroo uranium deposits, contains up to 40 ppm uranium. The Honeymoon Granite shows locally intensive potassic alteration (Fricke and Reid, 2009). Unaltered Honeymoon Granite, however, has an abundance of uranium-bearing minerals (uranium oxides in pyrite, monazite, allanite, zircon and apatite).

The felsic rocks in the Olary Domain are associated with a number of orthomagmatic and hydrothermal uranium deposits (Crocker Well, Mount Victoria and Radium Hill). The main uranium mineral at the Crocker Well deposit is thorian brannerite. Davidite is the main uranium mineral at the Mount Victoria and Radium Hill deposits. These deposits also contain monazite and xenotime and minor uranophane (McKay and Miezitis, 2001). Thus, although uranium-bearing minerals are present in felsic rocks and deposits in this part of the Lake Frome region, they are not as readily leachable as uraninite, which is far more abundant in the Mount Painter and Mount Babbage inliers.

Felsic rocks at the margins of Amadeus and Ngalia basins contain up to 32 ppm and 55 ppm uranium respectively (OZCHEM database). These felsic rocks also host several uranium-bearing pegmatite bodies and fluorapatite veins, which contain good sources of leachable uranium. Additionally, uranium may have been sourced from detrital minerals in the sandstones. Schmid et al. (2012) have documented removal of uranium and vanadium from clasts containing detrital roscoelite in the sandstone unit at the Bigrlyi deposit.

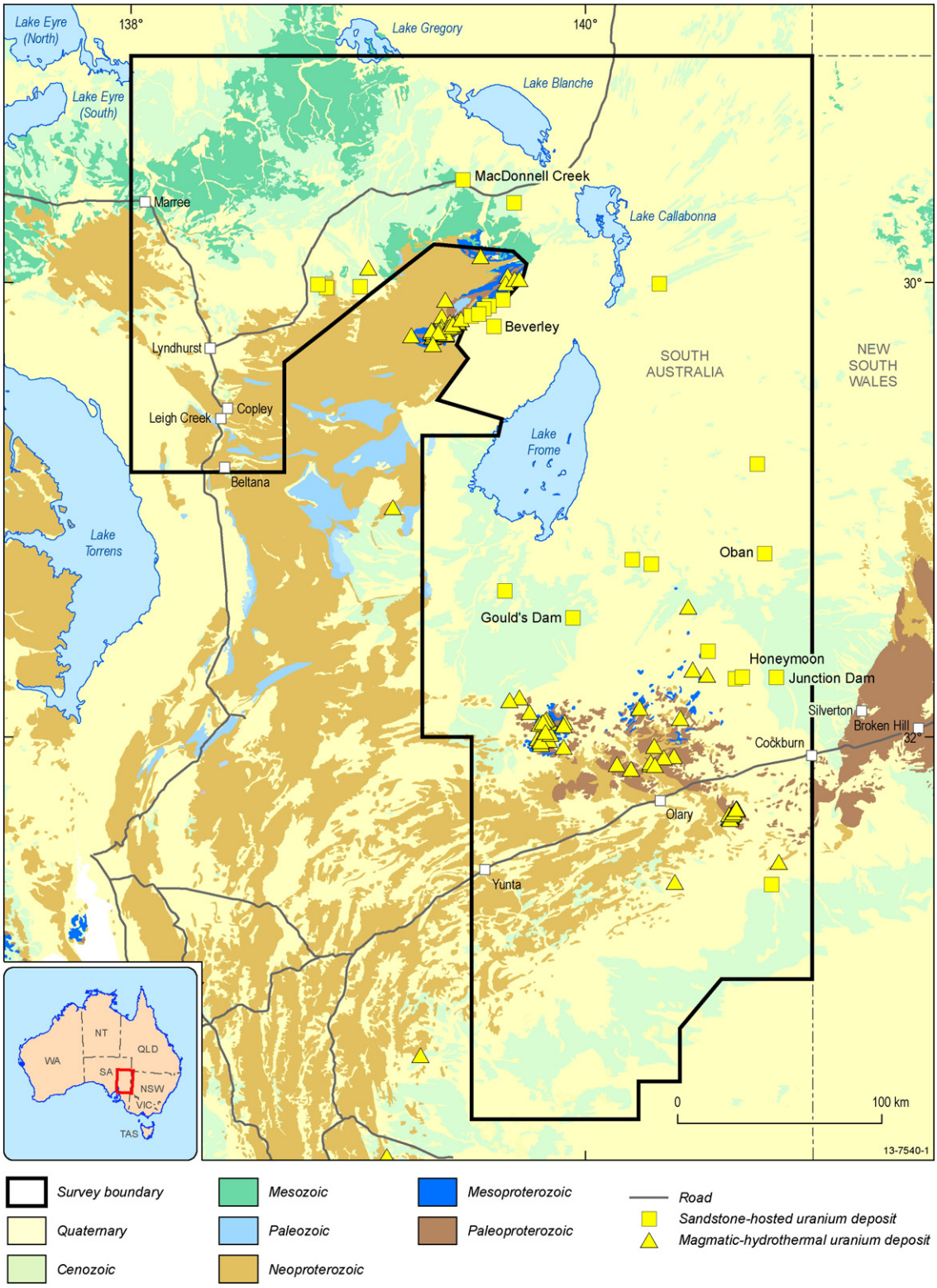

Fig. 13. Location map of the Lake Frome region (Callabonna Sub-basin) showing the boundary of the Frome AEM Survey, main uranium occurrences and principal bedrock units. From Roach et al. (2014).

3.3. Source and nature of fluids

In sandstone-hosted uranium systems, uranium is transported in oxidised groundwaters of variable salinity and pH. The salinity of present-day groundwaters in the Eyre Formation in the Callabonna Sub-basin is higher (10000 ppm to 20000 ppm TDS or Total Dissolved Salt; Southern Cross Resources, 2000) than those in the sandstone aquifers in the Shirley Basin, Wyoming (170 to 1250 ppm TDS; Harshman,

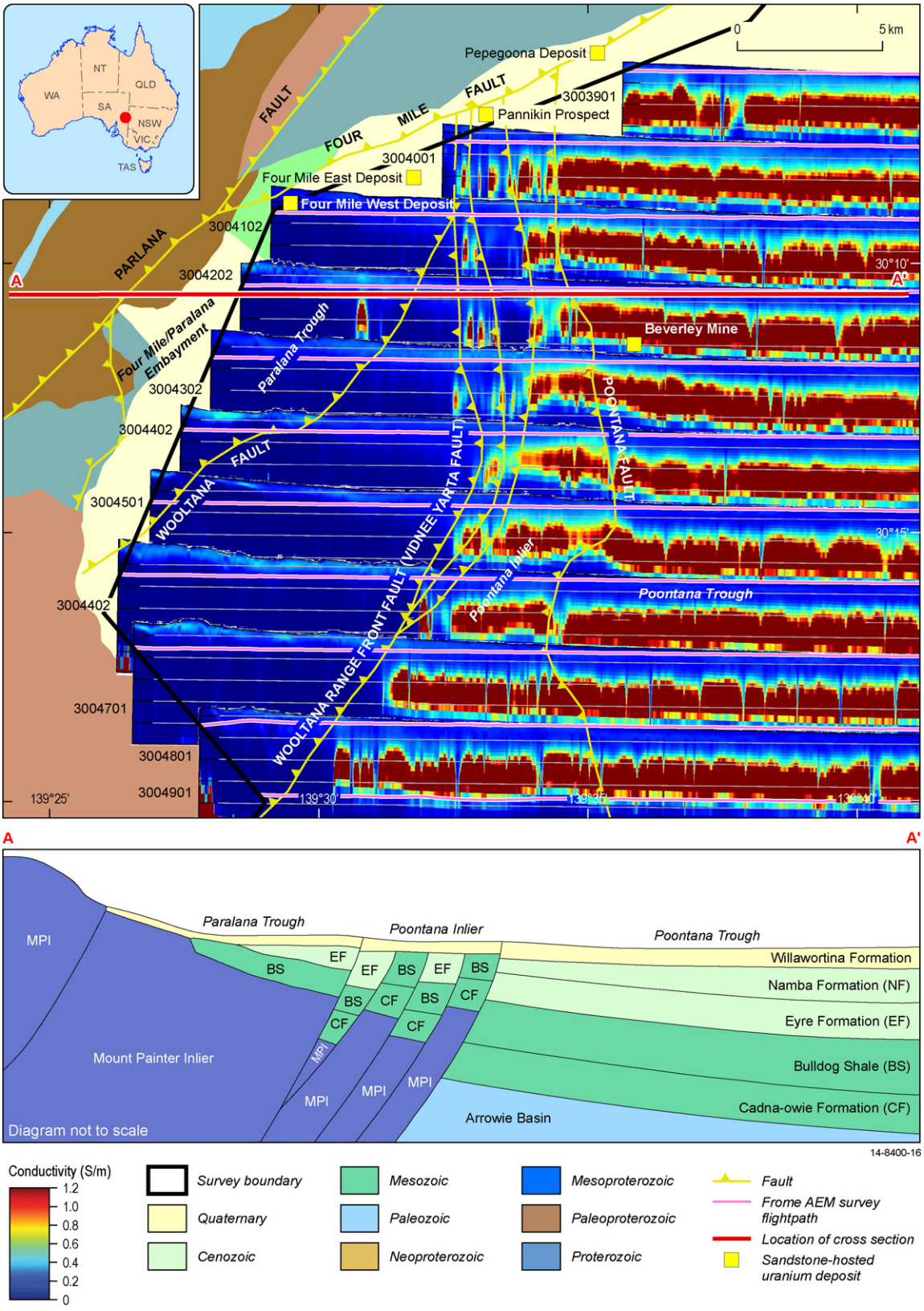

Fig. 14. A geological model highlighting major fault lines and the association of fault blocks and uranium mineralization around the Beverley area, eastern Lake Frome region. Airborne electromagnetic conductivity sections overlying the geological base map highlight resistive Proterozoic (Mount Painter Inlier) basement in the west and conductive basement, generally salt water-saturated Paleocene–Eocene Eyre Formation and Cretaceous Bulldog Shale, in the east, separated by the uplifted block of the Poontana Inlier.
From Roach et al. (2014).

Table 5
Ages, U and Th contents of U-bearing granites and felsic rocks within the Curnamona Province, including the Ninnerie Supersuite.
Modified after Roach et al. (2014).

Domain	Province	Name	Age Ma	± Ma	Description	Comments	Reference	U RANGE PPM	U AVG PPM	Th AVG PPM	Th/U AVG	main U-bearing minerals
Moolawatana	Mount Babbage	Terrapinna Granite	1560	3	Coarse-grained granite	Magmatic crystallisation age	Fraser and Neumann (2010)	2–28	8	49	7	Zircon, monazite, allanite
		Yerilla Granite	1558	4	Coarse-grained granite	Magmatic crystallisation age	Fraser and Neumann (2010)	4–270	107	355	4.1	Uraninite in pyrite, monazite, xenotime, allanite, zircon, apatite, titanite (Ti-silicate)
		Wattleowie Granite	1563	3	Biotite granite with biotite foliation	Magmatic crystallisation age	Fraser and Neumann (2010)	2–50	7	35	6.2	Zircon, monazite
		Petermorra Volcanics	1560	3	Deformed felsic extrusive, volcaniclastics, epiclastic sandstone	Magmatic crystallisation age	Teale and Flint (1993)	2–34	10	32	6.4	Zircon, monazite, allanite
		White Well Granite	1556	4	Biotite granite	Age assumed to be similar to the Yerilla Granite	Sheard et al. (1992)	4–16	9	45	7.1	Zircon, monazite
		Prospect Hill Granite	1556	4	Biotite granite	Age assumed to be similar to the Yerilla Granite	Sheard et al. (1992)	–	96	207	2.2	Monazite, allanite
	Mount Painter	Mount Neill Granite, Coulthard Suite	1585	3	Coarse-grained granite	Magmatic crystallisation age	Fraser and Neumann (2010)	3–380	30	90	5.4	Zircon, titanite, epidote
		Box Bore Granite, Coulthard Suite	1583	2	Coarse-grained granite, gneissic fabric	Magmatic crystallisation age	Fraser and Neumann (2010)	5–79	41	130	4.2	Allanite, monazite, zircon
Moolawatana	Mount Painter	Nooldoonooldoona Trondhjemite, Coulthard Suite	1575	3	Na-altered Mount Neill Granite	Magmatic age of precursor Mount Neill Granite. Age of metasomatism ?1555 Ma	Elburg et al. (2001)		17	67	3.9	Zircon, monazite
		Hot Springs Gneiss	1582	6	Coarse-grained augen granitic gneiss with strong biotite foliation	Magmatic crystallisation age	Fraser and Neumann (2010)	7–427	98	330	3.4	Zircon, trace allanite
		Hodgkinson Granodiorite (4 Mile Creek)	1552	4	Medium-grained granodiorite	Magmatic crystallisation age	Fraser and Neumann (2010)		5	12	2.4	Zircon
		Pepegoona Porphyry	1576	2	Rhyolitic and rhyodacitic metavolcanics	Magmatic crystallisation age	Teale and Flint (1993)	13–34	24	72	3.2	Zircon, titanite, ?xenotime
		British Empire Granite	455	8	Granite batholith with S-type intruded by I-type	Pb–Pb stepwise leaching of garnet	McLaren et al. (2002), Elburg et al. (2003)	2–32	11	9	1.2	Zircon, monazite, xenotime
		Radium Creek Metamorphics (Lower metasediments)	1600	8	Quartzofeldspathic gneiss with bands of heavy minerals	Maximum age of deposition	Fraser and Neumann (2010)	2–5	3	16	5.7	Zircon
		Radium Creek Metamorphics (Upper metasediments)	1591	6	Quartzofeldspathic gneiss with bands of heavy minerals	Maximum age of deposition	Fraser and Neumann (2010)	2–5	3	16	5.7	Zircon
		Golden Pole Granite	1560		Even textured brick red coloured granite	Maximum interpreted age of emplacement	Wall (1995)	1–10	4	36	18	Zircon, xenotime
Moolawatana	Olary	Honeymoon Granite	1541	59	Quartz–plagioclase–alkali feldspar–muscovite–biotite granite	Concordia intercept age	Jagodzinski and Fricke (2010)	13.5–40	27.6	8.4	0.4	Monazite, zircon, apatite, allanite, titanite, U-oxides in pyrite
		Lake Charles Diorite	1585	195	Medium- to fine-grained hornblende-bearing	Magmatic crystallisation age	Fanning (1995)	0.4–6	2.4	7	3.1	Zircon

(continued on next page)

Table 5 (*continued*)

Domain	Province	Name	Age Ma	± Ma	Description	Comments	Reference	U RANGE PPM	U AVG PPM	Th AVG PPM	Th/U AVG	main U-bearing minerals
					diorites to granodiorites							
Olary		Mindamereeka Trondhjemite, Crocker Well Suite	1580	21	White, coarse-grained and massive leucocratic phlogopite trondhjemites grading into alaskites, characterised by opalescent blue quartz	Magmatic crystallisation age	Ludwig and Cooper (1984)	0.9–110	13.9	72.8	13	Allanite, monazite, zircon, thorian brannerite
		Mount Victoria Granite, Crocker Well Suite	1579	2	Biotite-only to biotite–muscovite-bearing monzogranites	Magmatic crystallisation age	Ludwig and Cooper (1984)	0.5-19.1	7	60.3	11.6	Zircon, monazite
		Bimbowrie Suite	1581	3	Medium- to coarse-grained muscovite–biotite granite characterised by large K-feldspar phenocrysts	Magmatic crystallisation age	Jagodzinski and Fricke (2010)	0.1–35	8.5	38.1	6.3	Zircon
		Windamerta Diorite	1581	6	Biotite and hornblende diorites, granodiorites and tonalites	Magmatic crystallisation age	Fanning (pers. Comm..)	0.3–51	9.2	47.2	2.3	Zircon, allanite
Olary		Billeroo Intrusive Complex	1610 to 1550	–	Alkaline magmatic rocks including syenite bodies, layered feldspathic ijolite phases and alkali lamprophyre dykes	Constrained by tectonic fabrics formed during the third phase of the Olarian Orogeny and layer parallel fabrics within Willyama Supergroup clasts	Rutherford (2006)	0.3–7.2	2.3	9.6	4.7	No information
Mudguard		Finlay Dam Rhyolite, Benagerie Volcanic Suite	1587	6	Porphyritic rhyolitic volcanic rocks	Magmatic crystallisation age	Jagodzinski and Fricke (2010)	11–21	16.2	55.1	3.4	Zircon
		Lake Elder Rhyodacite, Benagerie Volcanic Suite	~1585	–	Porphyritic rhyodacitic volcanic rocks	–	Wade (2011)	8.5–18.5	11.8	35.8	3	Zircon
		Benagerie 1, Benagerie Volcanic Suite	–	–	Extensively altered porphyritic amygdaloidal trachytes occurring as a series of flows with scoriaceous tops	–	Wade (2011)	8–18	10.8	37.6	3.6	No information
		Ninnerie 1, Ninnerie Supersuite	1550–1590	–	Fine-grained basalt	Max depositional ages of overlying and underlying sediments	Fraser and Neumann (2010)	4–10.5	6.5	14.7	2.3	No information

1972) and Chu-Sarysu Basin, Kazakhstan (900 to 6000 ppm TDS; Fyodorov, 2001a, 2001b).

As coffinite is one of the main ore minerals in many deposits, the concentration of dissolved silica in groundwaters can be of critical importance. Unfortunately, the problem of thermodynamic stability of coffinite with respect to uraninite remains unresolved (Hemingway, 1982; Langmuir, 1978; Brookins, 1975). This is because of two important reasons; the variation in the composition of natural coffinite, $U(SiO_4)1 - x(OH)_4x$, and uraninite, $UO_{2-2.6}$, and the uncertainty in the thermodynamic data for coffinite. Calculations suggest that in order to form coffinite, the concentration of dissolved silica in groundwater should exceed its average measured concentration of about 17 ppm (Langmuir, 1978). As this concentration is less than the equilibrium concentration of dissolved silica, estimated from the thermodynamic data of coffinite, it is argued that the natural coffinite coexisting with quartz and uraninite is in a metastable state (Hemingway, 1982). Langmuir (1978) noted that waters in the Grants mineral belt in New Mexico, where both uraninite and coffinite coexist, contain 19 ppm to 120 ppm dissolved silica, and suggested that coffinite became stable relative to uraninite at intermediate levels of dissolved silica; that is, at a level above those in average groundwater but below the saturation with amorphous silica. Thus formation of coffinite requires groundwaters supersaturated with respect to quartz. A number of different processes have been discussed to explain silica supersaturation. They include: the suppression of silica precipitation (Goldhaber et al., 1987); the presence of organo-silica complexes (Bennett and Siegel, 1987); and, step-wise reduction of uranium from waters in the presence of silica gel (Hemingway, 1982).

The involvement of mobile reductants has been reported in many sandstone-hosted uranium deposits (see below for more detailed discussion). These reductants are either generated from hydrocarbon-bearing basins underlying sandstone-hosted uranium deposits, or from more proximal sources such as biogenic and non-biogenic H_2S produced from the interaction of groundwater with pyrite in the sandstone (Spirakis, 1996).

3.4. Fluid-flow pathways

Sandstone-hosted uranium deposits are formed by oxidised, uranium-bearing fluids flowing in permeable sandstones interbedded between relatively impermeable shaly sediments. In the Callabonna Sub-basin, the Paleocene to Eocene Eyre Formation sands, which host more than 90% of known mineralisation in the Lake Frome area, are highly permeable. The mature, fine- to coarse-grained, unconsolidated, carbonaceous, pyritic sands give a measured permeability of 5 m^2/day in the Four Mile East ore zone (Heathgate Resources, 2008). The overlying Late Oligocene to Miocene Namba Formation is characterised by an overall low permeability.

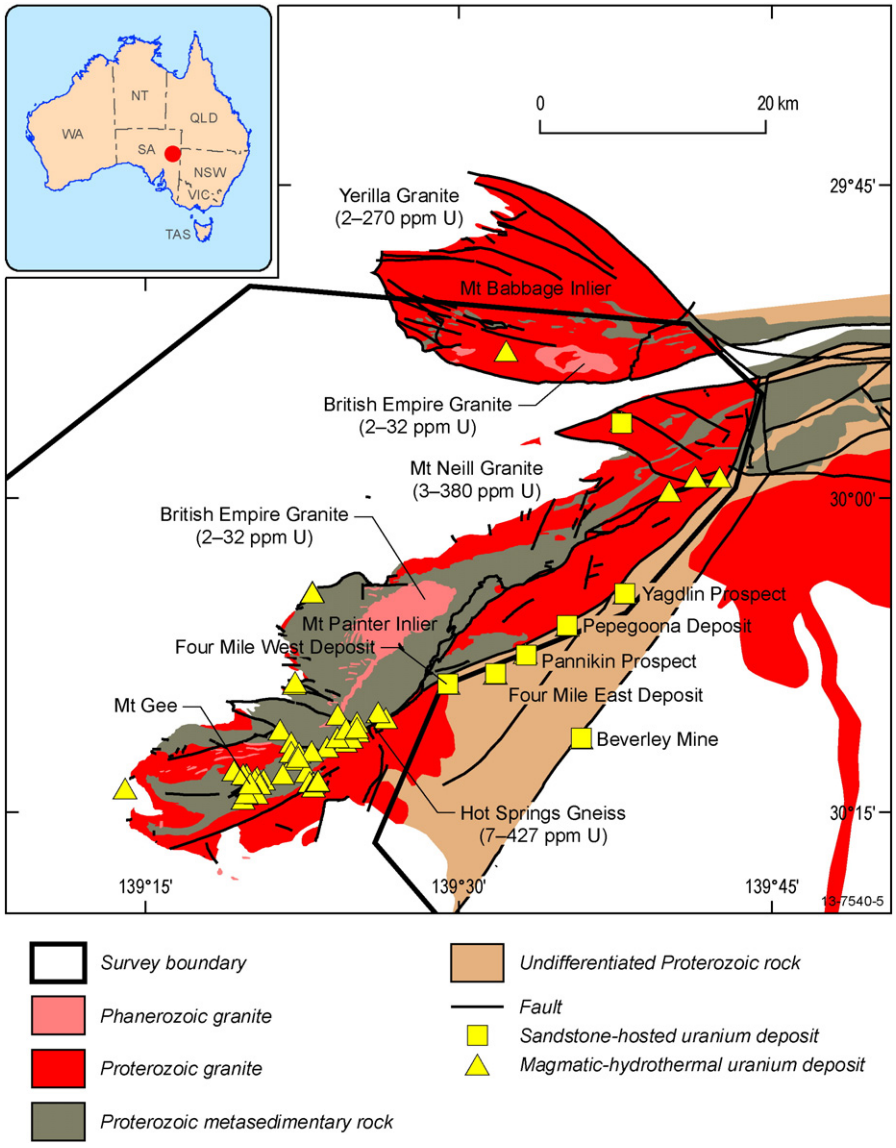

Fig. 15. Uranium source rocks in the Mount Painter and Mount Babbage inliers. Solid geology is modified from SARIG, 2014 (http://minerals.statedevelopment.sa.gov.au/sarighelp/home), with uranium concentration data from sources quoted in Table 5.
From Roach et al. (2014).

In the Namba Formation, the lenticular Beverley Sands, which host the Beverley Deposit, are interbedded between the Beverley Clay and the Alpha Mudstone. The Beverley Sands aquifer is made up of four units, of which the main mineralised sands have moderate permeability, whereas the two underlying sandy units are more permeable (Heathgate Resources, 2007).

An important factor in the formation of sandstone-hosted uranium systems is the direction of fluid-flow at the time of mineralisation. In many mineralised basins it is known to be different from the present-day fluid-flow direction (Sanford, 1992, 1994; Dzhakelov, 1993). In the southern part of the Lake Frome region mineralisation is located in the Paleocene to Eocene palaeovalley systems, which generally run northward from the uplifted parts of the Olary Domain (Alley, 1998). In the past, the Oban uranium deposit was shown as sitting in the Lake Charles Palaeovalley, which was previously interpreted running southeast to northwest (Hou et al., 2007a, 2007b), although the new palaeovalley map of South Australia now shows Oban as sitting in sediments emptying northeast from the Yarramba Palaeovalley (Hou et al., 2012). Eyre Formation sediments in the northern part of the Lake Frome region were deposited predominantly in alluvial fans (Alley, 1998), although some basal channel deposits may also be present to the north of the Mount Babbage Inlier. The top of the Eyre Formation in the Paralana Trough (Fig. 13), which hosts significant uranium deposits, slopes southwest to northeast. Present-day hydrogeological measurements in wells show that the present-day groundwater flow is from southwest to northeast (SKM, 2008). It is therefore possible that in the Eocene, when uranium deposits were formed, the groundwater also flowed in the same direction, linking the groundwaters with the source of leachable uranium. A similar scenario of north- to northeasterly fluid-flow was proposed by Skirrow et al. (2009).

The Beverley Palaeochannel represents a cyclic cut-and-fill (channel-in-channel) system and is filled with Beverley Sands (Namba Formation) incised into Alpha Mudstone (Namba Formation). It runs generally from northwest to southeast. Its shape is controlled by movements along the Poontana Fault Zone, which was active during deposition of the Beverley sequence and also after deposition of the Willawortina Formation (Heathgate Resources, 2008). If the fluid-flow during the formation of the Beverley deposit was also from northwest to southeast, it would link the fluids with the sources of leachable

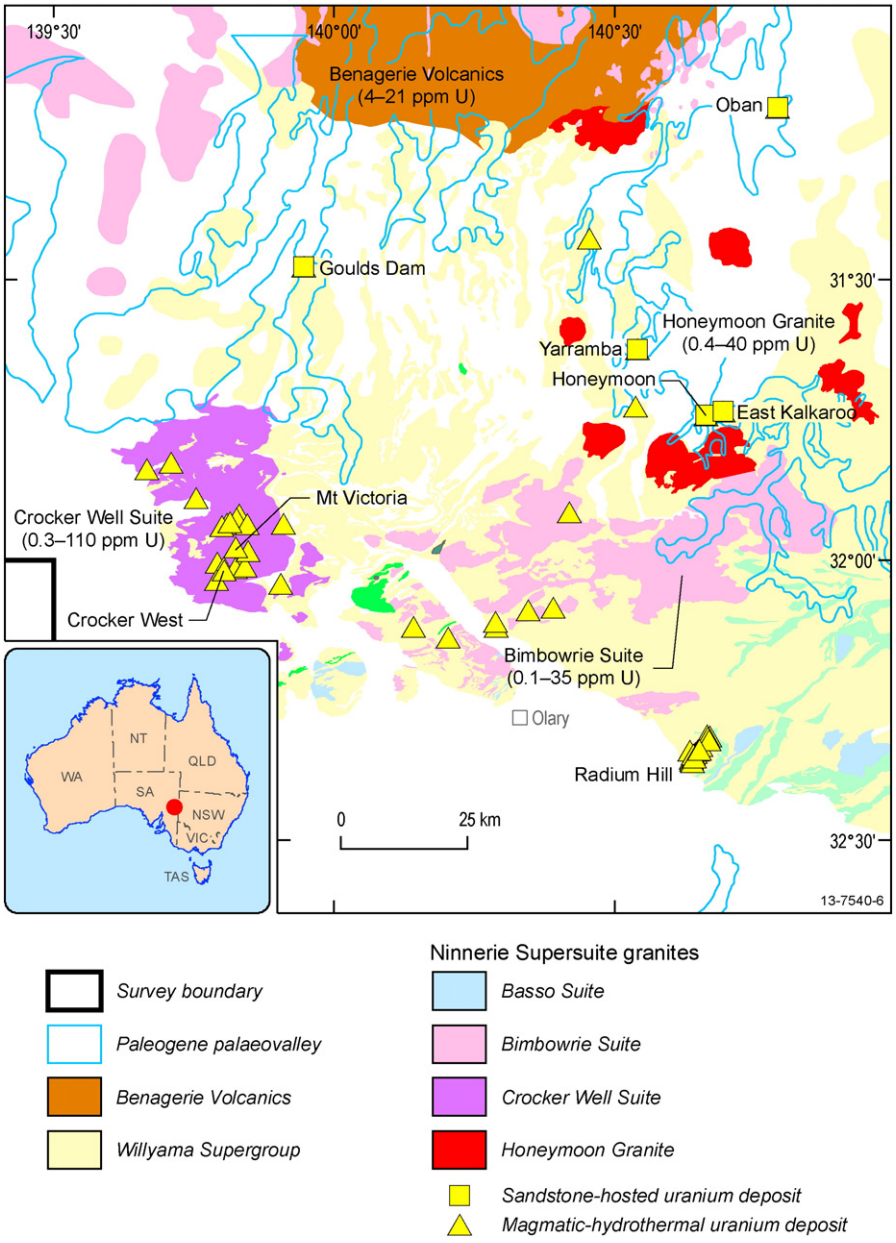

Fig. 16. Uranium source rocks in the Olary Domain, southern Lake Frome area. Solid geology is modified from SARIG, 2014 (http://minerals.statedevelopment.sa.gov.au/sarighelp/home), with uranium concentration data from sources quoted in Table 5. The map includes palaeovalley outlines from Hou et al. (2012). From Roach et al. (2014).

uranium in the northern Mount Painter and Mount Babbage inliers, rather than bringing fluids east across the hydrological barrier formed by the uplifted Poontana Inlier. It is important to note that while the dominant fluid flow directions are along the palaeovalleys, lateral fluid flow has been documented in many palaeovalley systems (Magee, 2009) and cannot be discounted in the Lake Frome region as a link between uranium sources and deposition sites.

3.5. Source of energy (energy drivers of fluid-flow)

In a single-fluid model of sandstone-hosted uranium systems (Jaireth et al., 2008) uranium is transported in oxidised shallow groundwater through sandstone aquifers. The flow of groundwater in this model is gravity driven and is controlled by hydrostatic head (created by relief) at the time when the uranium mineral system was established. The landscape evolution history in the Callabonna Subbasin outlined by Roach et al. (2014) and Skirrow et al. (2009) summarises important episodes of cooling/uplifting in the Lake Frome region. Of these, two episodes are considered critical as energy drivers of uranium systems:

1. Paleocene to Eocene (before ~55 Ma), caused either by the removal of ~1.5–2.0 km of rocks or by a decrease in geothermal gradient accompanied by minor erosion (Mitchell et al., 2002). The uplifted Mount Painter Inlier could have not only provided material for the Eyre Formation sediments, but also created the needed hydrostatic head to generate fluid flow in Mesozoic aquifers (such as the Algebuckina Sandstone and the Cadna-owie Formation).
2. Pliocene (before ~6–4 Ma), when the present day relief in the modern Flinders Ranges was formed from tectonic movement along major faults such as the Paralana Fault (Quigley et al., 2007). This episode is broadly related to the deposition of the Willawortina Formation, which unconformably overlies the Namba Formation that hosts the Beverley uranium deposit. The tectonic uplift in the Pliocene thus

created the needed hydrostatic head for fluids in the sandy aquifers of the Namba Formation.

A hiatus (~5 million years) in sedimentation is recorded between the Lower and Upper Eyre Formations in the southern Callabonna Sub-basin (Alley, 1998). A more prolonged hiatus (~15 million years) is also documented between the Upper Eyre Formation and the Namba Formation (Alley, 1998). Zircon provenance studies at Beverley, summarised in Roach et al. (2014), show that basal sediments of both the Eyre Formation and the Namba Formation were mostly derived from rocks in the Mount Painter Inlier, before becoming mixed with sediments from other sources in their upper parts, indicating that the provenance area (Mount Painter Inlier) was uplifted during the Middle Oligocene (before ~28 Ma; Fig. 17). This indicates the presence of a possible hydrostatic head necessary to drive fluids in the aquifers of the Eyre Formation.

A two-fluid model (Fig. 18; Jaireth et al., 2008), considered to be important for some sandstone-hosted uranium systems, cannot be ruled out for the Lake Frome region (see Michaelsen and Fabris, 2011 and Skirrow et al., 2009, for further discussion). In this model uranium precipitation is caused by interaction with mobile reductants (hydrocarbons and/or H_2S). Mobile reductants can be derived either from hydrocarbon accumulations in the Eromanga and Arrowie basins or from thermal degradation of organic material in the sediments. Reactivation of faults in the Lake Frome region can trigger movement of reductants from underlying basins. Hot fluids along the Paralana Fault (such as those occurring in the Paralana Hot Springs) can also cause reduction of uranium-bearing fluids in the aquifer. The principal driver of the Paralana Hot Springs is probably the thermal gradient created by the high heat flow zone in the Mount Painter Inlier. Apatite fission-track thermochronology studies near the Paralana Fault indicate that it created heating of >~100 °C in the area at ca. 20–25 Ma (Mitchell et al., 2002). This heating is capable of generating mobile reductants from the degradation of organic material from shales in various sedimentary rocks in the three basins, especially in the Eromanga Basin and Callabonna Sub-basin.

A tectonic driver of fluid-flow has also been suggested in the Amadeus (Angela and Pamela deposits) and Ngalia Basins (Bigryli and Walbiri deposits). The peak of deformation associated with the Alice Springs Orogeny (450 Ma–300 Ma), which initiated thrusting and folding in a near the basin, could have also triggered groundwater flow in the sandstone units hosting uranium deposits (Edgoose, 2013a, 2003b; Schmid et al., 2012).

3.6. Physical and chemical traps/sinks

The presence of redox fronts in uranium deposits shows that uranium deposition was caused predominantly by reduction of oxidised uranium-bearing fluids flowing in sandy aquifers. In most cases reduction occurs from reaction with an in situ reductant (organic material in the aquifer and/or in the shaly sediments underlying it). In recent years the role of mobile reductants (hydrocarbons and other associated gases, such as H_2S, CH_4, N_2 and H_2) has been documented in a number of sandstone-hosted uranium deposits outside Australia (Pechenkin, 2014; Jaireth et al., 2008; Huang et al., 2005). The role of H_2S as an effective reductant was demonstrated by Goldhaber et al. (1978) and Reynolds and Goldhaber (1978) in a number of roll-type uranium deposits in South Texas, where uranium mineralisation is hosted by organic-poor sandstone. H_2S can also be produced by sulphate-reducing bacteria, as demonstrated by Bonnetti et al. (2014a, 2014b) for uranium deposits located in the Erlian Basin, China. The process suggested by Bonnetti et al., 2014a, 2014b may be important for many other deposits, because the close spatial correlation between Fe–Ti oxides, uraninite and pyrite, documented at the Bayinwula deposit (Erlian Basin), is also seen in a number of other uranium deposits (Reynolds and Goldhaber, 1978; Schofield et al., 2009).

At the Bigryli deposits (Ngalia Basin), uranium minerals are closely associated with degraded vanadium-bearing roscoelite (Schmid et al., 2012), suggesting that V^{+3} in roscoelite may have acted as a reductant of uranium in oxidised waters. According to Schmid et al. (2012), uranium may also have been sourced from roscoelite.

In the Callabonna Sub-basin, the Eyre Formation is known be rich in organic material. In the Yarramba Palaeovalley, which hosts the Honeymoon deposit, it contains an average 0.3% organic material in the form of lignite, plant fragments and woody material (Bampton et al., 2001; Skidmore, 2005). The sediments are also locally enriched in pyrite (averaging 7%), estimated on the basis of sulphur analysis by Bampton et al. (2001).

The Beverley Sands in the Namba Formation do not contain organic material but the Alpha Mudstone underlying the sands is enriched in carbonaceous matter. The ore zones contain 0.05% to 0.5% organic carbon in grey sands and up to 2% in selected samples. The Alpha Mudstone has abundant plant fragments and large pieces of carbonised wood (Heathgate Resources, 2007). Michaelsen and Fabris (2014, 2011) have recently identified six organic facies, of which three are in the Eyre Formation and two are in the Namba Formation. Their "Namba Facies 1" is dominated by liptinite and contains abundant lamalginite and telaginite. The facies is developed at the base of the Namba Formation. Their "Namba Facies 2" is developed within mudstones and the humic material is considered to have undergone extensive transportation and oxidation. As the upper Namba Formation lacks effective (hydrogen-rich detrital organic) reductants, mobile reductants (hydrocarbon gases) could have been involved in the formation of the Beverley and other uranium deposits in the northern part of the Lake Frome region (Michaelsen and Fabris, 2011, 2014). The generation of hydrocarbons was facilitated by heat resulting from relatively high geothermal gradient in the area (Michaelsen and Fabris, 2014).

Sulphur isotope composition of framboidal pyrites in host rocks of Pepegoona and Pannikan deposits in the Lake Frome regions show that they are isotopically light with $\partial^{34}S$ values ranging between −43.8‰ and −18.3‰ (Ingham et al., 2014). These values are similar to the values reported from several other sandstone-hosted uranium deposits (Bonnetti et al., 2014a, 2014b; Northrop and Goldhaber, 1990; Goldhaber et al., 1983). The isotopically light sulphur isotopic composition is interpreted to indicate involvement of sulphate reducing bacteria in the generation of H_2S and formation of pyrite (Bonnetti et al., 2014a, 2014b; Northrop and Goldhaber, 1990; Goldhaber et al., 1983; Cheney and Jensen, 1965). Uranium mineralisation at the Bayinwula deposit in the Erlian Basin (NE China) is thought to have resulted form redox reactions caused by detrital organic material and biogenic sulphate reduction (Bonnetti et al., 2014a, 2014b).

Sandstones near redox zones in sandstone-hosted uranium deposits often contain calcite cement (Dong et al., 2005; Langen and Kidwell, 1961). Carbon isotope analysis of shows that the carbonate is isotopically light (average $\partial^{13}C = -1.5‰$ for dolomite in Henry Basin, Utah; Northrop and Goldhaber, 1990; and $\partial^{13}C = -6.8‰$ for calcite at the Qianjiadia deposit in Inner Mangolia; Dong et al., 2005) indicating that the source of carbon was organic produced by anaerobic bacteria. At the Qianjiadia deposit, Dong et al. (2005) do not rule out the possibility that carbonate was formed from the migration of oil and gas-bearing water. This carbonate is much lighter than the diagenetic carbonate (with average $\partial^{13}C = -0.87‰$) observed in the sandstone. Diagenetic carbonate is isotopically similar to sedimentary carbonates (Dong et al., 2005).

In a large number of sandstone-hosted uranium deposits, mineralisation is structurally controlled. The structural control has been more clearly demonstrated in deposits where mineralisation is thought to have occurred due to mixing of uranium-bearing oxidised waters with mobile reductants (e.g., Sun et al., 2009; Goldhaber et al., 1983). For example, mineralisation in the tectonic-lithologic type of sandstone-hosted uranium deposits (e.g. the Mikouloungou deposit the Franceville Basin, Gabon) is controlled by permeable fault zones

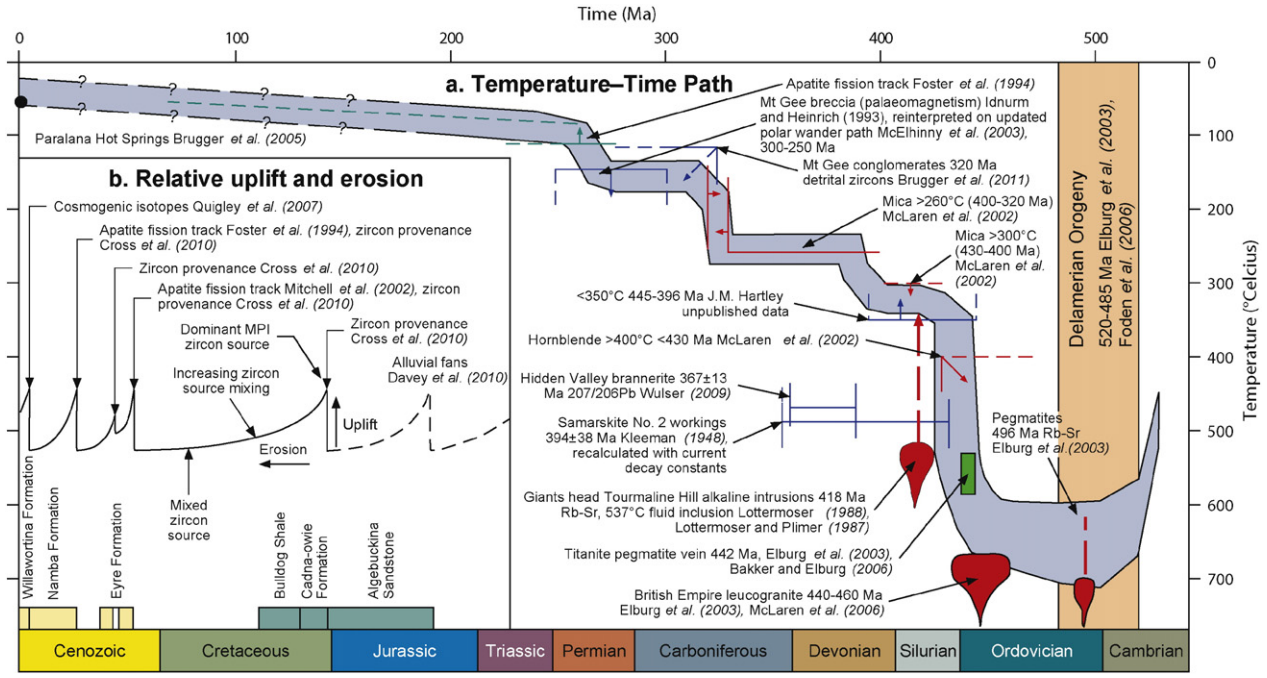

Fig. 17. Landscape evolution model for the Mount Painter Inlier. A (main diagram): Thermochronology, isotopic dating, palaeomagnetic dating and thermal history path modified from Wülser (2009). Figure includes data from Bakker and Elburg (2006), Brugger et al. (2005), Brugger et al. (2011a), Cross et al. (2010), Davey et al. (2010), Elburg et al. (2003), Foden et al. (2006), Foster et al. (1994), J. M. Hartley (pers. comm. to P.-A. Wülser, 2009), Idnurm and Heinrich (1993), Kleeman (1946), Lottermoser (1988), Lottermoser and Plimer (1987), McElhinny et al. (2003), McLaren et al. (2002), McLaren et al. (2006) and Wülser (2009). Box B: Relative uplift and erosion events interpreted using cosmogenic isotopic dating by Quigley et al. (2007), apatite fission-track dating by Foster et al. (1994) and Mitchell et al. (2002), zircon provenance studies by Cross et al. (2010) and regolith-landform mapping Davey et al. (2010).

extending into clastic sediments adjacent to the fault. A similar structural control has been speculated for world-class uranium deposits in the Chu-Sarysu basin in Kazakhstan (Aubakirov, 1998). In uranium deposits underlain by hydrocarbon basins, areas at the margins of the hydrocarbon cap-rocks and areas in proximity to tectonically active structures can function as important conduits of mobile reductants (Jaireth et al., 2008).

In basal channel deposits, mineralisation is controlled by the shape of palaeochannels. Mineralisation is often located in the basal scours (e.g. mineralisation in the Chinle Member, central Utah, USA, and in the Stráž deposit in the Czech Republic), bends (e.g. the Honeymoon and East Kalkaroo deposits), sites of confluences with tributaries (the Beverley, Goulds Dam and Oban deposits), and areas of channel-widening and bar-heads (Jaireth and Huston, 2010; Demko, 2003; Fiedler and Slezak, 1992). At this stage processes, which influence accumulation of uranium mineralisation at these sites, are not clear, but they may be related to the amount of organic material concentrated in the sediments. These sites may also exert control on the changes in the flow of groundwater in the channel sands.

3.7. Age and relative timing of mineralisation

Although it has been difficult to obtain accurate age data for uranium mineralisation in sandstone-hosted uranium deposits, available information suggests that most mineralised basins commonly witness more than one episode of mineralisation. For example, two episodes

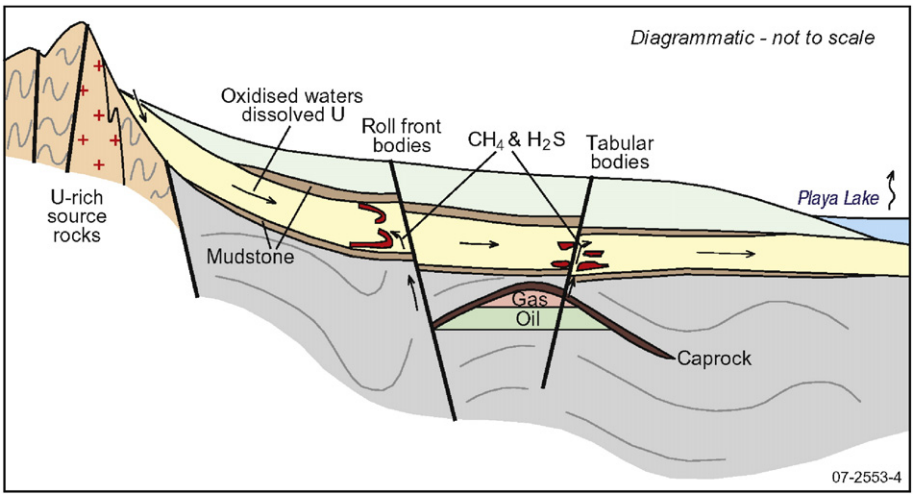

Fig. 18. Diagram showing a two-fluid uranium deposition model. Uranium is carried in oxidised groundwaters and is reduced by hydrocarbons and/or H_2S released from the underlying oil and/or gas field. Both roll-front and tabular ore bodies can result from the process. During ore deposition hydrocarbons are often oxidised to form carbonates.

of mineralisation are reported in the uranium deposits of the Grants Mineral Belt, New Mexico (Ludwig et al., 1984). The primary uranium ore is thought to have been formed (minimum age of mineralisation of ca. 130 Ma) early in the history of the host rock, whereas redistributed ore resulted from remobilisation of primary ore between ca. 3.3 Ma and 12.5 Ma. The whole-rock, Pb–Pb model ages in the Chu-Sarysu Basin in Kazakhstan suggest a more prolonged process of mineralisation spanning four stages (Mikhailov and Petrov, 1998): Late Cretaceous (mineralisation hosted in Jurassic sediments); Eocene (mineralisation in sediments of Late Cretaceous–Paleocene age); Late Oligocene–Middle Miocene (mineralisation in Jurassic, Cretaceous and Paleogene sediments); and Late Oligocene–Quaternary (remobilisation of mineralisation in all host sediments)

A similar episodic nature of mineralisation can also be deduced for uranium deposits in the Callabonna Sub-basin. Wulser et al. (2011) dated coffinite grains at the Beverley deposit. The grains were inhomogeneous and porous and the LA-ICPMS analysis showed the presence of high proportions of common lead, indicating that the grains were open to lead loss since their formation. Three intersepts on the concordia plot of Wulser et al. (2011) gave sub-concordant to concordant apparent ages between 6.7 Ma and 0.4 Ma. Uranium–lead (U–Pb) dating by LA-ICPMS of carnotite disseminated in the Beverley Sands (upper mineralisation zone), and also filling cracks within kaolinite and alunite in the Beverley Clay unit, gave concordant to sub-concordant ages between 5.5 Ma and 3.4 Ma (Wulser et al., 2011). The age data were interpreted to suggest that uranium mineralisation (coffinite and late-stage carnotite) at Beverley is of Pliocene age (6.7 Ma–3.4 Ma; Wulser et al., 2011).

The disequilibrium $^{234}U/^{238}U$ ratio in groundwaters in the Pepegoona deposit, however, suggests that uranium mineralisation has probably been deposited or remobilized within 1 Ma (Murphy et al., 2011, 2014).

Fig. 16 summarises evidence for the landscape evolution of the northern Flinders Ranges in terms of its temperature–time path and relative uplift history. The figure is developed from the temperature–time path (Box 'A') of Wülser (2009), which represents the Paleozoic to Mesozoic thermal history of the region until about 250 Ma using collated thermochronology, isotopic and palaeomagnetic data. The inset (Box 'A' in Fig. 16) shows a collation of data including regolith-landscape mapping, thermochronology and zircon provenance work undertaken around the Beverley uranium mine. The relative uplift history indicates that pulsatory uplift of the northern Flinders Ranges continued from 320 Ma as evidenced by the presence of alluvial fans around its flanks, mapped by Davey et al. (2010). Following this, thermochronology data correlate strongly with zircon provenance data from Beverley that indicate pulses of uplift and associated erosional stripping occurred before the commencement of deposition in the Cadna-owie Formation, the Eyre Formation (including a hiatus in deposition), the Namba Formation and the Willawortina Formation. The data serve to illustrate that the ancient Flinders Ranges have been sub-aerially exposed since at least 320 Ma, and have undergone pulsatory periods of uplift and erosion since then.

The history of landscape evolution in the Lake Frome region (Fig. 16) suggests at least three episodes that could have generated flows of uranium-bearing fluids in sandy aquifers important to present uranium deposits (Roach et al., 2014; Skirrow et al., 2009): before ~55 Ma (uranium systems in Mesozoic aquifers as Eocene Eyre Formation sediments were being deposited); before ~28 Ma (uranium systems in Mesozoic and Eocene Eyre Formation aquifers as Miocene Namba Formation sediments were being deposited); and, before ~6 Ma to 4 Ma (uranium systems in Mesozoic, Eocene Eyre Formation and Miocene Namba Formation aquifers as Quaternary Willawortina Formation sediments were being deposited). It is possible that emplacement of younger systems not only remobilized uranium deposits formed during preceding events, but also formed new zones of mineralisation in older aquifers, i.e. the Miocene event could have formed new uranium deposits in Mesozoic and Eocene aquifers as well as redistributing mineralisation formed during Mesozoic and Eocene events.

3.8. Preservation

Preservation is of critical importance for sandstone hosted deposits. Uranium mineralisation can be partially or completely destroyed, especially in deposits formed at shallower depths (< a few hundred metres), by post-mineralisation uplift and erosion. It can also be remobilised and degraded by oxidised waters flowing through the aquifer host-rock.

Adams et al. (1978) studied post-depositional processes related to the formation and destruction of uranium mineralisation at the Jackpile-Paguate deposit, northwest New Mexico. The destruction of mineralisation is thought to be caused by pre-Cretaceous weathering and erosion, which also generated regional-scale alteration of detrital feldspar in the sandstone. In the Callabonna Sub-basin, reactivation of faults has led to selective erosion of aquifers. In the Poontana Inlier, the Eyre Formation has been eroded, which means that mineralised zones, if formed, were destroyed resulting from movement on the Wooltana Fault in west and Poontana Fault Zone in the east (Fig. 13).

Dispersion of U-series isotopes around known deposits shows that in many areas mineralisation is actively remobilized by groundwaters (e.g. the Pepegoona deposit; Murphy et al., 2011). Detailed isotopic studies in the Chu-Sarysu Basin in Kazakhstan show that uranium mineralisation at the redox front is undergoing reworking (Fyodorov, 2001a, 2001b). The flow of groundwaters is controlled predominantly by hydrogeological gradients, which depend on the reactivation of faults. In the Callabonna Sub-basin, the present-day groundwater flow is controlled by relief generated during the most recent uplift of the northern Flinders Ranges, in the Mount Painter and Mount Babbage inliers. Penetration of groundwaters in Mesozoic and Cenozoic aquifers is remobilizing uranium from known deposits in the Lake Frome region.

Critical features of sandstone-hosted uranium mineral system discussed in the above section are summarised in Table 6.

4. Calcrete-hosted uranium mineral systems

In Australia, most calcrete-hosted uranium deposits are located in the Cenozoic palaeochannels in the Yilgarn Craton, WA (Table 7). Some deposits and prospects are also found in the Paterson and Gascoyne regions (WA), Arunta region (NT) and Gawler region (SA). Description of the geology of some major deposits and prospects can be found in McKay and Miezitis (2001), Lally and Bajwah (2006) and in a technical document (TECDOC) by IAEA (1984). Uranium mineralisation at the Yeelirrie deposit is described by Cameron (1990).

Calcrete-hosted uranium deposits are generally of small to medium tonnage (<~10 million tonnes) with low grades (<~0.1 wt.% U_3O_8; Fig. 6). The two largest calcrete-hosted deposits in the world are Yeelirrie (WA) and Langer-Heinrich, Namibia, with ~56 000 tonnes (Table 6) and ~41 000 tonnes (UDEPO) of uranium respectively.

4.1. Geological setting

Butt et al. (1984) classified calcrete-hosted uranium deposits by their geomorphological setting into three main types: valley; playa; and, terrace. Valley deposits, such as Yeelirrie, Hinkler–Centipede and Lake Raeside, in the Yilgarn Craton, occur in calcretes and associated sediments in the central channels of major (palaeo)drainages, and in the platforms and chemical deltas where the drainage enters playas (Figs. 19 and 20). The calcretes generally change vertically downwards into an alluvial clay–quartz unit (Fig. 21). Uranium mineralisation is not limited to the calcretes but transgresses into underlying units, with the greatest concentration located in the vicinity of the groundwater table

Table 6
Critical features of sandstone-hosted uranium mineral systems.

Deposit types (including synonyms)
- Roll-front, tabular, basal channel, tectonic/lithologic, epigenetic strata-infiltration

Geological setting
- Intracratonic basin, continental margin basin, intermontane basin.
- Embayment of basins rimmed by uranium-rich felsic rocks.
- Permeable sands in channels in palaeovalleys.
- Shallow dipping (normally between 5 and 10°) basin sequences.
- Often basin sequences tilted in the direction of a major reservoir (outflow zone): lake or sea.
- Sandstone aquifers sealed by over- and under-lying impermeable layers (mudstone, etc.).

Source (fluid, metal, energy)

Fluids
- Meteoric water. Locally diagenetic. Salinity variable but mostly not very saline (can locally reach ~5 wt.% NaCl). Oxidised. Neutral to moderately acidic.
- In rock sequence devoid of organic material a second reduced fluid sourced from hydrocarbon or coal-bearing basins may be involved.

Uranium
- Peraluminous felsic rocks (intrusive and volcanic), especially two-mica leucocratic granites. Peralkaline volcanics. Uranium either derived from volcanic glass or from uraninite. Minerals such as zircon, monazite and uranium-bearing thorite become leachable sources after metamictisation (100 to 150 Ma after emplacement of felsic rocks). Locally uranium can be sourced from the lithic material in the sandstone, volcanic ash in overlying or underlying beds.
- Presence of orthomagmatic and/or magmatic-hydrothermal uranium mineralisation in the source area is important in forming bigger deposits.

Energy drivers of fluid-flow
- Dominantly gravity-driven fluid-flow. Reactivation of faults at the basin margin (causing tilting and doming of the basin) can trigger groundwater flow.

Fluid pathway
- Lithified and/or unlithified immature and permeable sands.
- If a second reduced fluid (mobile reductant) is involved, faults within the basin sequence can be important.
- In palaeochannels, groundwater flows occurs both along the channel as well as across the channel.

Trap

Physical
- Contact with carbonaceous shales underlying sandstone. In palaeochannel systems mineralisation can be found in basement scours, at meandering bends, at sites of channel widening and at sites of confluence with tributaries.

Chemical
- Carbonaceous material in the sands is the most common reductant (biogenic reduction in the presence of anaerobic and sulphate-reducing bacteria). Locally Fe^{+2}- and vanadium-bearing clays and silicates can be important. In some regions Fe^{+2}-bearing silicates, especially chlorite in mafic rocks, can serve as effective reductants. Mobile reductants, such as CH_4, CO, H_2S, N_2 and H_2, and other hydrocarbons derived from hydrocarbon and coal basins, can also cause reduction

Age and relative timing of mineralisation
- Generally Paleozoic and younger. In older basins, mineralisation can form if the sandstones contain algal material and/or Fe^{+2}-bearing silicates and sulphides.
- Mineralisation often occurs in unconsolidated and semi-consolidated sands soon after the deposition of overlying shales. In many basins with significant resources mineralisation is formed in more than one episode of groundwater flow, closely related to uplift history of sediment provenance areas. The uplift is caused by reactivation of faults.

Preservation
- Critical. As mineralisation often occurs in good aquifers, it can be easily dissolved and redeposited or completely destroyed. Preservation requires physical isolation of mineralisation from the flow of oxidised groundwater. Slowing down of groundwater or its cession can also promote preservation.

Main references
Kyser and Cuney (2009), Dahlkamp (2009), Jaireth et al. (2008)

(Fig. 21). Mineralisation occurs almost entirely as carnotite, generally as a late-stage precipitate in cavities, lined by thin coatings of minerals such as calcite, dolomite, silica and/or sepiolite. Carnotite may also form fine disseminations in the clay–quartz units.

The playa deposits, such as the Lake Maitland and Lake Austin deposits in the Yilgarn Craton, occur in near-surface evaporitic and alluvial sediments (Cavaney, 1984; Heath et al., 1984). The calcretes near playas act as principal aquifers to the playas (Fig. 19). In the Yilgarn, mineralised playas are usually closely associated with calcretes in the

Table 7
Major calcrete uranium deposits and prospects in Australia. Uranium resource data from OZMIN.

Name	State	Deposit type	Ore (Mt)	Grade (%)	U (t)
Anketell	WA	Valley	16.300	0.014	2308
Bellah Bore East	WA	Valley	0.35	0.018	62
Centipede	WA	Valley	12.94	0.043	5531
Dawson-Hinkler Well	WA	Valley	13.09	0.026	3463
Double 8 — Ponton	WA	Valley	26.000	0.025	6614
Hillview	WA	Valley	27.6	0.015	4072
Jailor Bore	WA	Unknown	1.430	0.050	716
Lake Maitland	WA	Playa	20.8	0.041	8564
Lake Mason	WA	Valley	9.1	0.016	1428
Lake Raeside	WA	Valley	6.800	0.025	1701
Lake Way	WA	Valley	9.95	0.045	4476
Lake Way South	WA	Playa	0.22	0.021	45.5
Lakeside (Lake Austin)	WA	Playa	0.62	0.042	265
Napperby	NT	Valley	9.340	0.030	2843
Nowthana	WA	Valley	11.9	0.047	8066
Peninsular Uranium	WA	Valley	9.75	0.014	1364
Thatcher Soak	WA	Valley	21.6	0.027	5916
Windimurra (U)	WA	Valley	19.000	0.015	2900
Wondinong	WA	Valley and Playa	6.500	0.016	1020
Yeelirrie	WA	Valley	50.05	0.111	55599
Yuinmery	WA	Playa	1.581	0.031	496

channels, often enriched in uranium. Mineralisation is generally concentrated near the groundwater table in sediments consisting of gypsiferous clays and muds. The sandy and silty clays locally contain calcareous nodules. In some deposits, such as Lake Maitland, the mineralisation occurs in thin calcretes in the playa itself. The terrace deposits are less common and occur in calcrete terraces in dissected valleys mainly in the Gascoyne Province.

Geologically significant uranium is associated with non-pedogenic calcrete or dolocrete formed within Cenozoic drainage systems incised into rocks containing leachable uranium and vanadium. Non-pedogenic calcrete (also known as groundwater or valley calcrete) is formed predominantly near the water table from groundwater moving along extremely low topographical gradients (Carlisle, 1984). The formation of non-pedogenic calcrete is generally controlled by climate and the type of soil. In the Yilgarn Craton, the distribution of non-pedogenic and pedogenic calcretes is defined by the Menzies Line (Butt et al., 1984). North of the Menzies Line, in the zone dominated by non-pedogenic calcretes, the soils are generally neutral to acid and the groundwaters are less saline and neutral to alkaline. South of the Menzies Line, in the zone dominated by pedogenic calcretes, the soils are neutral to alkaline and the groundwaters are saline and neutral to acidic (Gray, 2001). The southern zone is characterised by higher annual rainfall (>225 mm), which is winter-dominated, and lower annual evaporation (<2500 mm) with average temperatures below 19 °C. The northern zone is characterised by summer-dominated rainfall, lower total rainfall, and higher annual evaporation in comparison with the southern zone.

4.2. Source and nature of fluids

One of the main components of the system is shallow-level groundwater in the palaeochannels. The groundwater is generally of variable salinity, ranging between 3000 mg/L and 6790 mg/L chloride in the Langer-Heinrich region in Namibia (Table 8). The pH varies between 6.6 and 7.8. The pH of calcrete groundwaters in Australia is very similar to those in Namibia. However the variation in salinity (chloride concentration) is large, ranging between 136 mg/L and 95 160 mg/L (Table 8).

4.3. Source of uranium, vanadium and potassium

All known calcrete-hosted uranium deposits are located in palaeochannels incised into potential source rocks of potassium,

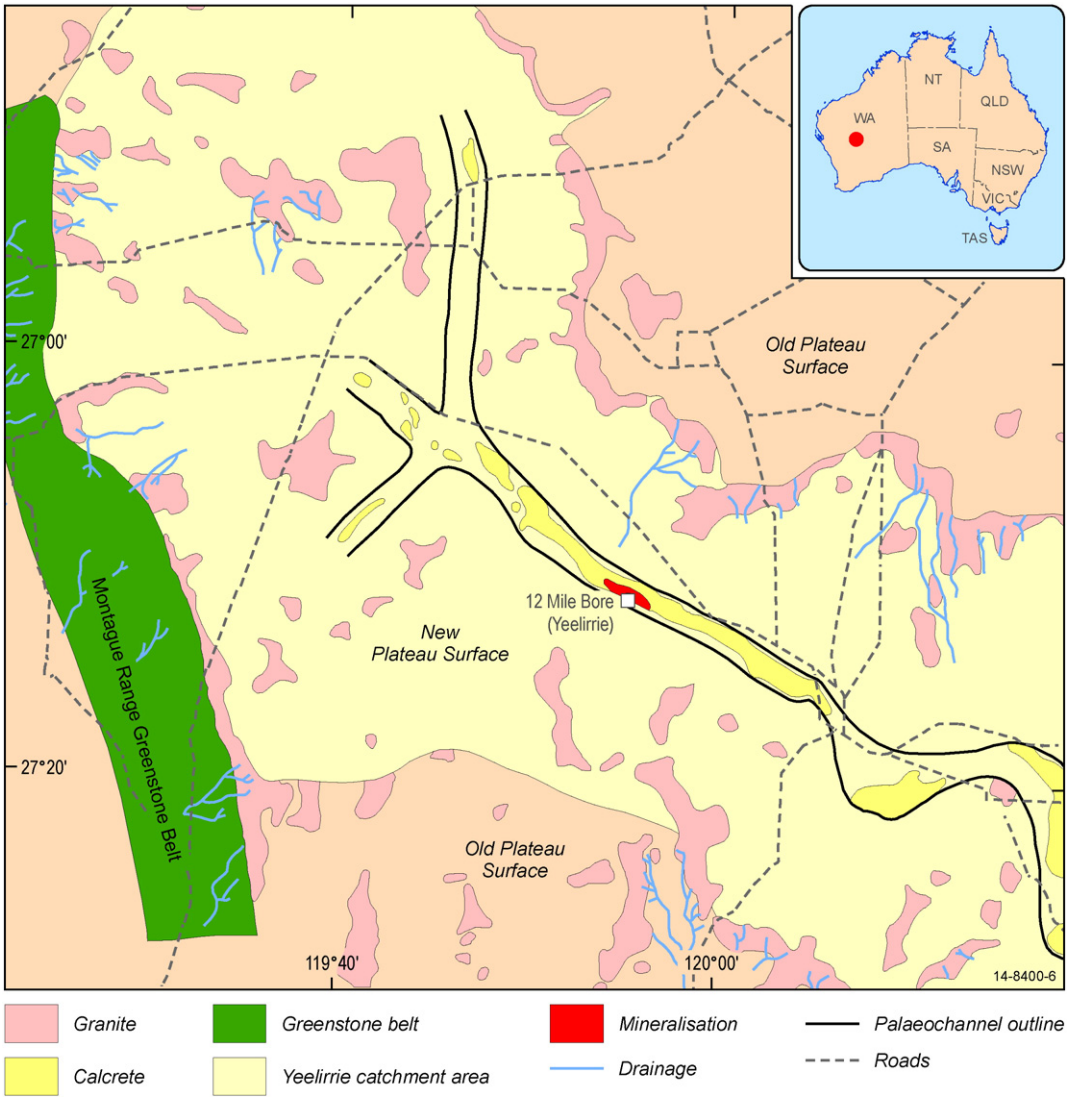

Fig. 19. Map of the Cenozoic palaeochannel hosting the Yeelirrie uranium deposit, modified after Cameron (1990). The figure also shows the Yeelirrie catchment and drainage system feeding into the palaeochannel. Note, the southward drainage in proximity to the deposit. A northward drainage in the direction of the deposit (not shown on the map) is can be seen on SANDSTONE 1:250000 topographic map.

uranium and vanadium. Felsic rocks in the Yilgarn Craton contain up to 20 ppm uranium (Schofield, 2009) and a granite in the upstream area of Lake Way deposit contains up to 25 ppm uranium (Mann and Deutscher, 1978). A monzogranite (adamellite) at Mount Cleaver, outcropping in the headwaters area of the Lake Way deposit, contains altered monazite, ilmenite and zircon (with metamict alteration halos) and contains up to 12 ppm uranium and up to 50 ppm vanadium (French and Allen, 1884). Intensive weathering and erosion of such felsic rocks can provide uranium as well as potassium to the calcrete-hosted uranium system. High uranium concentrations (up to 400 ppb) in groundwaters in the Lake Way area supports the leaching of uranium from the felsic rocks (Mann and Deutscher, 1978).

Mafic igneous rocks, sediments with vanadium-rich clays and ironstones such as banded iron-formation and ferricrete are often enriched in vanadium (Bastrakov et al., 2010). For example, lateritic ironstones in the Yilgarn Craton commonly contain up to 1000 ppm vanadium (Butt et al., 1978). Such rocks are generally present in the vicinity of calcrete-hosted uranium deposits (Mann and Deutscher, 1978; Karner and Becker, 2009).

4.4. Source of energy (energy drivers of fluid-flow) and fluid-flow pathways

The calcrete-hosted uranium system is driven by shallow groundwater drainage of extremely low topographic gradients, ca. 1% (10 m/km; Karner and Becker, 2009), established in permeable sediments infilling palaeochannels. In the drainage area near the Lake Way deposit, the gradients are also low, ranging between 0.155% in the north and northeast to 0.06% near the lake (French and Allen, 1884). In the drainage area of the Yeelirrie deposit, longitudinal gradients decrease from approximately 0.12% upstream to 0.06% near the ore body (Cameron, 1984).

The drainage in the region is controlled by a recharge area upstream and a system of playa lakes in the discharge area. In addition to the infill sediments, calcretes also represent good aquifers. For example, pumping tests near the Yeelirrie deposit produced a yield of approximately 4.5 million litres a day from an excavation measuring $450 \times 40 \times 9$ m (Cameron, 1984). In many palaeovalleys, lateral flow may be critical in fertile systems (Magee, 2009), because it may provide more effective hydrogeological connection with leachable sources of uranium and vanadium.

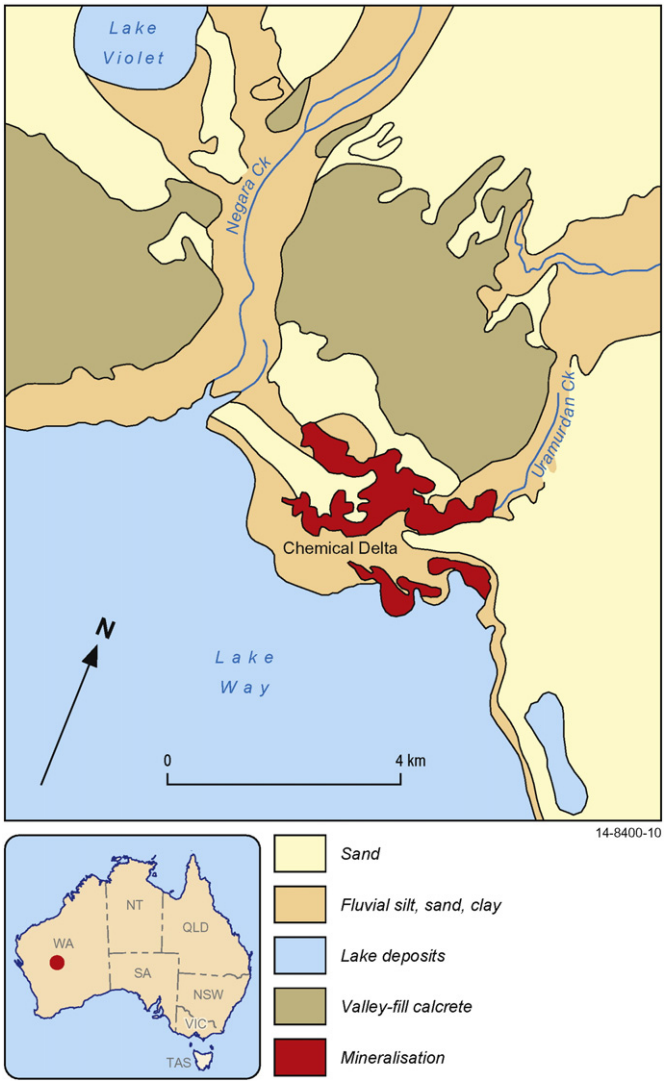

Fig. 20. Geological setting of the Lake Way uranium deposit, modified after French and Allen (1884). Most of the carnotite is located in the carbonated fluvial clastics. Significant mineralisation also occurs in valley-type calcretes and carbonates at the edge of Lake Way (French and Allen, 1884).

The presence of playa lakes creates conditions where groundwaters in the palaeovalleys can mix with relatively more saline waters in the playas.

4.5. Physical and chemical traps/sinks

Carnotite is a hydrated uranium- and potassium-bearing vanadate with the formula $K(U^{+6}O_2)(V^{+5}O_4)\cdot xH_2O$. Its solubility and precipitation depend on the:

- Concentration of potassium, uranium and vanadium in the fluid;
- Oxidation state of the fluid, because in oxygen-saturated, low-temperature surficial fluids, uranium and vanadium form aqueous complexes of uranyl ($U^{+6}O_2$) and V^{+4} and V^{+5} respectively; and,
- Type of oxidation-reduction reaction. As the valence states of uranium and vanadium in carnotite are +6 and +5 respectively, oxidation-reduction reactions are important with respect to vanadium only in conditions where vanadium forms complexes containing V^{+3} and V^{+4}. In such cases, precipitation of carnotite will require oxidation and not reduction of the fluid (see discussion below).

Calculations on the speciation of uranium and vanadium and on the stability of carnotite in shallow-level groundwaters show that geologically realistic concentrations of uranium and vanadium (>0.01 mg/L each of uranium and vanadium) can be transported in oxidised fluids (Bastrakov et al., 2010). In such conditions, uranium forms aqueous uranyl complexes and vanadium forms complexes containing either V^{+4} or V^{+5}. The calculations also show that precipitation of carnotite can occur due to changes in any of the following:

- pH; decrease in pH if the groundwater is alkaline (pH >8) or increase in pH if the groundwater is acidic (pH < 7);
- Oxidation state. At oxidation states where vanadium is transported as complexes of V^{+3} and/or V^{+4}, an increase in the oxidation state is essential to form carnotite;
- Concentration of dissolved potassium. An increase in the concentration of potassium will cause precipitation of carnotite;
- Partial pressure of CO_2, which controls the concentration of carbonate complexes in the groundwater. As uranium in these conditions is transported as a uranyl-carbonate complex, any decrease in the concentration of carbonate ions in groundwater will favour precipitation of carnotite;
- Concentration of dissolved calcium in the groundwater. As addition of calcium to the groundwater can cause precipitation of carbonate, the associated decrease in the concentration of dissolved carbonate ions in the groundwater can cause precipitation of carnotite; or,
- Concentration of dissolved sulphur in the groundwater. In oxidised groundwater sulphur is dissolved to form sulphate ions, which control the solubility of uranium as uranium forms uranyl-sulphate complexes. A decrease in the concentrations of sulphate ions, caused often by the deposition of gypsum and barite, can thus favour the precipitation of carnotite.

The formation of carnotite in valley calcretes is closely related to the seasonal fluctuation of the groundwater table. The fluctuation is associated with evaporation of groundwaters, which can lead to an increase in the concentration of dissolved potassium, vanadium and uranium (Butt et al., 1984). It can also change the concentration of carbonate ions in the water, affecting the solubility of uranium.

Evaporation is also important in the playa deposits, where it can control the salinity of lake waters and the precipitation of gypsum-bearing sediments. However, mixing of more saline lake waters, relatively enriched in potassium and calcium, and the incoming groundwaters from the drainage channel can be equally important in the formation of carnotite. Such mixing can cause an increase in the concentration of potassium and calcium in groundwater, which may lead to the precipitation of carnotite. In a similar way, an increase in the concentration of calcium can destabilise uranyl carbonate or uranyl sulphate complexes by precipitating calcite and gypsum, respectively, and thereby facilitate the formation of carnotite (Mann and Deutscher, 1978).

According to Mann and Deutscher (1978), redox processes can also contribute to the formation of carnotite in some calcrete-hosted uranium deposits. In this model the interaction of mildly reduced groundwaters with mafic rocks in the greenstones can cause dissolution of vanadium to form V^{+4}-bearing complexes. Vanadium from these groundwaters mixes with overlying uranium-bearing fluids either through diffusion and/or by upwelling of the waters caused by a subsurface hydromorphic barrier. Mixing causes oxidation of vanadium from V^{+4} to V^{+5} to form carnotite. The presence of dark-green coloured (relatively reduced with V^{+4}) carnotite deep in the calcrete profile, and of more yellow-coloured (relatively oxidised, with V^{+5}) carnotite toward the surface in some deposits is cited in support of this model.

The shape, size and basement topography of the palaeochannel can be of critical significance in the formation of calcrete-hosted uranium mineralisation. Butt et al. (1978) noted that the location of the thickest and most extensive calcrete can be influenced by the occurrence of

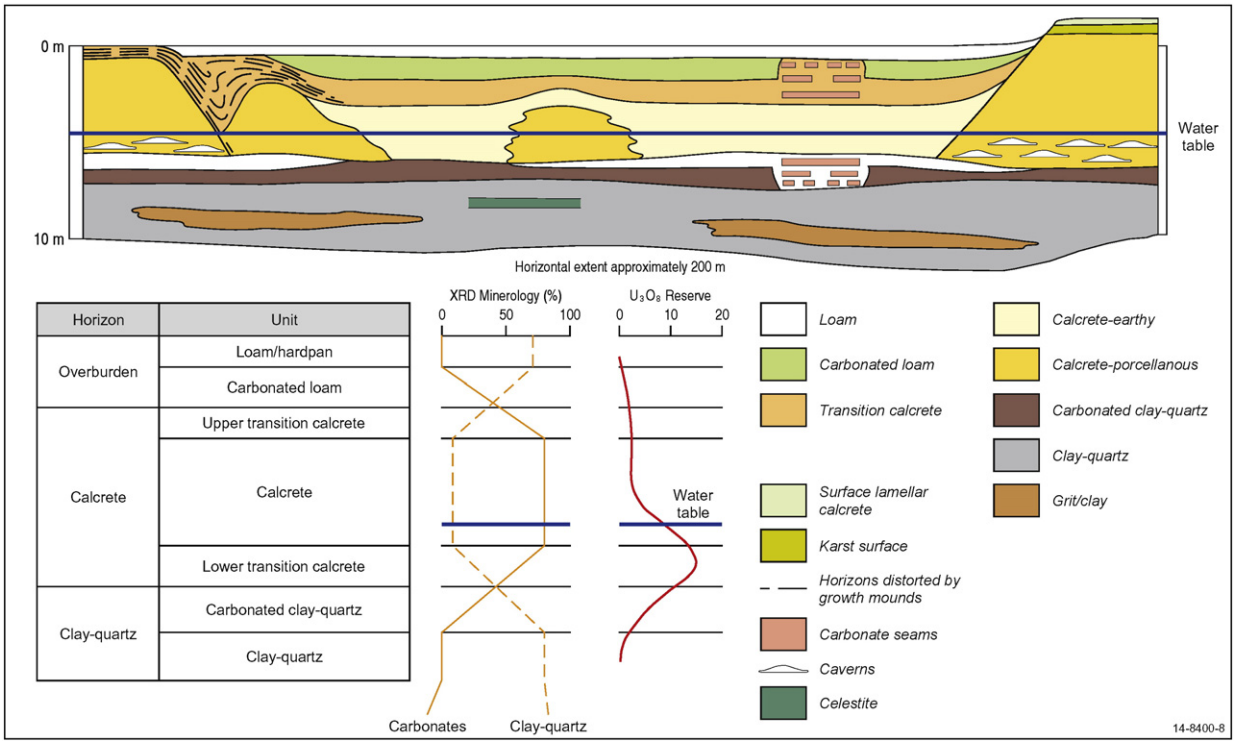

Fig. 21. Schematic cross section of the palaeochannel at the Yeelirrie uranium deposit. The main ore zone is located just below the water table in the calcrete as well as in the carbonated clay-quartz fluvial unit.
Modified after Cameron (1990).

subsurface barriers restricting drainage flow and causing ponding of groundwater. The presence of such barriers can affect formation of calcrete as well as carnotite in two ways: firstly by increasing the concentration of dissolved species as a result of evaporation and thereby causing precipitation of carbonates; and, secondly by causing upwelling of water into a more oxidising environment and thereby causing precipitation dissolved uranium and vanadium as carnotite. The existence of a barrier down-stream from the mineralisation at the Yeelirrie is speculated by Butt et al. (1978). At the Windimurra prospect, the calcrete outcrop widens upstream of a narrow constriction in the channel. The widened part is more mineralised than the rest of the calcrete in the channel (Butt et al., 1978). Cameron (1984) noted a significant drop in the longitudinal gradient in the palaeochannel hosting the Yeelirrie deposit, from 0.12% upstream to 0.06% near the orebody. This drop in the gradient can cause slowing of groundwater flow and its ponding, facilitating upwelling and evaporation, which can trigger the precipitation of carnotite. At the Yeelirrie deposit, the main palaeochannel is connected to a drainage-system running southward (north of the channel) and running northward (south of the channel). These two drainage systems can provide additional hydrological connection to more proximal leachable sources of uranium and vanadium. The presence of additional drainage can be critical in forming fertile mineral systems

4.6. Age and relative timing of mineralisation

All calcrete-hosted deposits show uranium disequilibrium (Dickson, 1984). This is not only because the systems are relatively young but also because of continuous dissolution and precipitation caused by the influx of waters in the channel aquifers. Therefore the precise age of mineralisation is not known for these deposits. The geological setting suggests that the age of calcrete-hosed deposits in Namibia (e.g., Langer-Heinrich) is at least 0.5 Ma (Kyser and Cuney, 2009).

Uranium series disequilibrium studies show that mineralisation at the Yeelirrie deposits is the youngest of the four other deposits in the Yilgarn Craton (Dickson, 1984). Yeelirrie appears to have formed between 0.1 Ma and 0.7 Ma. Mineralisation at the Centipede, Lake Way and Lake Maitland deposits is thought to be older than that at the Yeelirrie deposit.

4.7. Preservation

As calcrete-hosted deposits are formed in relatively shallow palaeochannels, which continue to be good aquifers, the preservation of mineralisation is critical for these deposits. The mineralisation can be destroyed (partially or completely) by tectonic activity and changes

Table 8
Groundwater salinity and pH in calcrete of selected mineralised areas.

Locality	pH	Cl (mg/L)	Source
Langer Heinrich, Namibia	6.6. to 7.8	3000 to 6790	Bowell et al. (2008)
Hinkler Well drainage, Yilgarn, WA	4.3 to 8.2	138 to 95160	Mann and Deutscher (1978)
Northern goldfields, Yilgarn, WA	7.6 to 8.2	610 to 2900	Johnson et al. (1999)
Paterson region, WA	7.4	136	Giblin (2001)
Napperby, Lake Lewis, NT	7.2 to 7.7	718 to 1600	English (2001)
Calcrete Tarcoola, Gawler, SA	6.0 to 7.7	1600 to 87000	Mernagh (2013)

in the climate. For example, Pleistocene uplift of parts of southern Africa has caused erosion of many calcrete-hosted deposits (Hambleton-Jones, 1982, cited in Boyle, 1984). To some extent large-size of some deposits may have resulted either from preservation of mineralisation at these deposits and/or from continuous enrichment of mineralisation by addition of uranium and vanadium removed from zones formed upstream.

Critical features of calcrete uranium mineral system discussed in the above section are summarised in Table 9.

4.8. Distinguishing features of large mineral systems

Features of basin-related uranium systems, discussed in this review, describe processes which may be critical to form fertile mineral systems. These features provide the basis to conduct mineral potential and prospectivity analyses in an area. Such analyses require identification of mappable signatures of the above-mentioned critical features in geological, geophysical and geochemical datasets.

National-scale mineral potential maps for basin-related minerals systems have been produced by Jaireth and Miezitis (2004), and Kreuzer et al. (2010) using this approach. Regional-scale prospectivity analyses using a mineral-systems approach have also been conducted for areas in north Queensland (Huston et al., 2010), east-central South Australia (Huston and van der Wielen, 2011) and the southern Northern Territory (Schofield, 2012).

The discussion of fertile basin-related systems summarised in this review shows that these systems require at least four interrelated ingredients: 1. Source(s) of leachable uranium (and vanadium and potassium for calcrete-uranium deposits); 2. A hydrological architecture enabling connection between the source and the sink (site of accumulation); 3. Physical and chemical sinks or traps; and, 4. A post-mineralisation setting favourable for preservation. These ingredients can help to distinguish fertile mineral systems from systems that are incapable of generating economic-grade concentrations of uranium. However, it is not clear if the above-mentioned ingredients on their own can assist in assessing the size (tonnage of contained uranium) of deposits resulting from fertile mineral systems. The challenges of identifying unique features that characterise world-class or giant mineral systems are involved and complex, and only in recent years has some significant progress been made in defining these features for some minerals systems (e.g., Laznicka, 2014; Richards, 2013; Jaireth and Huston, 2010; McCuaig et al., 2010; Jaques et al., 2002). Unfortunately, little progress has been made to understand critical features of world-class and giant uranium mineral systems. In the PCO, world-class uranium deposits are located exclusively in the South Alligator Rivers Uranium Field (Fig. 7). A multi-scale edge analysis ('worming') of the gravity data suggests that world-class deposits are located near the edges of gravity highs, spatially associated with the 'worms' of the upward continuation heights (UCH) of 20 km (Jaireth et al., 2007). Relatively smaller deposits in the Rum Jungle Uranium Field (Fig. 7) are associated with shallower 'worms' (1 to 5 km). Uranium deposits in the South Alligator Uranium Field (Fig. 7) do not show a clear association with the 'worms'.

According to Richard et al. (2012) some giant unconformity-related uranium deposits may have resulted from special fluids capable of dissolving high concentration of uranium. Their calculations suggest that oxidised and acidic fluids (pH ranging between 2.5 and 4.5) can dissolve up to ~2 wt.% uranium (at 155 °C and pH ~ 2). They also report high uranium concentrations (~500 ppm) in fluid inclusions from a number of deposits in the Athabasca Basin.

The Chu-Sarysu Basin in Kazakhstan (with a total uranium resource of ~790 000 tonnes; IAEA's UDEPO database) contains a number of world-class sandstone-hosted uranium deposits, such as Inkai (~153 000 tonnes) and Mynkuduk (~127 000 tonnes). The organic content of the sandstone aquifer, which hosts the uranium deposits, is low (generally < 0.03 to 0.05 wt.%) compared to the organic content of host sandstone units in the Wyoming Basin (0.5 wt.%; Jaireth et al., 2008). It has been suggested that the large sizes of the uranium deposits may have resulted from the influx of mobile reductants (hydrocarbons and associated gases) leaking from the hydrocarbon basins underlying the sandstone units hosting uranium deposits (Pechenkin, 2014; Jaireth et al., 2008).

World-class and giant mineral deposits are often thought to result from mineral systems that are more 'efficient' than those which produce deposits of average size. By and large, the efficiency of a mineral system depends on how well the critical ingredients (e.g. the four ingredients listed above) come to be interlinked in space as well as in time. Hronsky (2011) describes them as self-organised critical systems (SOC), in which ore formation results from rare periods of anomalous dynamics during the evolution of large-scale fluid flux systems.

In general, the amount of uranium accumulated in a deposit (U_t) formed from basin-related uranium systems is equal to the product of

Table 9
Critical features of calcrete-hosted uranium systems.

Deposit types (including synonyms)
- Fluvial valley-fill or valley-type, lacustrine or playa-type.

Geological setting
- Cenozoic palaeovalleys and channels in arid zones.
- Palaeochannels filled with sediments containing non-pedogenic calcrete. Formation of non-pedogenic calcrete is controlled by climate (arid) and by the soil-type (neutral to acid soils).
- Playa lakes with evaporitic sediments.

Source (fluid, metal, energy)

Fluids
- Meteoric water, lake water, shallow to deep (~400 m) ground water.
- Salinity (chloride): variable ranging between 136 mg/L and 95 160 mg/L. High salinity waters can transport more uranium and vanadium; pH varies between 6.0 and 8.2. pH is not considered important for the transport of uranium and vanadium.

Potassium, uranium, and vanadium source
- Felsic rocks for uranium (rocks with >~20 ppm U).
- Mafic rocks and banded iron formations for vanadium. Average abundance (in ppm) of vanadium in major rock types (Krauskopf, 1982): Basalt (250); Shale (130); Granite (50).
- Potassium from felsic rocks.

Energy drivers of fluid-flow
- Dominantly gravity-driven fluid-flow. Seasonal variation of the groundwater table is considered important. Hydrological gradients are low (~0.12% and lower).

Fluid pathway
- Permeable sands in palaeochannels.
- Efficient hydrological system involves a good connection between aquifers in palaeochannels and salt lakes (discharge areas).

Trap

Physical
- Changes in the shape of palaeochannels and subsurface barriers in palaeochannels can restrict flow of groundwater causing its ponding and upwelling.

Chemical
- For valley-type calcrete deposits: changes in pH and concentration of potassium, vanadium and uranium, and dissolved CO_2 due to evaporation of upwelling groundwater.
- For playa-type deposits: mixing of groundwater with saline lake water and changes in the concentration of K, Ca, CO_3 and SO_4.
- Less frequently: mixing of relatively reduced waters carrying vanadium with more oxidised waters carrying uranium.

Age and relative timing of mineralisation
- Cenozoic age.
- Paragenetically, carnotite mineralisation is late and replaces carbonate minerals in the calcrete. Activation of the mineral system depends on the hydrogeological connection between aquifers in the palaeochannels and playa lakes.

Preservation
- Critical. As mineralisation is formed in relatively shallow palaeochannels with good aquifers, it can be dissolved, re-precipitated and enriched or completely destroyed. Mineralisation can also be destroyed by changes in the climate

Main references
Bastrakov et al. (2010), Dahlkamp (2009), Boyle (1984), Butt et al. (1984)

concentration of uranium in the fluid (C), the amount of fluid passing through the systems per unit time (Q), the duration of the fluid-flow (T), and the extraction efficiency (E) of uranium at the trap or sink site (Hobday and Galloway, 1999):

$$U_t = C \times Q \times T \times E.$$

This simple equation can provide a rough estimate of uranium available for accumulation in a deposit. For example, a sandstone unit with a thickness of 10 m and a strike extension of 1000 m, and with a dip of 10° and a hydraulic conductivity of 1 m/year, can allow 1700 tonnes/year of fluid to pass through it. With a concentration of 100 ppm (100 g/t) uranium, this fluid can bring through the sandstone aquifer around 170 000 tonnes of uranium over one million years (or 85 000 tonnes uranium over half a million years). However, this total amount of uranium in the fluid (e.g., 85 000 tonnes) can accumulate either in one large or in many relatively smaller deposits (Jaireth, 2011a, 2011b). The number of deposits and the uranium grade of these will depend on the extraction efficiency of the mineral system.

4.8.1. Differences between sandstone-hosted mineral systems in the Chu-Sarysu and Syrdarya basins (Kazakhstan) and the Callabonna Sub-basin (South Australia)

Groundwaters which form sandstone-hosted and calcrete-uranium deposits are highly oxidised. Therefore, the concentration of uranium in these fluids largely depends on the concentration of leachable uranium in the source rocks. As the solubility of uranium in peraluminous felsic magmas is by an order of magnitude smaller than the solubility in peralkaline magmas, peraluminous felsic rocks can reach saturation with respect to uraninite at a much lower total concentration of uranium (<~30 ppm, Kyser and Cuney, 2009). In contrast, peralkaline rocks can have much higher concentrations of uranium but most of the uranium in these rocks is trapped in accessory minerals, such as zircon, apatite and monazite. Uranium from these minerals becomes leachable only after they have gone through metamictisation. Felsic volcanics (more commonly associated with peralkaline magmas) can contain the most readily leachable source of uranium in the form of volcanic glass (Kyser and Cuney, 2009).

The influence of the leachable source of uranium on the size of uranium deposits can be illustrated by comparing uranium deposits in the Lake Frome region. More than 80% of uranium resources in the Lake Forme region are located in its northern part (Figs. 12, 14, and 15), which hosts three large deposits (Beverley, Four Mile East and Four Mile West). In contrast uranium deposits in the southern part of the Lake Frome region are small, e.g. Goulds Dam, Honeymoon, East Kalkaroo, Yarramba and Oban (Fig. 15). One of the striking differences between the two areas is the presence of felsic rocks with much higher concentration of uranium in the northern part (see Section 3.2), suggesting that the sandstone mineral systems in the northern part were tapping a relatively larger source-reservoir of uranium. An additional element that favoured formation of relatively large deposits was the activation of a more efficient hydrological architecture in the northern part, which linked source rocks with reductant-bearing permeable sands (Figs. 13 and 14). The landscape evolution history summarised in Section 3.7 indicates the possibility that sandstone uranium mineral system in the northern part operated for a longer duration spanning three episodes. In this regard the mineral system is similar to the uranium mineral system in the Chu-Sarysu Basin in Kazakhstan, where four episodes have been revealed by dating of uranium minerals (Section 3.7). However, uranium deposits in the Chu-Sarysu Basin are larger than those in the northern part of the Lake Frome region.

A comparison of the regions (Lake Frome in South Australia and Chu-Sarysu and Syrdarya basins in Kazakhstan, Table 10) shows that Chu-Sarysu and Syrdarya basins are much larger (~7 times) than the Callabonna Sub-basin in the Lake Frome region. Most importantly, the sandstone-bearing host units are thicker in the Chu-Sarysu and Syrdarya basins than in the Callabonna Sub-basin and contain much larger proportions of sands. In the Lake Frome region, the Beverly deposit is hosted by the Namba Formation, which is predominantly composed of clay with sand lenses of variable thickness. The Eyre Formation, which hosts most of the sandstone-hosted uranium deposits in the Lake Frome region, is dominated by sands but the maximum thickness is much smaller than the host units in the Chu-Sarysu and Syrdarya basins. Thus, the quantity of oxidised groundwater passing through aquifers in the Chu-Sarysu and Syrdarya basins was much larger than the host units in the Callabonna Sub-basin. In addition, the duration of flow of these waters in the Chu-Sarysu and Syrdarya Basins was much longer, as shown by four episodes of uranium mineralisation (Table 10). A prolonged duration is also supported by the large distance of redox fronts from the uranium source regions (up to 350 km) observed in Chu-Sarysu and Syrdarya Basins. In contrast, the distance of redox fronts from the uranium source regions in the Callabonna Sub-basin is much smaller (up to 10 km).

The large size of uranium deposits in the Chu-Sarysu and Syrdarya basins can also be associated with a more efficient mechanism of extracting uranium from oxidised groundwaters. The organic content of host units in these basins is much lower than that of the Callabonna Sub-basin (Table 10). However, the Chu-Sarysu and Syrdarya basins overlie hydrocarbon-bearing basins, capable of releasing mobile reductants such as H_2S, N_2, H_2 and CH_4. Gaseous reductants are known to be more effective reductants than plant organic material commonly observed in many sandstone-hosted deposits (Pechenkin, 2014, Fyodorov, 2005).

Table 10
Comparison of critical features of sandstone-hosted uranium mineral systems in the Lake Frome region (Australia) and Chu-Sarysu and Syrdarya basins (Kazakhstan).

Feature\Region	Lake Frome (Callabonna Sub-basin)[a]	Chu-Sarysu–Syrdarya basins[b]
Size of the basin (km^2)[c]	32 800	216 326
Age of the host rock	Cretaceous (Bulldog Shale equivalent) Paleogene (Eyre Formation) Neogene (Namba Formation)	Cretaceous, Paleogene
Maximum thickness of host unit (m)	Eyre Formation: 120 Namba Formation[d]: 250	Cretaceous: 320 Paleogene: 200
Lithology of host unit	Cretaceous: sandy diamictite, silt, basal conglomerate Paleogene: sand, carbonaceous sand, gravel, silt, minor clay and lignite Neogene: predominantly clay, fine sand, silt, dolomitic palygorskite	Cretaceous and Paleogene: fine-grained sand and gravel (clay units < 20%)
Source of leachable uranium	Felsic rocks (intrusive and volcanic); uraninite–bearing veins and breccia zones	Felsic rocks (intrusive and volcanic); uraninite–bearing veins
Organic carbon (wt.%)	<0.05 to 0.5	<~0.03 to 0.05%
Mobile reductant (Hydrocarbon-related)	Not prominent	Prominent
Distance of redox front from recharge area (Km)	Up to 10	Up to 350
Number of mineralising events	Possibly 3 but only one documented by dating methods	4 events documented by dating methods
Resources[e]	~62 000 tonnes U	~790 000 tonnes U

[a] Michaelsen and Fabris (2014); Alley (1998), Heathgate Resources (2008).
[b] Petrov (1998), Fyodorov (2005), Fyodorov (1996).
[c] Size of the basin approximate.
[d] Namba Formation is dominated by clay units which enclose sand lenses of variable thickness.
[e] UDEPO, IAEA.

4.8.2. The world-class Yeelirrie deposit

The Yeelirrie deposit is the largest valley-type calcrete-hosted uranium deposit in the Yilgarn region. It is ~10 times larger than other calcrete uranium deposits in the region (Table 7). Leachable sources of uranium and vanadium are present in proximity to all known calcrete deposits in the area. The palaeovalley system which hosts this deposit is similar in size and shape to other palaeovalley systems that host smaller deposits.

An important distinguishing feature observed in the palaeovalleys at the Yeelirrie deposit is the significant decrease in its longitudinal gradient, from 0.12% upstream to 0.06% near the orebody (Cameron, 1984). This change in gradient can cause slowing of groundwater flow and its ponding. The ponding in its turn can result in upwelling of groundwaters, facilitating effective evaporation and loss of dissolved CO_2, triggering the precipitation of carnotite.

The presence of drainage systems, running southward (north of the channel) and running northward (south of the channel), can provide additional hydrological connection to more proximal leachable sources of uranium and vanadium.

Carnotite mineralisation at the Yeelirrie deposit is known to be the youngest of other calcrete uranium deposits in the area (see Section 4.6). It is possible that mineralisation at other, relatively older deposits has been remobilised and partially destroyed.

4.9. Conclusions

This review discussed critical features of fertile basin-related uranium mineral systems in Australia. The discussion shows that fertile minerals systems require the presence of four ingredients: 1. Source rocks of leachable uranium (and vanadium and potassium for calcrete-uranium deposits); 2. Hydrological architecture enabling connection between the source and the sink (site of accumulation); 3. Physical and chemical sinks or traps; and, 4. Post-mineralisation setting favourable for preservation.

This review also discusses factors which may control the efficiency of basin-related mineral systems. A rough estimate of the efficiency of a mineral system can be made by assessing the amount of uranium available for extraction at the site of mineralisation (sink or trap). In the unconformity-related uranium mineral systems, this is determined by the concentration of leachable uranium in source rocks (Archean and Paleoproterozoic felsic rocks and hydrothermally altered palaeoregolith) and in the amount of fluid released from the diagenesis of sandstone overlying the unconformity. Fluid-flow modelling suggests that an effective convection system can be generated in basins with a thickness of >~3 km (Raffensperger and Garven, 1995a, 1995b). Diagenesis of sandstones produces a system of aquifers and aquitards, which not only controls fluid flow, but also creates hydrological compartmentalisation of the basin (Hiatt and Kyser, 2007). Another factor which determines fluid-flow in these systems is the tectonic activation of faults. Fluid-flow modelling suggests that during extensional deformation, basinal diagenetic fluids begin to penetrate the basement below the unconformity along fault zones, whereas compressional deformation causes expulsion of fluids from the basement into the sandstones above the unconformity (Cui et al., 2012). This periodic interaction of basinal fluids with the basement rocks is critical because it can not only facilitate sourcing of uranium from them, but can also produce mobile gaseous reductants (H_2S, N_2, H_2 and CH_4) from dissolution of minerals (e.g., graphite, sulphides) in the basement rocks. The involvement of mobile reductants is thought to be one of most critical factors in generating world-class uranium deposits (Jefferson et al., 2007; Pascal, 2014; cited in Potter, 2014). The high grades (>10 wt.% U) in some world-class deposits in the Athabasca Basin may be related to intensive dissolution of quartz by silica-undersaturated ore fluids (Cuney, 2005).

In the sandstone-hosted uranium systems, the efficiency of the mineral system is controlled by the concentration of leachable uranium in the source rocks (peraluminous felsic intrusives and peralkaline intrusives and volcanics, especially after metamictisation of uranium-bearing minerals) and by the quantity of groundwaters flowing through the aquifers. The latter can be estimated by the permeability of sands, their thickness and by the hydrological gradient at the time of mineralisation. These two factors determine the quantity of uranium carried to the potential site of mineralisation. As a general rule, mineral systems in which uranium is sourced from detrital minerals in the sandstone itself (intrinsic source) form relatively smaller deposits (e.g. Bonnetti et al., 2014a, 2014b). It was noted that uranium deposits in the northern Lake Frome region are bigger than similar deposits in the southern part of the region. One possible explanation of their larger size is the high concentration of leachable uranium in the felsic rocks of the Mount Painter and Mount Babbage inliers. However, uranium deposits in the Lake Frome region are much smaller than similar deposits in the Chu-Sarysu and Syrdarya Basins in Kazakhstan. We argue that this is because sandstone aquifers in these basins are thicker and contain a larger proportion of permeable sands. In addition, low organic carbon content of these aquifers may have allowed oxidised groundwaters to flow to considerable distance, building up the concentration of dissolved uranium in them. This is supported by the large distance (~350 km) of redox fronts from source rocks, observed in the sandstones in the Kazakhstan deposits. The influx of mobile gaseous reductants from the hydrocarbon-bearing basins underlying the sandstone aquifers could have provided an efficient mechanism for extracting uranium from oxidised groundwaters. In contrast, in the sandstone-hosted uranium mineral systems in the Lake Frome region, the most common reductant is the plant organic material in the sands.

In the calcrete-uranium mineral systems, the efficiency is also controlled by the concentration of leachable uranium and vanadium in the source rocks and by the amount of groundwater channelled in the palaeochannel aquifers (sands and calcretes). We argue that the mineral system at the Yeelirrie deposit was more efficient, resulting in the formation of a deposit ten times larger than average calcrete-uranium deposits. It has been noted that there is a significant drop in the longitudinal gradient of the channel, from 0.12% upstream to 0.06% near the orebody (Cameron, 1984). This drop in the gradient can cause slowing of groundwater flow and its ponding. The ponding, in its turn, can result in the upwelling of groundwaters, facilitating effective evaporation and loss of dissolved CO_2 and triggering precipitation of carnotite. The presence of drainage systems, feeding the palaeochannel from north and south is an additional important factor determining the large size of the Yeelirrie deposit, because the drainage could have provided additional, more proximal, hydrological connections to the leachable sources of uranium and vanadium.

Acknowledgements

The authors gratefully acknowledge the contributions of many colleagues in Geoscience Australia who were involved in various research and data acquisition projects conducted as part of the Australian Government's 2006–2011 Onshore Energy Security Program. The review draws on a large number of papers and records published by Geoscience Australia (listed in the references). The authors gratefully acknowledge constructive discussions with colleagues in Geoscience Australia, especially Yanis Miezitis, Aden McKay, Marina Costelloe, Andrew Cross, David Huston, Roger Skirrow, Anthony Schofield, and Patrice de Caritat. We thank the reviewers David Huston, Roger Skirrow, Susan Hall and Michel Cuney for their constructive comments. The authors also acknowledge Daniel McIlroy and Chris Evenden for drafting figures. This paper is published with the permission of the CEO, Geoscience Australia.

References

Adams, S.S., Curtis, H.S., Hafen, P.L., Salek-Nejad, H., 1978. Interpretation of postdepositional processes related to the formation and destruction of the Jackpile-Paguate uranium deposit, Northwest New Mexico. Econ. Geol. Bull. Soc. Econ. Geol. 73, 1635–1654.

Ahmad, M., Hollis, J.A., 2013. Pine Creek Orogen. In: Ahmad, M., Munson, T.J. (Eds.), Geology and mineral resources of the Northern Territory. Northern Territory Geological Survey 5, pp. 1–133.

Ahmad, M., Lally, J.H., McCready, A.J., 2006. Economic Geology of the Rum Jungle Mineral Field. Northern Territory Geological Survey, Darwin.

Alley, N.F., 1998. Cainozoic stratigraphy, palaeoenvironments and geological evolution of the Lake Eyre Basin. Palaeogeogr. Palaeoclimatol. Palaeoecol. 144, 239–263.

Aubakirov, K.B., 1998. On the deep origin of ore-forming solutions in the uranium deposits in platform sequence of depression (with Chu-Sarysu Province as an example). Geol. Kazakhstan 2, 40–47.

Bagas, L., 2004. Proterozoic evolution and tectonic setting of the northwest Paterson Orogen, Western Australia. Precambrian Res. 128, 475–496.

Bagas, L., Nelson, D.R., 2007. Provenance of Neoproterozoic sedimentary rocks in the northwest Paterson Orogen, Western Australia. Special Publication — Northern Territory Geological Surveypp. 1–10.

Bakker, R.J., Elburg, M.A., 2006. A magmatic-hydrothermal transition in Arkaroola (northern Flinders Ranges, South Australia); from diopside–titanite pegmatites to hematite–quartz growth. Contrib. Mineral. Petrol. 152, 541–569.

Bampton, K.F., Haines, J.B., Randell, M.H., 2001. Geology of the Honeymoon uranium project. AusIMM Proc. 306, 17–27.

Bastrakov, E.N., Jaireth, S., Mernagh, T.P., 2010. Solubility of uranium in hydrothermal fluids at 25°–300°: implications for the formation of uranium deposits. Geoscience Australia, Record 2010/XX. Geoscience Australia, p. 86.

Bennett, P., Siegel, D.I., 1987. Increased solubility of quartz in water due to complexing by organic compounds. Nature 326, 684–686.

Bonnetti, C., Cuney, M., Malartre, F., Michels, R., Bourlange, S., Liu, X., 2014. Genesis of roll front-type uranium deposits in the Erlian Basin, NE China: the Bayinwula deposit. AusIMM Uranium Conference, 10–11 June, Perth.

Bonnetti, C., Cuney, M., Michels, R., Truche, L., Malartre, F., Liu, X., Yang, J., 2014. The multiple roles of sulphate-reducing bacteria and Fe-Ti oxides in the genesis of Bayinwula roll front-type uranium deposit, Erlian Basin. NE China Econ. Geol. 110 (4), 1059–1081.

Borshoff, J., Faris, I., 1990. Angela and pamela uranium deposits. In: Hughes, F.E. (Ed.), Geology of the Mineral Deposits of Australia and Papua New Guinea. Australasian Institute of Mining and Metallurgy, Melbourne, Victoria, Australia, pp. 1139–1142.

Bowell, R.J., Barnes, A., Grogan, J., Dey, M., 2008. Geochemical controls on uranium precipitation in calcrete paleochannel deposits of Namibia. http://www.srk.com.au/files/File/SRK%20UK/Publisher%20Articles/24th%20_IAGS_%20Symposium.pdf.

Boyle, D.R., 1984. The genesis of surficial uranium deposits. Surficial Uranium Deposits IAEA TECDOC-322. IAEA, Vienna, pp. 45–52.

Brookins, D.G., 1975. Coffinite–uraninite stability relations in Grants Mineral Belt, New Mexico. AAPG Bull. 59, 905.

Brugger, J., Long, N., McPhail, D.C., Plimer, I., 2005. An active amagmatic hydrothermal system; the Paralana hot springs, northern Flinders Ranges, South Australia. Chem. Geol. 222, 35–64.

Brugger, J., Wulser, P.-A., Foden, J., 2011. Genesis and preservation of a uranium-rich Paleozoic epithermal system with a surface expression (northern Flinders Ranges, South Australia); radiogenic heat driving regional hydrothermal circulation over geological timescales. Astrobiology 11, 499–508.

Brunt, D.A., 1990. Miscellaneous uranium deposits in Western Australia. In: Hughes, F.E. (Ed.), Geology of the Mineral Deposits of Australia and Papua New Guinea. Australasian Institute of Mining and Metallurgy, Melbourne, Victoria, Australia, pp. 1615–1620.

Bull, S.W., Rogers, J.R., 1996. Recognition and significance of an early compressional deformation event in the Tawallah Group, McArthur Basin, N.T. (Abs.). In: Baker, T., et al. (Eds.), MIC '96: New Developments in Metallogenic Research, The McArthur–Mount Isa–Cloncurry Minerals Province, Townsville, April 22–23, 28–31.

Butt, C.R.M., Horwitz, R.C., Mann, A.W., 1978. Uranium occurrences in calcretes and associated sediments in Western Australia. CSIRO Minerals Research Laboratories, Division of Mineralogy, p. 67.

Butt, C.R.M., Mann, A.W., Horwitz, R.C., 1984. Regional setting, distribution and genesis of surficial uranium deposits in calcretes and associates sediments in Western Australia. Surficial Uranium Deposits, IAEA TECDOC-322. IAEA, Vienna, pp. 121–127.

Cameron, E., 1984. The Yeelirrie calcrete uranium deposit, Western Australia. IAEA TECDOC-322. IAEA, Vienna, pp. 157–164.

Cameron, E., 1990. Yeelirrie uranium deposit. In: Hughes, F.E. (Ed.), Geology of the Mineral Deposits of Australia and Papua New Guinea. Australasian Institute of Mining and Metallurgy, Melbourne, Victoria, Australia, pp. 1625–1629.

Carlisle, D., 1984. Surficial uranium occurrences in relation to climate and physical setting. Surficial Uranium Deposits TECDOC-322. IAEA, Vienna, pp. 121–227.

Carson, L.J., Haines, P.W., Brakel, A.T., Pietsch, B.A., Ferenczi, P.A., 1999. Milingimbi SD; 53-2. Northern Territory Geological Survey, Darwin, Northern Territory, Australia, p. 46.

Carson, C.J., Hollis, J.A., Glass, L.M., Close, D.F., Whelan, J.A., Wygralak, A.S., 2011. Summary of results. Joint NTGS-GA geochronology project: Pine Creek Orogen, eastern Arunta Region, Murphy Inlier and Amadeus Basin, July 2007–July 2009. Northern Territory Geological Survey Record 2010–004. Northern Territory Geological Survey, Darwin.

Cavaney, R.J., 1984. Lake Maitland uranium deposit. Surficial Uranium Deposits, TECDOC-322. IAEA, Vienna, pp. 137–140.

Cheney, E.S., Jensen, M.L., 1965. Stable carbon isotopic composition of biogenic carbonates. Geochim. Cosmochim. Acta 29, 1331–1346.

Chi, G., Bosman, S., Card, C., 2013. Numerical modelling of fluid pressure regime in the Athabasca basin and implications for fluid flow models related to the unconformity-type uranium mineralization. J. Geochem. Explor. 125, 8–19.

Chipley, D., Polito, P.A., Kyser, T.K., 2007. Measurement of U–Pb ages of uraninite and davidite by laser ablation-HR-ICP-MS. Am. Mineral. 92, 1925–1935.

Coats, R.P., Blissett, A.H., 1971. Regional and economic geology of the Mount Painter Province. Geological Survey of South Australia, Department of Mines, Bulletin 43, p. 417.

Craig, M.A. (Ed.), 2011. Geological and energy implications of the Pine Creek region airborne electromagnetic (AEM) survey, Northern Territory, Australia. Geoscience Australia, Canberra, A.C.T., Australia.

Cross, A., Jaireth, S., Hore, S.B., Michaelsen, B., Schofield, A., 2010. SHRIMP U–Pb detrital zircon results, Lake Frome region, South Australia. Geoscience Australia Record 2010/46.

Cross, A., Jaireth, S., Rapp, R., Armstrong, R., 2011. Reconnaissance-style EPMA chemical U–Th–Pb dating of uraninite. Aust. J. Earth Sci. 58, 675–683.

Cui, T., Yang, J., Samson, I.M., 2012. Tectonic deformation and fluid flow: implications for the formation of unconformity-related uranium deposits. Econ. Geol. 107, 147–163.

Cuney, M., 2005. World-class unconformity-related uranium deposits: key factors for their genesis. In: Mao, J., Bierlein, F. (Eds.), Mineral Deposit Research: Meeting the Global Challenge. Proceedings of the Eighth Biennial SGA Meeting Beijing, China, 18–21 August 2005, pp. 245–248.

Cuney, M., 2010. Evolution of uranium fractionation processes through time; driving the secular variation of uranium deposit types. Econ. Geol. Bull. Soc. Econ. Geol. 105, 553–569.

Curtis, J.L., Brunt, D.A., Binks, P.J., 1990. Tertiary palaeochannel uranium deposits of South Australia, Geology of the Mineral Deposits of Australia and Papua New Guinea. In: Hughes, F.E. (Ed.), Geology of the Mineral Deposits of Australia and Papua New Guinea. Australasian Institute of Mining and Metallurgy, Melbourne, Victoria, Australia, pp. 1631–1636.

Dahlkamp, F.J., 2009. Uranium Deposits of the World: Asia. Springer-Verlag, Berlin (493 pp.).

Davey, J.E., Mcavaney, D.J., Hill, S.M., 2010. Parabarana, northern Flinders Ranges, Australia. In: Davey, J.E. (Ed.), Mesozoic Palaeolandscape Reconstruction, Southern Eromanga Basin Margins. University of Adelaide (PhD thesis).

de Vries, S.T., Pryer, L.L., Fry, N., 2008. Evolution of Neoarchaean and Proterozoic basins of Australia. Precambrian Res. 166, 39–53.

Demko, T.M., 2003. Sequence stratigraphy of a fluvial-lacustrine succession in the Triassic lower Chinle Formation, central Utah, USA. Geol. Soc. Am. Abstr. Programs 35, 426.

Derome, D., Cuney, M., Cathelineau, M., Fabre, C., Dubessy, J., Bruneton, P., Hubert, A., 2003. A detailed fluid inclusion study in silicified breccias from the Kombolgie sandstones (Northern Territory, Australia); inferences for the genesis of middle Proterozoic unconformity-type uranium deposits. J. Geochem. Explor. 80, 259–275.

Derome, D., Cathelineau, M., Cuney, M., Fabre, C., Lhomme, T., 2005. Mixing of sodic and calcic brines and uranium deposition at McArthur River, Saskatchewan, Canada: a Raman and laser-induced breakdown spectroscopic study of fluid inclusions. Econ. Geol. 100, 1529–1545.

Dickson, B.L., 1984. Uranium series disequilibrium in the carnotite deposits of Western Australia. Surficial Uranium Deposits TECDOC-322. IAEA, Vienna, pp. 165–170.

Dong, W., Lin, J., Xia, Y, Qi, D., 2005. Alteration characteristics of the sandstone-type uranium deposit in Qianjiadian, Inner Mongolia. In: Mao, J., Bierlein, F. (Eds.), Mineral Deposit Research: Meeting the Global Challenge. Proceedings of the Eighth Biennial SGA Meeting Beijing, China, 18–21 August 2005, pp. 249–251.

Dorling, S., Belyk, C.L., Bishop, J., 2011. Kintyre uranium deposit: geology and mineralisation styles. Presentation at the AusIMM Uranium 2011 Conference, 10–14 June 2011, Perth.

Douglas, G.B., Butt, C.R.M., Gray, D.J., 2011. Geology, geochemistry and mineralogy of the lignite-hosted Ambassador palaeochannel uranium and multi-element deposit, Gunbarrel Basin, Western Australia. Mineral. Deposita 46, 761–787.

Drexel, J.F., Major, R.B., 1990. Mount Painter uranium-rare earth deposit. In: Hughes, F.E. (Ed.), Geology of the Mineral Deposits of Australia and Papua New Guinea. Australasian Institute of Mining and Metallurgy, Melbourne, pp. 993–998.

Dzhakelov, A.K., 1993. The Origin of Groundwaters in Chu-Sarysu Artesian Basin: Resources and Perspectives on Their Usage. U. M. Akhmedsafina Institute of Hydrogeology and Hydrophysics, Gylym, Almaty (in Russian, 238 pp.).

Edgoose, C.J., 2013a. Amadeus Basin. In: Ahmad, M., Munson, T.J. (Eds.), Geology and Mineral Resources of the Northern Territory. Northern Territory Geological Survey, Darwin, pp. 23:21–23:70.

Edgoose, C.J., 2013b. Ngalia Basin. In: Ahmad, M., Munson, T.J. (Eds.), Geology and Mineral Resources of the Northern Territory. Northern Territory Geological Survey, Darwin, pp. 24:21–24:24.

Elburg, M.A., Bons, P.D., Dougherty-Page, J., 2001. Age and metasomatic alteration of the Mt Neill Granite at Nooldoonooldoona Waterhole, Mt Painter Inlier, South Australia. Aust. J. Earth Sci. 48, 721–730.

Elburg, M.A., Bons, P.D., Foden, J., Brugger, J., 2003. A newly defined Late Ordovician magmatic–thermal event in the Mt Painter Province, northern Flinders Ranges, South Australia. Aust. J. Earth Sci. 50, 611–631.

English, P.M., 2001. Formation of analcime and moganite at Lake Lewis, central Australia: significance of groundwater evolution in diagenesis. Sediment. Geol. 143, 219–244.

Fabris, A.J., Gouthas, G., Fairclough, M., 2010. The new 3D sedimentary basin model of the Curnamona Province: geological overview and exploration implications. MESA J. 58, 16–24.

Fanning, C.M., 1995. SADME Data Package. Geochronological synthesis of South Australia. Part 1: The Curnamona Province. South Australia Department of Primary Industries and Resources. Open File Envelope, pp. 1–12, 08918.

Fayek, M., Kyser, T.K., 1997. Characterization of multiple fluid-flow events and rare-earth-element mobility associated with formation of unconformity-type uranium deposits in the Athabasca Basin, Saskatchewan. Can. Mineral. 35 (Part 3), 627–658.
Ferenczi, P.A., Sweet, I.P., 2004. Mount Evelyn Northern Territory; sheet SD 53-05. Northern Territory Geological Survey, Darwin, Northern Territory, Australia.
Fidler, R.W., Pope, G.J., Ivanac, J.F., 1990. Bigrlyi uranium deposit. In: Hughes, F.E. (Ed.), Geology of the Mineral Deposits of Australia and Papua New Guinea. Australasian Institute of Mining and Metallurgy, Melbourne, Victoria, Australia, pp. 1135–1138.
Fiedler, J., Slezak, J., 1992. Experience with the coexistence of classical deep mining and in-situ leaching of uranium in Northern Bohemia. IAEA TECDOC-720, pp. 115–128.
Fisher, L.A., Cleverley, J.S., Pownceby, M., MacRae, C., 2013. 3D representation of geochemical data, the corresponding alteration and associated REE mobility at the Ranger uranium deposit, Northern Territory, Australia. Mineral. Deposita 48, 947–966.
Foden, J., Elburg, M.A., Dougherty-Page, J., Burtt, A., 2006. The timing and duration of the Delamerian Orogeny; correlation with the Ross Orogen and implications for Gondwana assembly. J. Geol. 114, 189–210.
Foster, D.A., Murphy, J.M., Gleadow, A.J.W., 1994. Middle Tertiary hydrothermal activity and uplift of the northern Flinders Ranges, South Australia; insights from apatite fission-track thermochronology. Aust. J. Earth Sci. 41, 11–17.
Fraser, G.L., Neumann, N.L., 2010. New SHRIMP U–Pb zircon ages from the Gawler Craton and Curnamona Province, South Australia, 2008–2010. Geoscience Australia Record 2010/16.
French, B.M., 1966. Some geological implications of equilibrium between graphite and a C–H–O gas phase at high temperatures and pressures. Rev. Geophys. 4, 223–253.
French, R.R., Allen, J.H., 1884. Lake Way uranium deposit, Wiluna, Western Australia. Surficial Uranium Deposits, TECDOC-322. IAEA, Vienna, pp. 149–157.
Fricke, C., Reid, A., 2009. Alteration of Uranium-rich Granite and Its Relationship to Uranium Mineralisation in the Honeymoon Area, South Australia. Department of Primary Industries and Resources, South Australia.
Frost, B.R., 1979. Mineral equilibria involving mixed-volatiles in a C–O–H fluid phase; the stabilities of graphite and siderite. Am. J. Sci. 279, 1033–1059.
Fulwood, K.E., Barwick, R.E., 1990. Mulga Rock uranium deposit; Officer Basin. In: Hughes, F.E. (Ed.), Geology of the Mineral Deposits of Australia and Papua New Guinea. Australasian Institute of Mining and Metallurgy, Melbourne, Victoria, Australia, pp. 1621–1623.
Fyodorov, G.V., 1996. A comparative description of the geological-technological characteristics of the sandstone hosted uranium deposits in Wyoming and Southern Kazakhstan. In: Slezak (Ed.), In-situ Leach Uranium Mining. Proceedings of IAEA Technical Committee Meeting, Almaty, Kazakhstan, September 1996, pp. 42–48.
Fyodorov, G.V., 2001a. Uranium deposits of the Inkay — Mynkuduk ore field, Kazakhstan. IAEA TECDOC-1425, pp. 95–112.
Fyodorov, G.V., 2001b. Industrial types of uranium deposits in Kazakhstan. IAEA TECDOC-1258, pp. 77–83.
Fyodorov, G.V., 2005. Uranium deposits of the Inkay-Mynkuduk ore field (Kazakhstan). Developments in uranium resources, production, demand and the environment TECDOC-1425. IAEA, Vienna, pp. 95–112.
Giblin, A., 2001. Groundwaters: Geochemical Pathfinders to Concealed Ore Deposits. CSIRO Exploration and Mining.
Goldhaber, M.B., Reynolds, R.L., Rye, R.O., 1978. Origin of a South Texas roll-type deposit; II, Sulfide petrology and sulfur isotope studies. Econ. Geol. Bull. Soc. Econ. Geol. 73, 1690–1705.
Goldhaber, M.B., Reynolds, R.L., Rye, R.O., 1983. Role of fluid mixing and fault-related sulfide in the origin of the Ray Point uranium district, south Texas. Econ. Geol. 78, 1043–1063.
Goldhaber, M.B., Hemingway, B.S., Mohagheghi, A., Reynolds, R.L., Northrop, H.R., 1987. Origin of coffinite in sedimentary rocks by a sequential adsorption-reduction mechanism. Bull. Mineral. 110, 131–144.
Gray, D.J., 2001. Hydrogeochemistry in the Yilgarn Craton. Geochem. Explor. Environ. Anal. 1, 253–264.
Greenhalgh, D., Jeffery, P.M., 1959. A contribution to the pre-Cambrian chronology of Australia. Geochim. Cosmochim. Acta 16, 39–57.
Hambleton-Jones, B.B., 1982. Uranium occurrences in the surficial deposits of southern Africa. In: Glen, H.W. (Ed.), Proceedings of the 12th CMMI Congress, Johannesburg. South African Institute of Mining and Metallurgy, pp. 123–136.
Harshman, E.N., 1972. Geology and uranium deposits, Shirley Basin area, Wyoming. U. S. Geological Survey Professional Paper 745. U. S. Geological Survey, Reston, VA, United States, Washington, D.C., p. 82.
Heath, A.G., Deutscher, R.L., Butt, C.R.M., 1984. Lake Austin uranium deposit, Western Australia. Surficial Uranium Deposits, IAEA TECDOC-322. IAEA, Vienna, pp. 129–132.
Heathgate Resources, 2007. Mining Proposal for Proposed Extension of Beverley Mine. Heathgate Resources Pty Ltd.
Heathgate Resources, 2008. Beverley Four Mile Project Public Environment Report and Mining Lease Proposal. Heathgate Resources Pty Ltd.
Hecht, L., Cuney, M., 2000. Hydrothermal alteration of monazite in the Precambrian crystalline basement of the Athabasca Basin (Saskatchewan, Canada); implications for the formation of unconformity-related uranium deposits. Mineral. Deposita 35, 791–795.
Hemingway, B.S., 1982. Thermodynamic Properties of Selected Uranium Compounds and Aqueous Species at 298.15 K and 1 bar and at Higher Temperatures; Preliminary Models for the Origin of Coffinite Deposits. U. S. Geological Survey, Reston, VA, United States.
Hiatt, E.E., Kyser, T.K., 2007. Sequence stratigraphy, hydrostratigraphy, and mineralizing fluid flow in the Proterozoic Manitou Falls Formation, eastern Athabasca Basin, Saskatchewan. Bull. Geol. Surv. Can. 4, 489–506.
Hiatt, E.E., Kyser, T.K., Fayek, M., Polito, P., Holk, G.J., Riciputi, L.R., 2007. Early quartz cements and evolution of paleohydraulic properties of basal sandstones in three Paleoproterozoic continental basins: evidence from in situ ^{18}O analysis of quartz cements. Chem. Geol. 238, 19–37.
Hickman, A.H., Clarke, G.L., 1993. Geology of the Broadhurst 1:100000 sheet, Western Australia. Geological Survey of Western Australia, Perth, West. Aust., Australia.
Hills, J.H., Richards, J.R., 1976. Pitchblende and galena ages in the Alligator Rivers Region, Northern Territory, Australia. Mineral. Deposita 11, 133–154.
Hobday, D., Galloway, W., 1999. Groundwater processes and sedimentary uranium deposits. Hydrogeol. J. 7 (1), 127–138.
Holland, H.D., 2006. The oxygenation of the atmosphere and oceans. Philos. Trans. R. Soc. Lond. Ser. B Biol. Sci. 361, 903–915.
Hou, B., Fabris, A.J., Keeling, J.L., Fairclough, M.C., 2007a. Cainozoic palaeochannel-hosted uranium and current exploration methods, South Australia. MESA J. 46, 34–39.
Hou, B., Zhang, W., Fabris, A.J., Keeling, J.L., Stoian, L., Fairclough, M.C., 2007b. Palaeodrainage and coastal barriers of South Australia 1:2000 000. CRC LEME, Geological Survey Branch, Primary Industries and Resources South Australia, Adelaide.
Hou, B., Fabris, A.J., MichaeIsen, B.H., Katona, L.F., Keeling, J.L., Stoian, L., Wilson, T.C., Fairclough, M.C., Cowley, W.M., Zang, W., 2012. Palaeodrainage and Cenozoic Coastal Barriers of South Australia. Digital Geological Map of South Australia, 1:2000000 Series (2nd edition). Geological Survey of South Australia, Department of Manufacturing, Innovation, Trade, Resources and Energy, Adelaide.
Hronksy, J.M.A., 2011. Self-organized critical systems and ore formation: the key to spatial targeting? SEG Newsl. 84.
Huang, X., Liu, D., Du, L., Zhao, Y., 2005. A new sandstone-type uranium metallogenetic type; structure-oil, gas type. In: Mao, J., Bierlein, F.P. (Eds.), Proceedings of the Biennial SGA (Society for Geology Applied to Mineral Deposits) Meeting. Springer, Berlin, Federal Republic of Germany, Beijing, pp. 265–268.
Huston, D.L. (Ed.), 2010. An assessment of the uranium and geothermal potential of north QueenslandGeoscience Australia, Record 2010/14. Geoscience Australia, Canberra (118 pp.).
Huston, D.L., van der Wielen (Eds.), 2011. An Assessment of the Uranium and Geothermal Prospectivity of East-central South Australia. Geoscience Australia, Canberra (Record 2011/34, 229 pp.).
Huston, D.L., Czarnota, K., Jaireth, S., Williams, N.C., Maidment, D., Cassidy, K.F., Duerden, P., Miggins, D., 2010. Minerals systems of the Paterson region. In: Roach, I.C. (Ed.), Geological and Energy Implications of the Paterson Airborne Electromagnetic (AEM) Survey, Western Australia. Geoscience Australia, Canberra, pp. 155–218.
IAEA, 1984. Surficial Uranium Deposits. IAEA TECDOC-322 (236 pp.).
IAEA, 2009. World distribution of uranium deposits (UDEPO) with uranium deposit classification. IAEA TECDOC-1629 (117 pp.).
Idnurm, M., Heinrich, C.A., 1993. A palaeomagnetic study of hydrothermal activity and uranium mineralization at Mt Painter, South Australia. Aust. J. Earth Sci. 40, 87–101.
Ingham, E.S., Cook, N.J., Cliff, J., Ciobanu, C.L., Huddleston, A., 2014. A combined chemical, isotopic and microstructural study of pyrite from roll-front uranium deposits, Lake Eyre Basin, South Australia. Geochim. Cosmochim. Acta 125, 440–465.
Jackson, D.G., Andrew, R.L., 1990. Kintyre uranium deposit. In: Hughes, F.E. (Ed.), Geology of the Mineral Deposits of Australia and Papua New Guinea. Australasian Institute of Mining and Metallurgy, Melbourne, Victoria, Australia, pp. 653–658.
Jagodzinski, E.A., Fricke, C.E., 2010. Compilation of new SHRIMP U–Pb geochronological data for the southern Curnamona Province, South Australia, 2010. Department of Primary Industries and Resources Report Book 2010/00014.
Jaireth, S., 2011a. Mineral systems overview. In: Craig, M.A. (Ed.), Geological and energy implications of the Pine Creek region airborne electromagnetic (AEM) survey, Northern Territory, AustraliaGeoscience Australia Record 2011/18. Geoscience Australia, Canberra, A.C.T., Australia, pp. 55–109.
Jaireth, S., 2011b. Sandstone-hosted uranium (and gold) mineral systems in the Frome region: implications of AEM data. Presentation at the Frome AEM Survey Interpretation Workshop, November 2011 (Presentation accessible at http://www.pir.sa.gov.au/minerals/geological_survey_of_sa/data/frome_embayment).
Jaireth, S., Huston, D.L., 2010. Metal endowment of cratons, terranes and districts: Insights from a quantitative analysis of regions with giant and super-giant deposits. Ore Geol. Rev. 38, 288–303.
Jaireth, S., Miezitis, Y., 2004. OZPOT GIS: Geoprovince-scale Assessment of Mineral Potential of Australia. Geoscience Australia, Canberra (accessed at http://www.australianminesatlas.gov.au/build/common/minpot.html).
Jaireth, S., Meixner, T., Milligan, P., Lambert, I., Miezitis, Y., 2007. Unconformity-related uranium systems; regional-scale constraints. Publication Series — Australasian Institute of Mining and Metallurgy 3/2007, pp. 31–32.
Jaireth, S., Mckay, A., Lambert, I., 2008. Association of large sandstone uranium deposits with hydrocarbons. AUSGEO News 89, 8–12 (Online: http://www.ga.gov.au/servlet/BigObjFileManager?bigobjid=GA11117).
Jaques, A.L., Jaireth, S., Walshe, J.L., 2002. systems of Australia; an overview of resources, settings and processes. Aust. J. Earth Sci. 49, 623–660.
Jefferson, C.W., Thomas, D.J., Gandhi, S.S., Ramaekers, P., Delaney, G., Brisbin, D., Cutts, C., Portella, P., Olson, R.A., 2007. Unconformity-associated uranium deposits of the Athabasca Basin, Saskatchewan and Alberta. In: Goodfellow, W.D. (Ed.), Mineral Deposits of Canada. Geological Association of Canada, Newfoundland, pp. 273–306.
Johnson, S.L., Commander, D.P., O'Boy, C.A., 1999. Groundwater resources of the Northern Goldfields, Western Australia. Western Australia Water and Rivers Commission, Report HG 4.
Karner, K., Becker, E., 2009. Geological setting of the Langer Heinrich uranium mine, Namibia. AusIMM International Uranium Conference 2009. AusIMM, Darwin, pp. 97–98.
Kleeman, A.W., 1946. An age determination on samarskite from Mount Painter, South Australia. Trans. R. Soc. S. Aust. 70 (Part 1), 175–177.
Kreuzer, O.P., Markwitz, V., Porwal, A.K., McCuaig, T.C., 2010. A continent-wide study of Australia's uranium potential. Part I: GIS-assisted manual prospectivity analysis. Ore Geol. Rev. 38, 334–366.

Kyser, K., Cuney, M., 2009. Unconformity-related uranium deposits. In: Cuney, M., Kyser, K. (Eds.), Recent and Not-So-Recent Developments in Uranium Deposits and Implications for Exploration. Mineralogical Association of Canada and Society for Geology Applied to Mineral Deposits, Quebec, pp. 161–219.
Kyser, K., Hiatt, E.E., Renac, C., Durocher, K., Holk, G., Deckart, K., 2000. Diagenetic fluids in Paleo- and Meso-proterozoic sedimentary basins and their implications for long protracted fluid histories. Short Course Handb. 28, 225–262.
Lally, J.H., Bajwah, Z.U., 2006. Uranium deposits of the Northern Territory. Northern Territory Geological Survey Report, p. 87.
Landais, P., 1996. Organic geochemistry of sedimentary uranium ore deposits. Ore Geol. Rev. 11, 33–51.
Langen, R.E., Kidwell, A.L., 1961. Geology and geochemistry of the Highland uranium deposit, Converse County, Wyoming. Amer. Inst. Mining and Metall. Engineers Paper 71-I-37, p. 17.
Langmuir, D., 1978. Uranium solution-mineral equilibria at low temperatures with applications to sedimentary ore deposits. Geochim. Cosmochim. Acta 42, 547–570.
Large, P., Bishop, J., Hawkins, D., Farias, P., Granholm, X., Perry, O., Mesthos, A., 2014. Kintyre uranium deposit: structural and alteration paragenesis. AusIMM International Uranium Conference 2014. AusIMM, Perth.
Larsen, E.S., Gottfried, D., 1961. Distribution of Uranium in Rocks and Minerals of Mesozoic Batholiths in Western United States. United States Department of Interior, Geological Survey.
Laznicka, P., 2014. Giant metallic deposits — a century of progress. Ore Geol. Rev. 62, 259–314.
Liu, S.F., Jaireth, S., 2010. Implications for uranium mineral systems. In: Roach, I.C. (Ed.), Geological and Energy Implications of the Paterson Province Airborne Electromagnetic (AEM) Survey, Western AustraliaGeoscience Australia Record 2012/12. Geoscience Australia, Canberra, pp. 219–275.
Lottermoser, B.G., 1988. A carbonatitic diatreme from Umberatana, South Australia. J. Geol. Soc. Lond. 145 (Part 3), 505–513.
Lottermoser, B.G., Plimer, I.R., 1987. Chemical variation in tourmalines, Umberatana, South Australia. Neues Jahrb. Mineral. Monatshefte 314–326.
Ludwig, K.R., Cooper, J.A., 1984. Geochronology of Precambrian granites and associated U–Ti–Th mineralisation, northern Olary Province, South Australia. Contrib. Mineral. Petrol. 86, 298–308.
Ludwig, K.R., Simmons, K.R., Webster, J.D., 1984. U–Pb isotope systematics and apparent ages of uranium ores, Ambrosia Lake and Smith Lake districts, Grants mineral belt, New Mexico. Econ. Geol. Bull. Soc. Econ. Geol. 79, 322–337.
Ludwig, K.R., Grauch, R.I., Nutt, C.J., Nash, J.T., Frishman, D., Simmons, K.R., 1987. Age of uranium mineralization at the Jabiluka and Ranger deposits, Northern Territory, Australia: new U–Pb isotope evidence. Econ. Geol. 82, 857–874.
Maas, R., 1989. Nd-Sr isotope constraints on the age and origin of unconformity-type uranium deposits in the Alligator Rivers uranium field, Northern Territory, Australia. Econ. Geol. 84 (1), 64–90 Available at: http://economicgeology.org/cgi/content/abstract/84/1/64.
Magee, J., 2009. Palaeovalley groundwater resources in arid and semi-arid Australia. Geoscience Australia Record 2009/03.
Malone, E.J., 1962. Darwin, N. T.; 1:250,000 geological series, sheet D/52-4, Australian national grid, explanatory notes. 20.
Mann, A.W., Deutscher, R.L., 1978. Genesis principles for the precipitation of carnotite in calcrete drainages in Western Australia. Econ. Geol. 73, 1724–1737.
McConachy, G., 2009. Pepegoona Deposit Northern Flinders Ranges, SA. SA Explorer's Conference, Adelaide (unpubl.).
McCready, A.J., Stumpfl, E.F., Melcher, F., 2003. U/Th-rich bitumen in Archean granites and Palaeoproterozoic metasediments, Rum Jungle mineral field, Australia; implications for mineralizing fluids. Geofluids 3, 147–159.
McCready, A.J., Stumpfl, E.F., Lally, J.H., Ahmad, M., Gee, R.D., 2004. Polymetallic mineralization at the browns deposit, Rum Jungle mineral field, Northern Territory, Australia. Econ. Geol. 99, 257–277.
McCuaig, T.C., Beresford, S., Hronsky, J., 2010. Translating the mineral systems approach into an effective exploration targeting system. Ore Geol. Rev. 38, 128–138.
McElhinny, M.W., Powell, C.M., Pisarevsky, S.A., 2003. Paleozoic terranes of eastern Australia and the drift history of Gondwana. Tectonophysics 362, 41–65.
McKay, A.D., Miezitis, Y., 2001. Australia's uranium resources, geology and development of deposits. AGSO-Geoscience Australia, Mineral Resource Report 1, p. 195.
McLaren, S., Dunlap, W.J., Sandiford, M., McDougall, I., 2002. Thermochronology of high heat-producing crust at Mount Painter, South Australia; implications for tectonic reactivation of continental interiors. Tectonics 21.
McLaren, S., Sandiford, M., Powell, R., Neumann, N., Woodhead, J., 2006. Palaeozoic intraplate crustal anatexis in the Mount Painter Province, South Australia; timing, thermal budgets and the role of crustal heat production. J. Petrol. 47, 2281–2302.
Mercadier, J., Skirrow, R.G., Cross, A.J., 2013a. Uranium and gold deposits in the Pine Creek Orogen (North Australian Craton): a link at 1.8 Ga? Precambrian Res. 238, 111–119.
Mercadier, J., Annelsey, I.R., McKechnie, C.L., Bogdan, T.S., Creighton, S., 2013b. Magmatic and metamorphic uraninite mineralisation in the western margin of the Trans-Hudson Orogen (Saskatchewan, Canada): a uranium source of unconformity-related uranium deposits? Econ. Geol. 108, 1037–1065.
Mernagh, T.P. (Ed.), 2013. A Review of Australian salt Lakes and Assessment of Their Potential for Strategic Resources. Geoscience Australia, Canberra (Record 2013/39).
Mernagh, T.P., Heinrich, C.A., Leckie, J.F., Carville, D.P., Gilbert, D.J., Valenta, R.K., Wyborn, L.A., 1994. Chemistry of low-temperature hydrothermal gold, platinum, and palladium (± uranium) mineralization at Coronation Hill, Northern Territory, Australia. Econ. Geol. 89, 1053–1073.
Michaelsen, B.H., Fabris, A.J., 2011. Organic facies of the Frome Embayment and Callabonna Sub-basin: what are the U reductants? In: Forbes, C.J. (Ed.), 2011 Sprigg Symposium: Unravelling the northern Flinders and beyond, Abstracts No. 100. Geological Society of Australia, Adelaide, pp. 49–52
Michaelsen, B.H., Fabris, A.J., 2014. Organic facies of the Frome Embayment and Callabonna Sub-basin, South Australia: what and where the uranium reductants. Presentation at the AusIMM Uranium 2014 Conference, 10–14 June 2014, Perth.
Mikhailov, V.V., Petrov, N.N., 1998. Age of exogene uranium deposits in south and southeast Kazakhstan according to the lead-isotope study. Geology of Kazakhstan 2 (354), 63–70.
Mitchell, M.M., Kohn, B.P., O Sullivan, P.B., Hartley, M.J., Foster, D.A., 2002. Low-temperature thermochronology of the Mt Painter Province, South Australia. Aust. J. Earth Sci. 49, 551–563.
Murphy, M.J., Dosseto, A., Turner, S.P., Schaefer, B.F., 2011. U-Series disequilibrium in groundwater as a vector for U mineralisation. Mineral. Mag. 75, 1516.
Murphy, M.J., Stirling, C.H., Kaltenbach, A., Turner, S.P., Schaefer, B.F., 2014. Fractionation of $^{238}U/^{235}U$ by reduction during low temperature uranium mineralisation processes. Earth Planet. Sci. Lett. 388, 306–317.
Needham, R.S., 1988. Geology of the Alligator Rivers uranium field, Northern Territory. Bulletin — Bureau of Mineral Resources, Geology & Geophysics, Australia 224.
Northrop, H.R., Goldhaber, M. (Eds.), 1990. Genesis of tabular-type vanadium-uranium deposits of the Henry Basin, Utah. Economic Geology 85, pp. 215–259.
NTGS, 2005. Pine Creek Orogen interpreted geology, Northern Territory Geological Survey, Darwin. 1: 500000 scale. Mapinfo dataset.
Orth, K., Meffre, S., Davidson, G., 2014. Age and paragenesis of mineralisation at Coronation Hill uranium deposit, Northern Territory, Australia. Mineral. Deposita 1–29.
Pascal, M., 2014. Graphite-bearing and graphite-depleted basement rocks in the Dufferin Lake Zone, south-central Athabasca Basin, Saskatchewan (M.Sc. Thesis) Department of Geological Sciences, University of Saskatchewan, Saskatoon, p. 179.
Pechenkin, I., 2014. Sandstone uranium deposits of Eurasia: from genetic concepts to forecasting new discoveries. URAM 2014. IAEA, Vienna, p. 68.
Pechmann, E., 1992. Mineralogy and Geochronology of U(–Au) Deposits from the Pine Creek Geosyncline, Northern Territory, Australia, and from the Athabasca Basin, Saskatchewan and Alberta, Canada. Heidelberg Universitat, Heidelberg, Federal Republic of Germany.
Petrov, N.N., 1998. Epigenetic stratified-infiltration uranium deposits of Kazakhstan. Geol. Kazakhstan 2, 22–39 (in Russian).
Polito, P.A., Kyser, T.K., Marlatt, J., Alexandre, P., Bajwah, Z., Drever, G., 2004. Significance of alteration assemblages for the origin and evolution of the Proterozoic Nabarlek unconformity-related uranium deposit, Northern Territory, Australia; reply. Econ. Geol. Bull. Soc. Econ. Geol. 99, 1045–1048.
Polito, P.A., Kyser, T.K., Rheinberger, G., Southgate, P.N., 2005a. A paragenetic and isotopic study of the proterozoic Westmoreland uranium deposits, Southern McArthur Basin, Northern Territory, Australia. Econ. Geol. 100, 1243–1260.
Polito, P.A., Kyser, T.K., Thomas, D., Marlatt, J., Drever, G., 2005b. Re-evaluation of the petrogenesis of the Proterozoic Jabiluka unconformity-related uranium deposit, Northern Territory, Australia. Mineral. Deposita 40, 257–288.
Polito, P.A., Kyser, T.K., Alexandre, P., Hiatt, E.E., Stanley, C.R., 2011. Advances in the understanding the Kombolgie Subgroup and unconformity-related uranium deposits in the Alligator Rivers Uranium Field and how to explore for them using lithogeochemical principles. Aust. J. Earth Sci. 58, 453–474.
Potter, E., 2014. Basement to surface expressions of deep mineralization and refinement of critical factors leading to the formation of unconformity-related uranium deposits. URAM 2014. IAEA, Vienna, p. 40.
Quigley, M., Sandiford, M., Fifield, K., Alimanovic, A., 2007. Bedrock erosion and relief production in the northern Flinders Ranges, Australia. Earth Surf. Process. Landf. 32, 929–944.
Quirt, D., Kotzer, T., Kyser, T.K., 1991. Tourmaline, phosphate minerals, zircon and pitchblende in the Athabasca Group; Maw Zone and McArthur River areas, Saskatchewan. Miscellaneous Report — Saskatchewan Mineral Resources, pp. 181–191.
Raffensperger, J.P., Garven, G., 1995a. The formation of unconformity-type uranium ore deposits 1. Coupled groundwater flow and heat transport modeling. Am. J. Sci. 295, 581–636.
Raffensperger, J.P., Garven, G., 1995b. The formation of unconformity-type uranium ore deposits; 2, Coupled hydrochemical modeling. Am. J. Sci. 295, 639–696.
Reynolds, R.L., Goldhaber, M.B., 1978. Origin of a South Texas roll-type uranium deposit; I, Alteration of iron–titanium oxide minerals. Econ. Geol. Bull. Soc. Econ. Geol. 73, 1677–1689.
Richard, A., Banks, D.A., Mercadier, J., Boiron, M.-C., Cuney, M., Cathelineau, M., 2011. An evaporated seawater origin for the ore-forming brines in unconformity-related uranium deposits (Athabasca Basin, Canada): Cl/Br and δ37Cl analysis of fluid inclusions. Geochim. Cosmochim. Acta 75, 2792–2810.
Richard, A., Rozsypal, C., Mercadier, J., Banks, D.A., Cuney, M., Boiron, M.-C., Cathelineau, M., 2012. Giant uranium deposits formed from exceptionally uranium-rich acidic brines. Nat. Geosci. 5, 142–146.
Richard, A., Kendrick, M.A., Cathelineau, M., 2014. Noble gases (Ar, Kr, Xe) and halogens (Cl, Br, I) in fluid inclusions from the Athabasca Basin (Canada): implications for unconformity-related U deposits. Precambrian Res. 247, 110–125.
Richards, J.P., 2013. Giant ore deposits formed by optimal alignments and combinations of geological processes. Nat. Geosci. 6, 911–916.
Roach, I.C., Jaireth, S., Costelloe, M.T., 2014. Applying regional airborne electromagnetic (AEM) surveying to understand the architecture of sandstone-hosted uranium mineral systems in the Callabonna Sub-basin, Lake Frome region, South Australia. Aust. J. Earth Sci. 61, 659–688.
Root, J.C., Robertson, W.J., 1994. Geophysical signature of the Kintyre uranium deposit, Western Australia. Publication — Geology Department and Extension Service, University of Western Australia 26, pp. 371–381.

Rutherford, L., 2006. Developing a tectonic framework for the southern Curnamona Cu–Au Province: geochemical and radiogenic isotope applications. PhD thesis, Department of Geology and Geophysics, University of Adelaide, Adelaide (unpubl.).
Sanford, R.F., 1992. A new model for tabular-type uranium deposits. Econ. Geol. 87, 2041–2055.
Sanford, R.F., 1994. A quantitative model of ground-water flow during formation of tabular sandstone uranium deposits. Econ. Geol. 89, 341–360.
SARIG, 2014. South Australian Resource Information Geoserver Accessible at http://minerals.statedevelopment.sa.gov.au/sarighelp/home.
Schmid, S., Foss, C., Hill, J., Quigley, M., Schaubs, P., Cleverley, J., Robinson, J., 2012. JSU Ngalia Basin Uranium Mineral System Project. In: Munson, T.J., Johnston, K.J. (Eds.), Geological Survey Record. Northern Territory Geological Survey, Darwin, Northern Territory, Australia, pp. 60–62.
Schofield, A., 2009. Uranium content of igneous rocks of Australia 1:5000000 maps — explanatory notes and discussion. Geoscience Australia, Canberra.
Schofield, A. (Ed.), 2012. An Assessment of the Uranium and Geothermal Prospectivity of the Southern Northern Territory. Geoscience Australia, Canberra (Record 2012/51, 220 pp.).
Schofield, A., Gleuher, M., Cross, A., Jaireth, S., 2009. Four Mile uranium deposit: mineralogy. In: Skirrow, R.G. (Ed.), Uranium ore-forming systems of the Lake Frome region, South Australia: regional spatial controls and exploration criteriaGeoscience Australia Record 2009/40. Geoscience Australia, Canberra, pp. 67–89.
Sheard, M.J., Fanning, C.M., Flint, R.B., 1992. Chronology and definition of Mesoproterozoic volcanics and granitoids of the Mount Babbage Inlier, northern Flinders Ranges. Quarterly Geological Notes, the Geological Survey of South Australia 123, pp. 18–32.
Skidmore, C., 2005. Geology of the Honeymoon uranium deposit. In: Taylor, G.F. (Ed.), 4th Sprigg Symposium Uranium: Exploration, Deposits, Mines and Mine waste Disposal Geology. Geological Society of South Australia, Adelaide.
Skirrow, R.G., Jaireth, S., Huston, D.L., Bastrakov, E.N., Schofield, A., van der Wielen, S.E., Barnicoat, A.C., 2009. Uranium mineral systems: processes, exploration criteria and a new deposit framework. Geoscience Australia Record, 2009/20 (44 pp.).
SKM, 2008. Environmental Studies for the Four Mile Project. Sinclair Knight Merz.
Southern Cross Resources, 2000. Honeymoon Uranium Project: Environmental Impact Statement (Toowong).
Spirakis, C.S., 1996. The roles of organic matter in the formation of uranium deposits in sedimentary rocks. Ore Geol. Rev. 11, 53–69.
Stuart-Smith, P.G., Wills, K., Crick, I.H., Needham, R.S., 1980. Evolution of the Pine Creek Geosyncline. Proceedings Series — International Atomic Energy Agency (Collection Comptes Rendus — Agence Internationale de l'Energie Atomique). pp. 23–37.
Sun, Y., Liu, C., Lin, M., Li, Y., Qin, P., 2009. Geochemical evidences of natural gas migration and releasing in the Ordos Basin, China. Energy Explor. Exploit. 27, 1–13.
Teale, G.S., 1993. Geology of the Mount Painter and Mount Babbage inliers. In: Drexel, J.F., Preiss, W.V., Parker, A.J. (Eds.), The Geology of South Australia Volume 1: The Precambrian, Bulletin 54. Geological Survey of South Australia, Adelaide, pp. 149–156.
Teale, G.S., Flint, R.B., 1993. Curnamona Craton and Mount Painter Province. In: Drexel, J.F., Preiss, W.V., Parker, A.J. (Eds.), The Geology of South Australia Volume 1: The Precambrian, Bulletin 54. Geological Survey of South Australia, Adelaide, pp. 147–155.
Teasdale, J., Pryer, L., Etheridge, M., Romine, K., Stuart-Smith, P., Cowan, J., Loutit, T., Vizy, J., Henley, P., 2001. Eastern Arrowie Basin SEEBASE Project, SRK Consulting, SRK Project Code: PI12.
Thundelarra Exploration, 2010. Exploration overview. Shaw Stockbroking Uranium Conference, Sydney (6 December, http://www.thundelarra.com.au/documents/6%20Dec%202010%20Sydney%20Uranium%20Conference%20Presentation.pdf).
Valenta, R.K., 1991. Structural Controls on Mineralisation of the Coronation Hill Deposit and Surrounding Areas. Geoscience Australia, Canberra, p. 220.
Wade, C.E., 2011. Definition of the mesoproterozoic ninnerie supersuite, Curnamona province, South Australia. MESA J. 62, 25–42.
Wall, N., 1995. Observations on the role of thermal regime on basement-cover deformation. BSc Honours thesis, Department of Geology and Geophysics, University of Adelaide, Adelaide (unpubl.).
Wilde, A.R., Wall, V.J., 1987. Geology of the Nabarlek Uranium Deposit, Northern Territory. Australia. Econ. Geol. Vol. 82, 1152–1168.
Wilde, A.R., Bloom, M.S., Wall, V.J., 1989. Transport and deposition of gold, uranium, and platinum-group elements in unconformity-related uranium deposits. Econ. Geol. Monogr. 6, 637–650.
Wilson, J.A., 1986. Geology of the Basement Beneath the Athabasca Basin in Alberta. Alberta Research Council, Edmonton, AB, Canada.
Worden, K.E., Carson, C.J., Scrimgeour, I.R., Lally, J., Doyle, N., 2008. A revised Palaeoproterozoic chronostratigraphy for the Pine Creek Orogen, Northern Australia; evidence from SHRIMP U/Pb zircon geochronology. Precambrian Res. 166, 122–144.
Wülser, P.-A., 2009. Uranium metallogeny in the North Flinders Ranges region of South Australia. PhD thesis, Department of Geology and Geophysics, University of Adelaide, Adelaide (unpubl.).
Wulser, P.-A., Brugger, J., Foden, J., Pfeifer, H.-R., 2011. The sandstone-hosted Beverley uranium deposit, Lake frome basin, South Australia: mineralogy, geochemistry, and a time-constrained model for its genesis. Econ. Geol. 106, 835–867.